

UC Irvine

UC Irvine Electronic Theses and Dissertations

Title

Analyzing the Long-Term Aging of Secondary Organic Aerosols and the Impacts of Acidity

Permalink

<https://escholarship.org/uc/item/76d6n5n1>

Author

Wong, Cynthia

Publication Date

2023

Peer reviewed|Thesis/dissertation

UNIVERSITY OF CALIFORNIA,
IRVINE

Analyzing the Long-Term Aging of Secondary Organic Aerosols and the Impacts of Acidity

DISSERTATION

submitted in partial satisfaction of the requirements
for the degree of

DOCTOR OF PHILOSOPHY

in Chemistry

by

Cynthia Wong

Dissertation Committee:
Professor Sergey A. Nizkorodov, Chair
Professor Annmarie G. Carlton
Professor James N. Smith

2023

Chapter 2 © 2021 American Chemical Society
Chapter 3 © 2022 American Chemical Society
All other materials © 2023 Cynthia Wong

DEDICATION

致爸爸、妈妈、哥哥——是你们的牺牲让这一切成为可能。我爱你

TABLE OF CONTENTS

	Page
LIST OF FIGURES	vi
LIST OF TABLES	x
LIST OF SCHEMES	xii
ACKNOWLEDGMENTS	xiii
VITA	xviii
ABSTRACT OF THE DISSERTATION	xxvii
1 Introduction	1
1.1 General Atmosphere Information	1
1.2 Atmospheric Aerosols	2
1.2.1 Aerosol Life Cycle	3
1.2.2 Volatile Organic Compounds and Secondary Organic Aerosol Formation	5
1.2.3 Secondary Organic Aerosol Composition and Complexity	5
1.3 Acidity of Aerosols	7
1.3.1 Effect of Acids on SOA Formation and Aging	9
1.4 Goals of the Thesis	10
2 Stability of α-Pinene and D-Limonene Ozonolysis Secondary Organic Aerosol Compounds Toward Hydrolysis and Hydration	13
2.1 Abstract	14
2.2 Introduction	14
2.3 Materials and Methods	18
2.3.1 SOA Generation	18
2.3.2 Aging by Exposure to Water Vapor followed by Low-Resolution Mass Spectrometry Analysis	19
2.3.3 Aging by Exposure to Water Vapor followed by High-Resolution Mass Spectrometry Analysis	21
2.3.4 Aging in Liquid Water followed by High-Resolution Mass Spectrometry Analysis	22
2.4 Results	23

2.4.1	Composition of SOA before aging	23
2.4.2	Aging by exposure to water vapor	26
2.4.3	Aging in liquid water	28
2.5	Discussion	34
2.6	Summary and Implications	38
3	Highly acidic conditions drastically alter chemical composition and absorption coefficient of α-pinene secondary organic aerosol	40
3.1	Abstract	41
3.2	Introduction	42
3.3	Experimental Methods	45
3.3.1	Secondary Organic Aerosol Generation	45
3.3.2	Aging in Sulfuric Acid	46
3.3.3	Measurements and Modeling of pH	47
3.3.4	Mass Spectrometry Analysis	48
3.3.5	Spectroscopic Measurements	49
3.4	Results and Discussion	50
3.4.1	Chemical Composition of Fresh α -pinene SOA	50
3.4.2	Chemical Composition of Aged α -pinene SOA	51
3.4.3	Optical Properties and Kinetics of Aged α -pinene SOA	56
3.4.4	HPLC Analysis of the Chromophores	59
3.4.5	Comparison of PDA and UV-Vis Absorption Spectra	62
3.5	Conclusions	66
4	Formation of chromophores from <i>cis</i>-pinonaldehyde in highly acidic conditions	68
4.1	Abstract	69
4.2	Introduction	69
4.3	Experimental Methods and Materials	72
4.3.1	Chemicals	72
4.3.2	Aging in Sulfuric Acid	73
4.3.3	Mass Spectrometry Analysis	74
4.3.4	Spectroscopic Measurements	75
4.3.5	NMR Spectroscopy Measurements	75
4.4	Results and Discussion	75
4.4.1	Ultra-Performance Liquid Chromatography	75
4.4.2	Kinetic Analysis	79
4.4.3	Product Identification	85
4.4.3.1	Purification and Separation of Chromophores	85
4.4.3.2	Confirmation of Chromophores	86
4.4.3.3	NMR Analysis and Possible Mechanisms	89
4.5	Conclusions	92

5	Biogenic and anthropogenic secondary organic aerosols become fluorescent after highly acidic aging	95
5.1	Abstract	95
5.2	Introduction	96
5.3	Experimental Methods and Materials	99
	5.3.1 Formation of SOA	99
	5.3.2 Aging in Sulfuric Acid	101
	5.3.3 Spectroscopic Measurements	101
5.4	Results and Discussion	103
	5.4.1 Fluorescence at Varying Acidities	103
	5.4.2 Fluorescence and Acid–Base Equilibria	108
	5.4.3 Interferences with Bioaerosol Fluorescence	112
5.5	Conclusions	113
6	Conclusions and Future Directions	115
	References	118

LIST OF FIGURES

	Page
1.1 Acidity of different aerosols and cloud water in the atmosphere (Adapted from Pye et al. 2020) ⁴⁷	8
2.1 Aging Experiments Summary. SOA were first generated in a flow tube reactor and collected on a foil substrate. Foil substrates were the cut into segments to age the SOA in humid conditions, dry conditions (control) or sealed and frozen (control) to understand the long-term aging of SOA by exposure to water vapor. Alternatively, the foil substrates were the cut into segments to age the SOA in liquid water, acetonitrile (control) or sealed and frozen (control) to understand the long-term aging of SOA by liquid water.	22
2.2 ESI-MS mass spectra of fresh α -pinene SOA (a,c) and α -pinene SOA in the presence of water vapor for 1 (b) and 2 (d) weeks. Peaks were normalized to the combined peak abundance.	24
2.3 ESI-HRMS mass spectra of fresh α -pinene (a) and d-limonene (d) SOA and α -pinene and d-limonene SOA after aging in liquid water for 1 (b,e) and 2 (c,f) days. Peaks were normalized to the combined peak abundance.	25
2.4 Difference low-resolution mass spectra of α -pinene SOA aged for 1 and 2 weeks by exposure to water vapor. Positive and negative peaks represent compounds that increased and decreased after aging by exposure to water vapor, respectively.	27
2.5 Difference high-resolution mass spectra of α -pinene SOA aged for 1 and 2 weeks in dry and humid conditions. Positive and negative peaks represent compounds that increased and decreased after aging by exposure to water vapor, respectively. (Trial 2)	28
2.6 Difference high-resolution mass spectra of α -pinene SOA aged for 1 and 2 weeks in dry and humid conditions. Positive and negative peaks represent compounds that increased and decreased after aging by exposure to water vapor, respectively. (Trial 3)	29
2.7 Difference high-resolution mass spectra of α -pinene and d-limonene ozonolysis SOA aged in liquid water for 1 and 2 days. Positive peaks represent compounds that increased after aging in water and negative peaks presents compounds that decreased after aging in water.	31

2.8	Difference high-resolution mass spectra of α -pinene SOA aged in acetonitrile and liquid water for 1 and 2 days. Positive peaks represent compounds that increased after aging in water and negative peaks presents compounds that decreased after aging in water. (Trial 2)	32
2.9	Difference high-resolution mass spectra of β -pinene SOA aged in acetonitrile and liquid water for 1 and 2 days. Positive peaks represent compounds that increased after aging in water and negative peaks presents compounds that decreased after aging in water. (Trial 3)	33
2.10	Van Krevelen diagram of fresh α -pinene SOA from Romonosky et al. (2017) compared to this study. Size of the markers are scaled to the normalized intensity.	37
3.1	Aging Experiments Summary. SOA were first generated in a flow tube reactor and collected on a foil substrate. Foil substrates were cut into three segments, extracted using acetonitrile, and acetonitrile was removed using a rotary evaporator. The corresponding acid was added to Sample A and Sample B. Sample C was extracted using the same method and dissolved in water for our control group.	47
3.2	Retention time integrated mass spectra of fresh α -pinene ozonolysis SOA. Peaks were normalized to the combined peak abundance.	51
3.3	Mass spectra of α -pinene ozonolysis SOA samples aged for 2 days in (a) 0 M (control), (b) 0.52 mM (pH 3.00), (c) 6.4 mM (pH 1.98), (d) 90 mM (pH 0.94), (e) 1.0 M (pH -0.01), (f) 1.8 M (pH -0.36), (g) 3.2 M (pH -0.62), (h) 5.6 M (pH -0.86), and (i) 10 M (pH -1.08) of H ₂ SO ₄ . Black traces correspond to CHO compounds, while red traces correspond to CHOS compounds. Mass spectra were derived by integrating over 2-16 min for each of the LC run and normalizing by the combined peak abundance.	53
3.4	Overall Amounts of CHO and CHOS Compounds. Relative ion abundance of the CHO (green) and CHOS (red) compounds present in fresh and aged α -pinene ozonolysis SOA samples. The labels on the x-axis represent pH values from the E-AIM model (Table 3.1), except for pH 4.3 sample, which corresponds to the pH meter reading. The ion peak abundances for all observed CHO and CHOS compounds were added. CHOS compounds may be overestimated in this approach as they have higher ionization efficiencies in ESI.	56
3.5	MAC spectra of α -pinene ozonolysis SOA samples aged for 0, 1, and 2 days in (a) 0 M (control), (b) 5.2×10^{-4} M (pH 3.00), (c) 6.4×10^{-3} M (pH 1.98), (d) 9.0×10^{-2} M (pH 0.94), (e) 1.0 M (pH -0.01), (f) 1.8 M (pH -0.36), (g) 3.2 M (pH -0.62), (h) 5.6 M (pH -0.86), and (i) 10 M (pH -1.08) solutions of H ₂ SO ₄	57
3.6	MAC absorption spectra of α -pinene ozonolysis SOA samples aged in (a) 5.6 M (pH -0.86) and (b) 10 M (pH -1.08) of H ₂ SO ₄ collected every 15 min over 24 h. Photographs of SOA and acid solution after \sim 5 min and \sim 24 h of aging	59
3.7	Time Dependent MAC for peaks of interest in SOA samples aged in pH -0.86 and pH -1.08	60

3.8	Fluorescence of APIN SOA Excitation-emission matrix plot for water (a), pH -1.08 solution (b), and SOA aged at pH -1.08. There is no visible fluorescence in the controls, however a relatively weak fluorescence band appeared at $\lambda_{\text{ex}} \approx 450 \text{ nm}/\lambda_{\text{em}} \approx 520 \text{ nm}$ in the aged SOA sample.	60
3.9	UPLC-PDA chromatograms of α -pinene ozonolysis SOA samples aged in (a) 5.6 M (pH -0.86) and (b) 10 M (pH -1.08) of H_2SO_4	62
3.10	Positive ion mode HRMS and PDA chromatogram between 3-15 min for α -pinene ozonolysis SOA aged in pH -1.08 conditions for 2 days.	63
3.11	MAC absorption spectra of α -pinene ozonolysis SOA samples aged in 10 M (pH -1.08) of H_2SO_4 diluted with 1:1 ACN/ H_2O and H_2O at various dilution factors. DF, dilution factor.	65
4.1	Structures of <i>cis</i> -pinonic acid and <i>cis</i> -pinonaldehyde	71
4.2	UPLC chromatograms of <i>cis</i> -pinonic acid aged in water for 2 days, 0.52 mM H_2SO_4 (pH 3.00), 5.6 M H_2SO_4 (pH -0.86), and 10 M H_2SO_4 (pH -1.08) in negative ion mode (b, e, h, k), position ion mode (c, f, i, l), and the corresponding PDA (a, d, g, j). Overlaid on the negative ion mode and positive ion mode TIC in red is the SIC for m/z 183.1028 and m/z 185.1177, respectively, except for TIC ESI (-) (pH -1.08). The PDA chromatograms were shifted 0.06 minutes to account for the time delay between the two detectors. All chromatograms were normalized based on the maximum peak intensity of their respective dataset.	77
4.3	Positive ion mode TIC for <i>cis</i> -pinonaldehyde aged in (a) H_2O , (b) 0.52 mM H_2SO_4 (pH 3.00), and (c) 1.0 M H_2SO_4 (pH -0.01).	80
4.4	UPLC chromatograms of <i>cis</i> -pinonaldehyde aged in 10 M H_2SO_4 (c,d) in positive ion mode for TIC (a), PDA (b), and SIC (m/z 151.1117) (c). The PDA chromatogram was shifted 0.06 minutes to account for the time delay between the two detectors.	81
4.5	Absorption spectra of <i>cis</i> -pinonic acid aged in (a) $5.2 \times 10^{-1} \text{ M}$ (pH 3.00), and (b) 10 M (pH -1.08) solutions of H_2SO_4 recorded every 15 min for 24 h.	82
4.6	Absorption spectra of <i>cis</i> -pinonaldehyde aged in (a) 5.6 M (pH -0.86) and (b) 10 M (pH -1.08) H_2SO_4 . Each spectrum was collected every 15 min over 24 h.	84
4.7	Absorption spectra of <i>cis</i> -pinonaldehyde aged in (a) 5.6 M (pH -0.86) and (b) 10 M (pH -1.08) H_2SO_4 for two days, compared to identical experiments with α -pinene SOA by Wong et al 2022. ¹⁸⁵	84
4.8	UPLC chromatograms of S5 and S6 isolated extracts in positive ion mode for TIC (a), PDA (b), and SIC (m/z 151.1117) (c). The PDA chromatogram was shifted 0.06 minutes to account for the time delay between the two detectors.	88
4.9	Absorption spectra from UV-Vis (red trace) and PDA (blue and green trace) from the purified sample	89
5.1	EEM plots for APIN/ O_3 and LIM/ O_3 SOA aged in H_2O , 0.52 H_2SO_4 (pH 3.00), and 10M H_2SO_4 (pH -1.08) for 2 days	103

5.2	EEM plots for APIN/OH and LIM/OH SOA aged in H ₂ O, 0.52 H ₂ SO ₄ (pH 3.00), and 10M H ₂ SO ₄ (pH -1.08) for 2 days	105
5.3	EEM plots for TOL/OH and XYL/OH SOA aged in H ₂ O, 0.52 H ₂ SO ₄ (pH 3.00), and 10M H ₂ SO ₄ (pH -1.08) for 2 days	107
5.4	MAC spectra of biogenic and anthropogenic SOA aged aged in H ₂ O, 0.52 H ₂ SO ₄ (pH 3.00), and 10M H ₂ SO ₄ (pH -1.08) for 2 days	107
5.5	MAC spectra of biogenic and anthropogenic SOA aged in 10 M (pH -1.08) of H ₂ SO ₄ and then diluted with 1:1 ACN/H ₂ O at various dilution factors . .	109
5.6	EEM plots for APIN/O ₃ and LIM/O ₃ SOA aged in 10M H ₂ SO ₄ (pH -1.08) for 2 days and then diluted with 1:1 ACN/H ₂ O at 1:2 (a,d), 1:3 (b,e), and 1:4 (c,f) dilution factors	110
5.7	EEM plots for APIN/OH and LIM/OH SOA aged in 10M H ₂ SO ₄ (pH -1.08) for 2 days and then diluted with 1:1 ACN/H ₂ O at 1:2 (a,d), 1:3 (b,e), and 1:4 (c,f) dilution factors	110
5.8	EEM plots for TOL/OH and XYL/OH SOA aged in 10M H ₂ SO ₄ (pH -1.08) for 2 days and then diluted with 1:1 ACN/H ₂ O at 1:2 (a,d), 1:3 (b,e), and 1:4 (c,f) dilution factors	111
5.9	Maximum fluorescence intensity as a function of mass concentration for each SOA sample aged in 10M H ₂ SO ₄ (pH -1.08) for 2 days and then diluted with 1:1 ACN/H ₂ O at various dilutions factors	112

LIST OF TABLES

	Page	
2.1	Aging Experiments Summary. APIN/O ₃ and LIM/O ₃ refer to SOA made by ozonolysis of α -pinene and d-limonene, respectively. “Humid Air” refers to samples that were aged in a relative humidity (RH 97%) aging chamber, while “Dry Air” refers to samples that were aged in a desiccator (RH <2%). “Liquid Water” and “Acetonitrile” correspond to samples that were extracted using the respective solvent and then aged. Dashes indicate that the corresponding control samples were frozen until analysis was performed. In the initial experiments, a low-resolution mass spectrometer was used; it was replaced by a high-resolution mass spectrometer for the rest of the study. The Solvent System column describes the solution composition adjusted for the ESI-MS analysis (e.g., by adding equal volume of acetonitrile of to an aqueous solution of SOA).	20
2.2	Major compounds in α -pinene SOA that changed after aging by exposure to water vapor. Ratios 1 indicate that the corresponding peak increased with aging while ratios <1 suggest that the peak decreased after aging.	27
2.3	Major compounds in α -pinene SOA that changed after aging by exposure to water vapor (humid conditions) or desiccant (dry conditions). Ratios >1 indicate that the correspond peak increased with aging while ratios <1 suggest that the peak decreased after aging. (Trial 2)	29
2.4	Major compounds in α -pinene SOA that changed after aging by exposure to water vapor (humid conditions) or desiccant (dry conditions). Ratios >1 indicate that the correspond peak increased with aging while ratios <1 suggest that the peak decreased after aging. (Trial 3)	30
2.5	Major compounds in α -pinene and d-limonene SOA that changed after aging in liquid water. Ratios >1 indicate that the correspond peak increased with aging while ratios <1 suggest that the peak decreased after aging.	32
2.6	Major compounds in α -pinene that changed after aging in acetonitrile and liquid water. Ratios >1 indicate that the correspond peak increased with aging while ratios <1 suggest that the peak decreased after aging. (Trial 2) .	33
2.7	Major compounds in α -pinene that changed after aging in acetonitrile and liquid water. Ratios >1 indicate that the correspond peak increased with aging while ratios <1 suggest that the peak decreased after aging. (Trial 3) .	34

3.1	Solution Acidity in Aging Experiments. The first column lists the molar concentration of H ₂ SO ₄ added to the solution. The molalities of [H ⁺] and other ions were calculated using the Extended Aerosol Inorganics Model (E-AIM, http://www.aim.env.uea.ac.uk/aim/aim.php). The effective pH values listed in the last column and quoted in the paper represent the negative logarithm of molality of [H ⁺].	48
3.2	Some of the major CHOS compounds detected in Aged APIN SOA in pH -1.08 by Mass Spectrometry	54
3.3	Lifetime of browning for several peaks on interest in α-pinene ozonolysis SOA samples aged in 5.6M (pH -0.86), and 10 M (pH -1.08) H ₂ SO ₄ . Lifetimes were calculated by assuming pseudo first order reactions in the times series fits for each peak.	61
3.4	Solution Acidity in Peak Shift Experiments. SOA samples aged at pH -1 were diluted with 1:1 ACN:H ₂ O and H ₂ O. Estimated pH was calculated using Extended Aerosol Inorganics Model (E-AIM (http://www.aim.env.uea.ac.uk/aim/aim.php)).	64
4.1	Solution Acidity in Aging Experiments. The first column lists the molar concentration of H ₂ SO ₄ added to the solution. The molalities of [H ⁺] and other ions were calculated using the Extended Aerosol Inorganics Model* (E-AIM, http://www.aim.env.uea.ac.uk/aim/aim.php). The effective pH values listed in the last column and quoted in the paper represent the negative logarithm of molality of [H ⁺].	74
4.2	Effective lifetimes of browning for of <i>cis</i> -pinonaldehyde aged in 5.6 M (pH -0.86) and 10 M (pH -1.08) H ₂ SO ₄ , calculated by assuming pseudo-first-order reactions in the time series fits for each peak.	85
4.3	Summary of the ¹ H and ¹³ C- NMR data from compounds S4, S5 and S6	90
5.1	Aging Experiments Summary	99
5.2	Solution Acidity in Dilution Experiments. SOA samples aged at 10M H ₂ SO ₄ were diluted in water. pH was estimated using Extended Aerosol Inorganics Model (E-AIM (http://www.aim.env.uea.ac.uk/aim/aim.php)).	101

LIST OF SCHEMES

	Page
4.1 Synthesis of <i>cis</i> -pinonaldehyde (S2)	72
4.2 Formation of homoterpenyl methyl ketone (S4) from <i>cis</i> -pinonic acid (S1) aged in H ₂ SO ₄ , adapted from Arcus and Bennett (1955) ¹⁸⁸ PT indicates proton transfer	78
4.3 Summary of products formed aging of <i>cis</i> -pinonaldehyde (S2)	86
4.4 Formation of 1-(4-(propan-2-ylidene)cyclopent-1-en-1-yl)ethan-1-one (S5), from the acid-catalyzed reaction of <i>cis</i> -pinonaldehyde (S2)	94
4.5 Formation of 1-(4-isopropylcyclopenta-1,3-dien-1-yl)ethan-1-one (S6, S7) from the acid catalyzed reaction of <i>cis</i> -pinonaldehyde (S2)	94

ACKNOWLEDGMENTS

Graduate school has, no doubt, been a rollercoaster – it’s full of ups and downs, twists and turns, and filled with moments of sheer exhilaration, gripping uncertainty, and heart-stopping fear. But just like a rollercoaster, I was never on this ride alone. I am deeply grateful to the numerous individuals and communities who have been by my side throughout my graduate school journey. Their unwavering support, guidance, and encouragement have been instrumental in helping me navigate the highs and lows of this rollercoaster ride and grow into the scientist I am today.

I am deeply grateful to my advisor, Sergey A. Nizkorodov, whose unwavering support has been integral in shaping my academic journey at UC Irvine. From the beginning, Sergey emphasized a collaborative partnership in our research endeavors, encouraging me to be creative and independent while providing the freedom to pursue extracurricular activities without pressure to spend more time in the lab. This autonomy gave me the confidence I needed to pursue my goals in graduate school and explore my passions without hesitation. Although we’ve had our differences, our conflicts have ultimately helped me become a better scientist and leader. Sergey has taught me invaluable lessons in both atmospheric chemistry and qualities that make a great mentor. I will always be grateful for his support and encouragement, and I hope to carry the lessons I’ve learned from him with me throughout my career.

I would like to express my gratitude to my committee members, Professor Annmarie G. Carlton and Professor James N. Smith, for their invaluable guidance, advice, and mentorship throughout my time at UC Irvine. I am also grateful for their willingness in allowing me to distract their students from time to time with my questions, ideas, and stories. The mentorship from both Professor Annmarie G. Carlton and Professor James N. Smith has been instrumental in fostering my growth as a scholar.

My time spent in and outside of the lab with the individuals of the Nizkorodov Group, both past and present has played a pivotal role in my growth and development. They have guided me in learning and repairing instrumentation, provided a space for exchanging ideas, and instilled the confidence to conduct independent research and for that I am incredibly thankful. I would like to offer a heartfelt appreciation to Dr. Natalie R. Smith and Dr. Alexandra L. Klodt (and sometimes Lena Gerritz) for their exceptional guidance and friendship throughout my research journey. They not only provided invaluable support in answering my questions, no matter how trivial they may have seemed, but they also went beyond their roles as mentors and truly became amazing friends, particularly during our thrilling climbing adventures and those memorable wine nights watching the Bachelor franchise (with of Dr. Annie Anderson). Their ability to create such an inclusive and joyful atmosphere has left an indelible mark on my heart, and I am forever grateful for their mentorship and the friendships we have formed. I would also like to express my heartfelt gratitude to Daniel Vite, Sijia (Lucia) Liu, and Jett Vuong for their unwavering dedication and hard work on their respective projects. Their commitment and passion have made my role as a mentor incredibly rewarding and fulfilling. I am immensely thankful for the opportunity to guide and

support them, and to be a part of their scientific journeys. Their enthusiasm and determination are truly inspiring, and I am honored to have played a role in their growth as scientists.

While at UC Irvine I was adopted into the Carlton Group, unofficially. These incredible individuals (with special thanks to Dr. Amy Christiansen, Madi Flesch, Alyssa Burns, and Yin Ting Chiu) provided me with a safe space to share the ups and downs of my research and even spill the latest news from the Chemistry Department. Despite my habit of barging into their meetings and occasional grad school meltdowns in their office, they tolerated me with a lot of patience. More importantly, they offered me a fresh perspective on problem-solving (both in science and in life), helping me see things from different angles. The Carlton group gave me an additionally amazing support system and expanded my horizons throughout my journey in graduate school.

I feel immensely grateful to be a part of the AirUCI community, which comprises a wonderful group of scientists always willing to collaborate, share expertise, and equipment. I cannot thank everyone at AirUCI enough for their assistance and friendship throughout my time here. In particular, I want to express my appreciation to Dr. Lisa Wingen and Dr. Veronique Perraud, who have been the backbone of this community and have taught me so much about instrumentation and research. Their willingness to spend countless hours discussing science with me over the years has been invaluable to my growth as a scientist. I am truly grateful for their mentorship and support.

The unwavering support of the UC Irvine Department of Chemistry and School of Physical Science throughout my journey deserves my utmost gratitude. Their continuous support enabled me to establish the chemistry graduate peer mentorship program, known as ChemUNITY, which focuses on fostering inclusivity within the department. Additionally, they provided me with the opportunity to serve as a Diversity, Equity, and Inclusion Graduate Fellow during the 2021-2022 academic year. These roles allowed me to have a profound impact on the academic culture by amplifying the voices of my peers and advocating for positive changes within our community. I am deeply grateful for the chance to work on issues close to my heart and contribute to creating a safe and welcoming environment for everyone in our community.

I am beyond thankful to a part of UC Irvine Ridge to Reef, a community of passionate leaders dedicated to creating meaningful change in the environment. This community sparked a renewed passion within me for environmental science and social justice, revitalizing my dedication to effecting positive change. I am particularly thankful for the support I received during my fourth year of graduate school, which included the Ridge to Reef Trainee Fellowship. This fellowship not only provided crucial support for my research but also opened doors for me to intern at IQAir North America during the summer of 2022. During this internship, I had the amazing opportunity to work with some amazing individuals (Amir Mousavi, Eric Klein, Harita Kandarpa, Casey Cheng and Misheel Enkhbold). I gained a broader perspective on air quality and had the privilege of collaborating with various non-profits and organizations in different countries. It allowed me to apply my technical skills to real-world applications and engage in hands-on work. I would like to extend a heartfelt

appreciation to Dr. Christi Chester Schroeder, my manager during my time at IQAir North America. Under her mentorship and leadership, I experienced significant growth and gained confidence as both a scientist and an ambassador of change. The dedication and effort she invested in cultivating a welcoming and inclusive work environment had a profound impact on me. Dr. Christi Chester Schroeder played a pivotal role in shaping my career trajectory, molding me into a scientist, and a leader. I am genuinely thankful to have her as one of my role models, and her influence will continue to resonate with me as I navigate future endeavors.

I would like to express my sincere gratitude to my peers and colleagues in the Grassian Research Group at UC San Diego, particularly Professor Vicki H. Grassian, Dr. Ellen M. Coddens, and Dr. Liora Mael. Their support and guidance have laid a solid foundation for my success as a researcher and scientist. Despite not being physically present during my time at UC Irvine, they have consistently challenged me to think critically, encouraged my intellectual curiosity, and pushed me to excel in my graduate studies. The Grassian Group fostered a stimulating and collaborative research environment, where ideas were nurtured and innovation thrived and their unwavering belief in my potential and their constant encouragement have been the driving force behind my achievements. I am truly honored and privileged to have had the opportunity to work with them, and I will forever cherish the lessons learned and the memories created during my time in the Grassian Group.

The fellowships, research funding sources, research journals, and facilities that have played a crucial role in enabling me to conduct impactful chemistry work during my time at UC Irvine and I am truly thankful for their crucial support and the opportunities they have afforded me. Firstly, I am incredibly thankful for being awarded the Ridge to Reef Trainee Fellowship (Ridge to Reef NSF Research Traineeship, award DGE-1735040), which provided invaluable support throughout my fourth year of graduate school. Chapters 2, 3, 4, and 5 received support from the National Science Foundation Grant AGS-1853639. The acquisition of the high-resolution mass spectrometer instrument mentioned in Chapters 2, 3, and 4 was made possible by the National Science Foundation Grant CHE-1337080. Furthermore, I would like to express my appreciation to the Nuclear Magnetic Resonance Spectroscopy Facility and the Laser Spectroscopy Labs at UC Irvine for their invaluable support and allowing me to utilize their instruments in Chapter 4 and Chapter 5, respectively. I extend my thanks to the Department of Chemistry for awarding me the Chemistry Dissertation Fellowship, which supported me during my final quarter at UC Irvine and allowed me to fully dedicate my time to the completion of this thesis. Lastly, I am grateful for ACS Earth Space Chemistry, for allowing me to reuse my published work as part of this dissertation. The support provided by these fellowships, funding sources, research journals, and facilities has been instrumental in the successful completion of my research, and I am truly grateful for their contributions.

Chapter 2 of this dissertation is a reprint of the material as it appears in Stability of α -Pinene and D-Limonene Ozonolysis Secondary Organic Aerosol Compounds Toward Hydrolysis and Hydration, American Chemical Society Earth and Space Chemistry (2021), 5, 2555-2564, DOI:10.1021/acsearthspacechem.2c00249, used with permission from American Chemical Society. The co-authors listed in this publication are Cynthia Wong, Daniel Vite, and

Sergey A. Nizkorodov.

Chapter 3 of this dissertation is a reprint of the material as it appears in *Highly Acidic Conditions Drastically Alter the Chemical Composition and Absorption Coefficient of α -Pinene Secondary Organic Aerosol*, *American Chemical Society Earth and Space Chemistry*, 2022, 6(12), 2983–2994, doi/10.1021/acsearthspacechem.2c00249, used with permission from American Chemical Society. The co-authors listed in this publication are Cynthia Wong, Sijia Liu, and Sergey A. Nizkorodov.

Without the support and friendship of the incredible individuals I've met during my time here in Irvine, there is no doubt in my mind that I would not have survived graduate school. I am immensely grateful for the cohort I had the privilege to enter graduate school with, as our collective experience was unlike any other, navigating through the trials of a global pandemic and witnessing a transformative societal awakening. The friendships I have made throughout my time here at Irvine have been a vital part of my success. Through chance encounters on Ring Road, brief exchanges at the shared facilities, catch-ups in the hallways and restrooms, or interactions through departmental organizations and activities, these friends helped preserve my sanity, but also empowered me to thrive and made the arduous path of grad school more bearable.

The first few friends I made in Irvine, Dora Kadish, Alexa Watson, Ryan Le Tourneau, and Ian Mercer, hold a special place in my heart. Their presence in my life has served as a constant reminder to seek joy, follow my passions outside the realm of academia, and make choices that prioritize my own happiness. It brings me immense happiness to witness their thriving journeys and their embrace of life's greatest opportunities.

It has been an absolute pleasure to share the atmosphere and work alongside other fierce and brilliant female scientists, Madi Flesch, Mooji Boldbataar, and Lia Dam (and Alyssa Burns). While our first meeting wasn't exactly smooth, they saw beyond my competitive exterior and recognized something more in me. The journey through classes and research, with all its highs and lows, brought us closer together, forging a bond that transcends mere colleagues. These friends were a breath of fresh air, constantly supporting one another, while pursuing our own endeavors in and outside of the lab.

I consider myself incredibly fortunate to have formed deep and meaningful friendships with Alissa Matus (<3), Mariana Navarro (Roomie), Aoon Rizvi (First Friend), and Sarah Bredekamp (Intimidating Friend). Each of them brings immense joy into my life, but collectively, they have a profound impact on me. They not only challenge me to think deeply about ideas and navigate life's situations, but they also possess the remarkable ability to transform even the most mundane errands into enjoyable adventures. These friendships extend far beyond our shared interest in science and chemistry. Together, they have created a safe and nurturing space where I can freely embrace and express my emotions, leaving me feeling seen, valued, and unconditionally loved. Throughout the course of my graduate school journey, I have encountered many challenges and tragedies, but with the unwavering support of these friends, I have grown into a stronger and more resilient individual. Laughter has become a

constant presence in our wine nights, craft sessions and taco Tuesdays, and it has undoubtedly been one of the most uplifting aspects of our friendships. As we eagerly anticipate the next chapter of our lives, I am filled with excitement to witness their accomplishments and wholeheartedly cheer them on from the sidelines.

While my friends outside of grad school may not have fully grasped the intricacies of my research, their presence served as a constant reminder that grad school was just one facet of my identity, not the entirety of who I am. They offered me a valuable perspective, emphasizing that life encompasses more than just school, and consistently encouraging me to recognize my own capabilities. For their enduring presence and the shared moments of joy, I am truly grateful.

I am beyond thankful for my partner, Eduardo Miguel Espinas Ilano (llama), and the countless ways in which he has uplifted and supported me. Regardless of the scale, he has consistently shown unwavering encouragement, attentively listening to every complaint, setback, failure, and accomplishment I have experienced throughout my graduate school journey. During my lowest moments, he has been a steadfast pillar of support, offering his unwavering presence and genuine care. Whether it's preparing meals for me, chauffeuring me around like a passenger princess, or simply being there during times of intense stress, his unwavering support has been a source of strength. His patience and unwavering belief in me have touched me deeply, and I am profoundly grateful to have the opportunity to share this remarkable journey called life together. I am so excited to start my next chapter with him and to pursue our incredible dreams as a team, knowing that with him by my side, anything is possible.

My love for my family (Baba, Mama, and Michael) is indescribable. Their unwavering dedication and care for their family in their native villages in China, along with the sacrifices they made to immigrate to the US, fills me with gratitude for having them as my parents. The challenges and microaggressions they have faced in this new country only amplify my appreciation for their resilience and courage, which continues to inspire me every single day. Their values have been instilled in me, shaping the person I am today. While I may not have been a perfect daughter, particularly during my adolescence, embarking on my own journey in the world allowed me to realize the depth of their love for me. Although we may not always have seen eye to eye, their unwavering support and sacrifices have made my educational pursuits and achievements possible, and I am eternally grateful for the opportunities they have afforded me to succeed. I owe every single accomplishment and success to my family, Baba, Mama, and Michael.

VITA

Cynthia Wong

EDUCATION

University of California, Irvine Irvine, CA
PhD in Atmospheric Chemistry 2018 - 2023
MS in Chemistry (2021, earned en route to PhD)
Thesis Advisor: Professor Sergey Nizkorodov

University of California, San Diego La Jolla, CA
Bachelor of Science, Environmental Chemistry 2014 - 2018
Minor in Business
Research Advisor: Professor Vicki H. Grassian

Honors and Awards:

Jacqueline Smitrovich Prize (2023), UC Irvine Department of Chemistry Dissertation Fellowship (2023), ACS Environmental Chemistry Graduate Student Award Honorable Mention (2023), UC Irvine Chemistry Excellence in Diversity, Equity, and Inclusion Award (2022), UC Irvine Department of Chemistry Diversity Fellow (2021-2022), National Science Foundation Ridge 2 Reef Fellow (2021-2022), National Science Foundation Ridge 2 Reef Trainee (2020-Present), National Science Foundation Graduate Research Fellowship Honorable Mention (2020), UC San Diego Chemistry Departmental Honors (2018), UC San Diego Thurgood Marshall College Provost Honors (2016-2018)

RESEARCH PROJECTS

Investigating the fluorescence of biogenic and anthropogenic secondary organic aerosols aged in highly acidic conditions

Graduate Project 2022-2023
Studied how the fluorescent properties of anthropogenic and biogenic SOA changed when aged in highly acidic conditions. The findings indicate that highly acidic conditions cause substantial changes to the absorption and fluorescence spectra of all SOA, and that the corresponding peaks differ depending on whether the VOC precursors are biogenic or anthropogenic.

Long term aging of *cis*-pinonic acid and *cis*-pinonaldehyde in highly acidic conditions

Graduate Project 2022-2023
Identified the mechanism and compound(s) responsible for the chromophores when α -pinene SOA was aged in highly acidic conditions. It was found that *cis*-pinonic acid formed homoterpenyl methyl ketone when aged in highly acidic conditions, as suggested by a previous

study, while *cis*-pinoaldehyde, undergoes multiple acid catalyzed reactions to form the chromophore of interest.

Acid catalyzed aging of α -pinene secondary organic aerosols

Graduate Project

2020-2022

Explored the effect of acidity on the chemical composition and optical properties of α -pinene secondary organic aerosol. It was found that acidity is a major driver of SOA aging, resulting in a large change in the chemical composition and optical properties of aerosols in regions where high concentrations of H_2SO_4 persist (e.g., upper troposphere and lower stratosphere).

Understanding the role of water vapor and aerosol liquid water on the molecular composition of α -pinene secondary organic aerosols

Graduate Project

2019-2021

Analyzed the effect of water vapor and aerosol liquid water on the molecular composition of biogenic monoterpene SOA. Results suggested that water led to changes in the chemical composition of these aerosols, but the extent of these changes was small, suggesting that hydrolysis and hydration is not a major aging mechanism.

Influence of organic compounds on the catalytic oxidation of S(IV) in acidic aqueous media

Undergraduate Project

2017-2018

Investigated the effect of carbonyls, specifically glyoxal, on S(IV) oxidation in acidic aqueous solutions catalyzed by iron using mass spectrometry, chromatography, and spectroscopy. The results suggest that impact of glyoxal on the catalytic oxidation of S(IV) is strongly influenced by various factors including the mechanism, form of iron, and ambient conditions such as pH, and concentration.

Effect of pH, temperature, and light on the dissolution of Arizona Test Dust and the catalytic oxidation of S(IV)

Undergraduate Project

2016-2017

Studied the factors (e.g., temperature, light, pH) that affect the dissolution of transitional metal ions in cloud droplets to gain better insight to the chemical pathways in the atmosphere. This work suggest the dissolution of transitional metals depends on ambient conditions - pH, temperature and light, which can further our understanding of how these metal ions catalyze reactions of atmospheric importance.

PROFESSIONAL EXPERIENCE

University of California, Irvine –Nizkorodov Research Lab

2018 - 2023

Graduate Student Researcher

- Designed and executed novel analytical experiments using techniques such as liquid chromatography-mass spectrometry and UV-Vis spectroscopy to investigate the chemical aging mechanisms of atmospheric particulate matter leading to the publication of 4 articles in scientific journals and 6+ presentations at national conferences.

- Trained and supervised 4 undergraduate students on various spectroscopy and mass spectrometry techniques, resulting in the successful completion of their research projects.
- Analyzed data from over 1,000 samples using software including, Microsoft Office, Igor Pro, and MATLAB.
- Demonstrated excellent communication skills by engaging with diverse groups, including weekly meetings with advisors, weekly meetings with the research lab, and conference presentations, resulting in collaborations with researchers and increased visibility for our research group.

IQAir North America

June 2022-December 2022

Air Quality Data Outreach and Science Specialist, Internship

- Validated and interpreted complex air quality data from diverse sources, including government regulatory monitors and low-cost sensors, to generate actionable insights and recommendations.
- Developed and implemented standardized procedures for the quality assurance of air quality data, leveraging programming software such as Excel, R, and Tableau. Created workflows to streamline data analysis and reporting for multiple projects.
- Conducted statistical analysis and dispersion modeling to process air quality data, resulting in the creation of clear, visually compelling graphs and figures that effectively communicated key insights to stakeholders.

UC Irvine Department of Chemistry Diversity Fellow

2021-2022

Fellow

- Implemented and organized programs and resources to promote inclusivity and equity, increasing access and support for underrepresented students in the field of science and engineering.
- Represented the department at the University of California Chemical Symposium, American Chemistry Society Conference, and the American Chemistry Society Bridge Program site visit, showcasing the department's commitment to diversity and inclusion.
- Collaborated with other fellows, the Associate Dean of Diversity, Equity, and Inclusion, and the Physical Sciences Access, Outreach, and Inclusion Program Coordinator to advance inclusive excellence within the School of Physical Sciences.

University of California, San Diego –Grassian Research Lab

2016-2018

Undergraduate Student Researcher

- Conducted innovative and impactful experiments investigating the effects of atmospheric conditions on the catalytic oxidation of sulfur in acidic aqueous media, working under the guidance of Professor Vicki H. Grassian.
- Acquired extensive hands-on experience in (but not limited to) mass spectrometry, spectroscopy, and chromatography techniques.
- Effectively communicated research results by presenting at 3 conferences and co-authoring 1 publication.

UC San Diego Sustainability Office

2016-2017

Renewable Energy and Green Technology Ambassador

- Spearheaded student education and community awareness initiatives centered around renewable energy and green technology, utilizing workshops, projects, and social media engagement activities to drive interest and engagement.

- Worked collaboratively with faculty members and administrative staff to better comprehend pressing environmental challenges, including climate change and public/environmental health issues. Fostered productive dialogue and cooperation to identify innovative solutions and drive progress.

UC San Diego Thurgood Marshall College

Fall 2017

Orientation Leader

- Assisted with the planning and execution of orientation events for incoming students, averaging 200 students per session.
- Conducted small group sessions, averaging 15 students each, and campus tours, sharing information about college resources and answering questions about academic programs and campus life.
- Provided guidance and support to new students throughout the orientation process, helping them acclimate to campus culture and build relationships with peers.
- Collaborated with fellow orientation leaders and college staff to ensure a positive and inclusive orientation experience for all participants.

UC San Diego Student Sustainability Collective

2015-2016

Intern

- Led the creation and delivery of educational events for 70 students, focused on critical issues such as water justice, water conservation, and the negative environmental impacts of plastics.
- Played a pivotal role in the design and execution of targeted strategies for the Plastics Water Bottle Ban campaign, an initiative aimed at reducing and eliminating the sale of plastic water bottles at the university. Collaborated effectively with stakeholders from across the institution to ensure the success of this effort.

Los Angeles Conservation Corps

2010-2011

Corpsmember

- Implemented sustainable practices by improving street sanitation, creating parks and community gardens, and restoring natural habitats to build a more sustainable community.
- Educated community members on sustainable practices at local events and engaged with them to promote awareness of environmental issues.
- Contributed to weekly beach and community clean-up efforts to maintain a clean and healthy environment.

TEACHING EXPERIENCE

UC Irvine Department of Chemistry

2018-2023

Teaching Assistant

- Served as a crucial link between professors and students, leveraging strong communication and interpersonal skills to enhance preparedness and engagement. Attended weekly TA meetings and provided targeted support and guidance to students as needed.

- Effectively conveyed complex concepts and theories in chemistry to students, leveraging a range of tools and techniques such as office hours, online discussion boards, emails, and sections. Demonstrated a keen ability to distill technical information into accessible, understandable language that resonated with students of varying skill levels.
- Classes taught include: General Chemistry Plus (2022), Analytical Chemistry Laboratory (Spring 2021), General Chemistry Laboratory (Fall 2018, Spring 2019), General Chemistry Lecture (Winter 2019, Fall 2020, Winter 2021), and Idiom of Science (H90) (Spring 2020)

UC San Diego Office of Academic Support and Instructional Services 2017
Math and Science Facilitator

- Provided vital support for Summer Bridge, a comprehensive transition program aimed at helping underrepresented and first-generation college students refine their academic skills and achieve success. Played an integral role in organizing activities, leveraging strong communication, and organizational skills to ensure the smooth functioning of the program.
- Facilitated weekly discussion sections for a cohort of 13 students, focused on key topics in math, science, and engineering. Created engaging activities and assignments that challenged students to develop their critical thinking, problem solving, and communication skills, while also providing targeted feedback and support to help them succeed.

OUTREACH AND TEACHING

UC Irvine Chemistry Peer Mentoring Program 2019-2023
Founder, Committee Chair, and Mentor

- Established a grad-to-grad mentoring program to assist incoming graduate students in navigating the challenges of graduate school, building a support network, and increasing their confidence and motivation in the program.
- Coordinated with the Department of Chemistry administration to recruit mentors and mentees, and organized quarterly events such as mentoring workshops, panel discussions, welcome socials, and organization mixers.
- Provided peer mentorship to incoming graduate students at UC Irvine, offering guidance and resources as needed.

UC Irvine Iota Sigma Pi 2018-2023
Member and Professional Development Chair

- Volunteered with multiple organizations and schools in Orange County to promote science education for the next generation.
- Collaborated with teachers to develop interactive activities, such as Invisible Ink and Rock Candy experiments, to teach acid-base chemistry and crystallization.
- Organized professional development events, including a NSF GRFP Peer Editing Workshop and LinkedIn Workshop.

UC Irvine Department of Chemistry 2018-2023
Recruitment Lead

- Developed social media content strategy and created compelling photos and videos to showcase the highlights of the department and recruitment weekends.
- Facilitated QA panels, campus tours, and meals for prospective graduate students to enhance their understanding of the department and foster relationships.
- Advocated for student needs and acted as a liaison between prospective students and graduate life services, including health insurance, financial aid, and counseling.

SoCal Undergraduate Research Symposium 2018-2022

Poster Judge

- Evaluated posters and presentations from undergraduate students conducting research in atmospheric chemistry.
- Engaged in discussions with undergraduate students to share my research experience and knowledge of graduate school.

Science Champions 4 Change 2021-2022

Poster Judge

- Provided guidance and resources to community college students to facilitate successful transfers to a university.
- Participated in monthly mentoring meetings to enhance mentoring skills, including effective techniques, active listening, building connections, tailored goal setting, and constructive feedback.

Ridge to Reef Summer Institute for Data Science Summer 2021

Participant

- Completed a 2-week program in Environmental Data Science, gaining expertise in R programming language and applying it to perform question-driven analysis on the data collected during the restoration of West Loma in Orange County.

Science Policy and Advocacy for STEM Scientists Program Summer 2021

Participant

- Completed an 8-week program with a focus on enhancing knowledge and experience with public policy processes and advocacy.
- Course modules include Introduction to Science Policy and Advocacy, Types of Policy, Effective Communication for Policymakers, Transitioning into Policy Careers, Effective Communications for Public Policy and Advocacy, Leveraging Science Policy Training for Industry Careers, and Ways to get Involved at your Local Level.

Mentoring Excellence Program Summer 2019

Participant

- Successfully completed a 6-week program on mentorship, enhancing my skills and resources related to effective mentoring.
- Gained valuable knowledge through program modules including The Lifecycle of the Mentoring Relationship, Effective Interpersonal Communication, Ethical Issues in Academia, Mentoring Across Differences, Resilience Conflict Resolution, and Balancing Academics/Wellness

UC San Diego Sustainability Office 2016-2017

Renewable Energy and Green Technology Ambassador

- Spearheaded student education and community awareness initiatives centered around renewable energy and green technology, utilizing workshops, projects, and social media engagement activities to drive interest and engagement.
- Worked collaboratively with faculty members and administrative staff to better comprehend pressing environmental challenges, including climate change and public/environmental health issues. Fostered productive dialogue and cooperation to identify innovative solutions and drive progress.

UC San Diego Department of Chemistry and Biochemistry

Spring 2017

Volunteer/Assistant

- Organized and facilitated CHEM 1: The Scope of Chemistry and Biochemistry, an undergraduate seminar with an average of 30 students per quarter, aimed at connecting students with the chemistry community and campus resources to support their career success.
- Participated in a student panel to share valuable information about campus resources and my own research experience, supporting students in navigating the demands of college life.
- Volunteered for a video project providing students with an immersive view of a research lab and sharing tips for academic success at UC San Diego.

PUBLICATIONS

Wong, C., Vuong, J., and Nizkorodov, S.A. “Fluorescence changes in biogenic and anthropogenic secondary organic aerosols under acidic aging”, *manuscript 25% completed, expected submission in June 2023*

Wong, C., Pazienza, J.E., Rychnovsky, S.D., and Nizkorodov, S.A. “Formation of chromophores from pinonaldehyde aged in highly acidic conditions”, *manuscript 90% completed, expected submission in May 2023*

Hill, R., Djokic, M.A., Anderson, A., Barbour, K., Guerra, A., Hunt, C., Jolly, A., Manley, K., Montoya, J., Norlen, C., Nugent, A., Washburn, K., Weber, S., Welch, A., Wong, C., and Allison, S. “Training a new generation of scholars: Ridge to Reef increases graduate student readiness to be interdisciplinary and community-based environmental problem solvers”, *manuscript 95% completed, expected submission in May 2023*

Wong, C., Liu, S., and Nizkorodov, S.A. “Highly-acidic conditions drastically alter chemical composition and absorption coefficient of α -pinene secondary organic aerosol” *ACS Earth & Space*, 2022, 6 (12), 2983–2994., DOI: 10.1021/acsearthspacechem.2c00249

Wong, C., Vite, D., and Nizkorodov, S.A. “Stability of α -pinene and d-limonene ozonolysis secondary organic aerosol compounds towards hydrolysis and hydration” *ACS Earth & Space*, 2021, 5, 2555-2564., DOI: 10.1021/acsearthspacechem.1c00171

Wei, J., Fang, T., Wong, C., Lakey, P.S.J., Nizkorodov, S.A., and Shiraiwa, M. “Superoxide formation from aqueous reactions of biogenic secondary organic aerosols” *Environmental Science & Technology*, 2020, 55, 260-270., DOI: 10.1021/acs.est.0c07789

Coddens, E.M., Huang, L., Wong, C., and Grassian, V.H., “Influence of glyoxal on the catalytic oxidation of S(IV) in acidic aqueous media” *ACS Earth & Space*, 2019, 260-270., DOI: 10.1021/acsearthspacechem.8b00168

CONFERENCE PRESENTATIONS

Platform Presentations:

Wong, C. and Nizkorodov, S.A., “Aging of Secondary Organic Aerosols at Atmospherically Relevant Acidities” , American Association for Aerosol Research 39th Annual Conference, October 2-7, 2022, Raleigh, NC

Wong, C., Liu, S., and Nizkorodov, S.A., “Long term aging of secondary organic aerosols under acidic conditions” , American Chemical Society Spring 2022 Meeting, March 20-24, 2021, San Diego, CA

Wong, C., Liu, S., and Nizkorodov, S.A., “Acidic-catalyzed aging of secondary organic aerosols” , American Association for Aerosol Research 39th Annual Conference, October 18-22, 2021, Virtual Conference

Wong, C., Coddens, E.M., Huang, L., and Grassian, V.H., “The Role of Inorganic and Organic Sulfur Oxidation in the Atmosphere” , Undergraduate Research Conference (URC), May 5, 2018, La Jolla, CA

Wong, C., Zhang, Y., Coddens, E.M., and Grassian, V.H., “Influence of temperature, light and pH on the dissolution of transitional metal ions in Arizona test dust” , Southern California Conference for Undergraduate Research, November 12, 2016, Riverside, CA

Poster Presentations:

Wong, C., Vite, D., Liu, S., and Nizkorodov, S.A. “Impact of water and sulfuric acid on the chemical composition and long-term aging of SOA” , The International Chemical Congress of Pacific Basin Societies (Pacifichem), December 16-21, 2021, Online Conference

Wong, C., Vite, D., and Nizkorodov, S.A. “Long-term aging of secondary organic aerosols in the presence of liquid water and water vapor” , American Association for Aerosol Research 38th Annual Conference, October 5-9, 2020, Virtual Conference

Wong, C., Fleming, L. T., Montoya-Aguilera, J. and S.A Nizkorodov, “Let’ s clear the air: water changes what we breathe” , 3rd Annual Environmental Research Symposium,

December 4, 2019, Irvine, CA

Wong, C., Fleming, L. T., Montoya-Aguilera, J. and S.A Nizkorodov, “Effects of relative humidity and aerosol liquid water on the molecular composition and aging of secondary organic aerosols” , American Association for Aerosol Research 37th Annual Conference, October 14-18, 2019, Portland, OR

Wong, C., Coddens, E.M., Huang, L., and Grassian, V.H., “Multiphase Reactions of Sulfur Oxidation and the Influence of Iron and Organics” , ACSSA-sponsored Undergraduate Research Symposium, May 17, 2018, La Jolla, CA

SKILLS

Instrumentation

Electrospray Ionization High-Resolution Mass Spectrometry, Direct Analysis in Real-Time Mass Spectrometry, Ultra-Performance Liquid Chromatography, UV-Vis Spectroscopy, Fluorescence Spectroscopy, Attenuated Total Reflectance - Fourier Transform Infrared Spectroscopy, Inductively Coupled Plasma Mass Spectrometry, Ion Chromatography

Software

Igor Pro, R Studio, Tableau, Microsoft Office, Xcalibur/Freestyle, MZMine, LabVIEW

ABSTRACT OF THE DISSERTATION

Analyzing the Long-Term Aging of Secondary Organic Aerosols and the Impacts of Acidity

By

Cynthia Wong

Doctor of Philosophy in Chemistry

University of California, Irvine, 2023

Professor Sergey A. Nizkorodov, Chair

Atmospheric aerosols, including secondary organic aerosols (SOA), are ubiquitous constituents in the atmosphere. During their transport over hundreds of kilometers from their sources, aerosols can undergo a variety of chemical and physical changes depending on the atmospheric conditions and interactions with other compounds, which is known as chemical aging. The SOA formation and aging processes—including the influence of acids on these processes—are the leading sources of uncertainty in aerosol radiative forcing in global climate models. The main objective of this thesis is to explore the influence of sulfuric acid on the chemical composition and optical properties of organic aerosols. This is achieved through laboratory studies that offer a detailed molecular-level understanding of the interactions between monoterpene oxidation products and inorganic compounds like sulfuric acid (H_2SO_4). Exploring the chemical reactions between organic aerosols and acids is crucial for understanding the evolution of SOA in the atmosphere.

The effect of water vapor and aerosol liquid water on the molecular composition of SOA derived from biogenic volatile organic compounds was studied to understand the chemical changes that can occur in SOA particles in the absence of sulfuric acid. SOA was generated and then aged by dissolving it in liquid water and keeping it in solution for 1-2 days or exposing it to water vapor for 1-2 weeks. The composition was monitored with mass spec-

trometry, and patterns of peak intensities and observed molecular formula were examined for evidence of water-mediated chemistry in the dark. The presence of water led to changes in the chemical composition of these particles, but the extent of these changes was small, suggesting that hydrolysis and hydration is not a major aging mechanism for atmospheric aerosols.

The second project discussed in this thesis tested the effect of sulfuric acid on the chemical composition and optical properties of α -pinene SOA. α -Pinene SOA was formed in an oxidative flow reactor and then aged in aqueous solutions containing various concentrations of H_2SO_4 . Composition changes were analyzed using mass spectrometry, while optical properties were studied using UV-Vis and fluorescence spectroscopy. This study found that SOA aged in moderately (pH 0 to 4) acidic conditions experienced relatively small changes in composition, while SOA aged in a highly (pH -1 to 0) acidic environment experienced more dramatic changes in composition. The aged SOA had compounds containing sulfur (accounting for 30% of the relative sample), as well as light-absorbing and fluorescent compounds. The findings in this study demonstrated that concentrated sulfuric acid plays a crucial role in the chemical composition and optical properties of aerosols in regions where high concentrations of H_2SO_4 persist, such as the upper troposphere and lower stratosphere.

To gain improved mechanistic understanding of the SOA acid-aging processes, two common monoterpene oxidation products from α -pinene, *cis*-pinonic acid and *cis*-pinoaldehyde, were then aged in highly concentrated sulfuric acid. All resulting reactions were analyzed using UV-Vis spectroscopy, high resolution mass spectrometry, and nuclear magnetic resonance spectroscopy to identify the products formed. Under highly concentrated sulfuric acid, it was found that *cis*-pinonic acid forms homoterpenyl methyl ketone, while *cis*-pinonaldehyde forms two regioisomers of 1-(4-isopropylcyclopenta-1,3-dien-1-yl)ethan-1-one.

The effect of highly concentrated sulfuric acid on the fluorescent properties of SOA from volatile organic compounds of anthropogenic and biogenic origin was investigated in the last study of this thesis. SOA was created with different combinations of oxidants and VOC precursors, followed by the analysis of absorption and fluorescence. The appearance of strongly light-absorbing and fluorescent compounds at $\text{pH} = \sim -1$ confirms that sulfuric acid is a major driver of SOA aging. The aged SOA from biogenic precursors (d-limonene and α -pinene) resulted in stronger fluorescence than aged SOA from anthropogenic toluene and xylene. The absorption spectra of aged SOA from biogenic precursors changed drastically in shape upon dilution, whereas the shapes of the fluorescence spectra remained the same, suggesting that fluorophores and chromophores in SOA are separate sets of species. Additionally, the fluorescence spectra of aged SOA and primary biological aerosol particles exhibited significant overlap, indicating that when subjected to highly concentrated sulfuric acid environments, aged SOA may be mistakenly identified as primary biological aerosol particles using fluorescence-based techniques.

SOA can exist under a range of acidities, providing a range of acid-catalyzed and acid-driven reactions. This thesis demonstrates that sulfuric acid is a strong driver in aging mechanisms for biogenic and anthropogenic SOA. By integrating these laboratory studies along with future field measurements and model predictions, informed decisions can be made to tackle the environmental issues associated with air quality and climate change.

Chapter 1

Introduction

1.1 General Atmosphere Information

Earth's atmosphere is essential to sustaining life as it provides key nutrients for living organisms. The atmosphere comprises 78% nitrogen (N_2), 21% oxygen (O_2), 0.9% argon (Ar), and 0.1% other trace gases, which includes water vapor.^{1,2} In addition to gases, the atmosphere contains particles that are naturally occurring and manmade. The understanding of these gases and particles, as well as their interactions, is crucial as their processes heavily influence different ecosystems on Earth.²⁻⁵

The Earth's atmosphere comprises of a series of layers, each with their own unique attributes. The closest part of the atmosphere to ground level is the troposphere, which spans up to 7-15 kilometers from the surface. The temperature, pressure, and density of air in this layer typically decreases with altitude. The troposphere is characterized by its strong vertical mixing and contains 75-80% of the mass of the atmosphere.⁶ Due to the complexity of this layer, the troposphere is heavily studied by many researchers. The second lowest layer

of the atmosphere is the stratosphere, separated from the troposphere by the tropopause, and marked by a temperature inversion.⁶ The stratosphere is notably known as the home to the ozone layer, which absorbs harmful UV radiation, protecting all living things, including humans and animals.^{1,2} The reactions that govern the ozone layer cause the temperature of the stratosphere to increase with altitude. This layer contains 10% of the air mass of the Earth, and contains significant amounts of sulfuric acid, H_2SO_4 , and organic compounds. Due to injection of SO_2 from volcanic eruptions and the long residence time, the stratosphere has been known to be very acidic, resulting in stratospheric aerosols that can contain 40-80 wt% H_2SO_4 .^{2-4,7-10} Although the mesosphere, thermosphere, and exosphere are additional layers in the atmosphere, the topics discussed in this thesis are primarily relevant to the troposphere and stratosphere.

1.2 Atmospheric Aerosols

Atmospheric aerosols are solid or liquid particles suspended in air. They can affect climate through their direct and indirect interactions with solar radiation. Aerosol particles can directly absorb and scatter solar radiation, altering the global radiative balance. Additionally, aerosols can act as cloud condensation and ice nuclei, resulting in changes in the microphysical and optical properties of cloud droplets. This alteration affects cloud albedo, droplet and particle number, as well as cloud size, impacting the radiation budget.

Aerosol particles have a wide size distribution, with the smallest particles being a few nanometers and the largest particles having a diameter (D_p) of over 10 microns. The particle size distribution can be defined by four distinct modes: nucleation mode ($D_p < 0.01 \mu\text{m}$), Aitken mode ($0.01 \mu\text{m} < D_p < 0.1 \mu\text{m}$), accumulation mode ($0.1 \mu\text{m} < D_p < 1 \mu\text{m}$), and coarse mode ($D_p > 1 \mu\text{m}$).^{1,2,11,12} Aerosol particle sizes can change due to a variety of processes, in-

cluding condensation, coagulation, fragmentation, evaporation, and abrasion.^{12,13} However, for air quality regulatory purposes, aerosol particles are categorized into either PM 2.5 or PM 10, which describes particle diameters that are 2.5 microns or less and 10 microns or less, respectively. These classifications allow for regulatory agencies to offer effective protection from the detrimental health effects of particulate matter, which are dependent on their size.

In addition to reduced visibility and negative impacts on ecosystems, aerosols can also contribute to adverse health effects. Epidemiological studies have shown that once inhaled, they can deposit into the parts of the respiratory system and blood stream. Depending on their size, aerosol particles can cause premature mortality and a variety of cardio-respiratory illnesses, including asthma, bronchitis, and inflammation and irritation in the respiratory track.^{14,15} Long term exposure to aerosol particles can have even more harmful health effects as it can worsen neurological diseases and cross the blood-brain barrier.^{14,15} However, in addition to concentration and duration of exposure, the extent and severity of which aerosol particles can influence health effects is in large part due to the composition, which will be addressed in greater detail in the following sections.

1.2.1 Aerosol Life Cycle

Aerosols result from both natural and anthropogenic sources. Primary aerosols are directly emitted into the atmosphere. Examples of primary aerosols include sea spray, release of soil and rock debris, biological aerosols, biomass burning smoke, and volcanic debris. They tend to be larger in size in comparison to secondary aerosols. Secondary aerosols are formed because of gas-to-particle conversion processes, such as gases condensing in and on to existing particles and gases reacting with each other and leading to the formation of new particles. Studies have also shown that secondary aerosols can be formed through cloud processing.¹⁶ Due to the variability of sources and formation mechanisms, extensive research has been

conducted on primary and secondary aerosols to understand their fate in the atmosphere.

Once emitted or formed, aerosol particles can reside in the atmosphere from hours to weeks, depending on their size and vertical distributions. Primary aerosols are relatively large (with diameters $>1\ \mu\text{m}$) and have short lifetimes, typically hours to days, mainly due to faster gravitational settling.¹⁷⁻¹⁹ On the other hand, because secondary aerosols are formed through new particle formation followed by condensation, they can be a few nanometers to $1\ \mu\text{m}$ in diameter. The lifetime of the smallest secondary aerosols is relatively short due to their diffusivity; however, larger secondary aerosols can reside in the atmosphere for several days to weeks.¹⁷⁻¹⁹ During their lifetimes, aerosols particles can be transported hundreds of kilometers from their source and can undergo a variety of chemical and physical changes depending on the environmental conditions, which is often referred to as “aging” (e.g., aging via exposure to acids, water, UV radiation, etc.).²⁰ Additionally, the lifetime of these particles can vary depending on which atmospheric layer they are present in. Aerosols present in the upper troposphere and the lower stratosphere have longer (days to years) lifetimes as compared to the lower troposphere (i.e., below the planetary boundary layer) because the removal mechanisms for particles at higher altitudes are inefficient.²¹

There are two types of deposition processes by which aerosols are removed from the atmosphere. Wet deposition removes particles via precipitation or in cloud processes such as through rain, snow, or cloud and fog droplets. On the other hand, dry deposition is the direct uptake of particles to surfaces (e.g., soil, water, and vegetation) following gravitational settling. Typically, smaller particles are removed via wet deposition while larger particles are expelled from the atmosphere by either dry or wet deposition.^{1,2,17}

1.2.2 Volatile Organic Compounds and Secondary Organic Aerosol Formation

Organic compounds account for a dominant fraction of aerosol mass in the lower troposphere. Primary organic aerosols are directly emitted, whereas secondary organic aerosols (SOA) are produced from atmospheric reactions involving volatile organic compounds (VOCs), which are emitted from natural and anthropogenic sources such as vegetation and motor vehicles, respectively.²² These reactions include the gas-phase oxidation of VOCs followed by condensation, heterogeneous oxidation of VOCs on particle surfaces, and aqueous processing in cloud or fog droplets.^{16,22} Due to the large variability of sources, chemical constituents, and transformations, SOA formation and aging processes are the leading source of uncertainty in aerosol radiative forcing in global climate models.²³ However, characterization of these compounds presents a major challenge in laboratory experiments and models.

1.2.3 Secondary Organic Aerosol Composition and Complexity

Due to the influence of various atmospheric factors and chemical diversity in the atmosphere, the chemical composition of secondary organic aerosols is highly complex.²² Depending on the precursors and conditions involved in their formation, SOA can exhibit varying degrees of physical and chemical properties, including viscosity, hygroscopicity, and light absorption. Consequently, the composition of SOA plays a crucial role in determining the extent to which aerosols can affect climate, health, visibility, and air quality.

The composition of secondary organic aerosols is significantly impacted by the chemical diversity of precursors in the atmosphere. VOCs such as α -pinene and isoprene originate from biogenic sources, while VOCs such as toluene and naphthalene come from anthropogenic sources. After being emitted, VOCs can undergo oxidation via hydroxyl radical ($\bullet\text{OH}$),

ozone (O_3), or nitrate radical ($\bullet NO_3$). These oxidation pathways result in compounds with oxygen (sometimes also nitrogen and sulfur) containing functional groups, such as carbonyl, carboxyl, and hydroxyl groups. In many cases, multiple oxygen-containing functional groups are needed to reduce vapor pressures, increase solubility, and partition into existing particles or nucleate new particles. Thus, VOC oxidation can result in a range of multi-functional products.

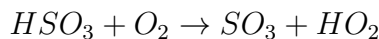
SOA complexity is also heavily influenced by the other atmospheric conditions, such as the presence of additional gases and pre-existing particles, temperature, relative humidity and aerosol liquid water, and particle acidity. During the formation of SOA in the presence of NO_x , yields are dependent on the presence of water. Studies have shown that the presence of NO_x could reduce SOA yields while others have noted the in the presence of water, SOA yields can be enhanced, depending on VOC precursors.²⁴⁻²⁹ Also, under high NO_x conditions, there can be a suppression of new particle formation and an increased likelihood of the formation of organonitrates.^{30,31} Previous studies have shown that introducing inorganic particles can enhance SOA formation due to its increased acidity and can impact phase state of aerosol particles.³²⁻³⁶ SOA formation at low temperatures can change the chemical makeup by increasing yields due to the low volatility environment, and therefore changing properties like refractive indices.³⁷⁻³⁹ The presence of water can also impact SOA production by increasing yields when SOA is formed in the presence of deliquesced seeds or by acting as medium for aqueous SOA formation.^{16,40,41}

After SOA are formed, these particles undergo a variety of aging processes depending on the environmental conditions (e.g., changes in acidity) during atmospheric transport.²⁰ As SOA particles age, they can undergo both physical and chemical transformations, including water uptake or loss, phase transitions, gas-to-particle partitioning, photolysis, hydrolysis,

and formation of salts.⁴²⁻⁴⁶ As they are of particular interest to this thesis, SOA and acidity will be discussed in more depth in the following section.

1.3 Acidity of Aerosols

The acidity of atmospheric aqueous phase (i.e., aerosol particles, cloud droplets, and fog droplets) is a crucial factor that can influence physical and chemical processes, and therefore impact human health, climate, and various ecosystems.^{47,48} SO₂ and NO₂ are the primary sources of acidity in the atmosphere over the polluted continental locations. Equations (1) and (2) show how the oxidation of these gases can produce strong acids.



There is a wide range of acidity in the atmosphere, evident in Figure 1.1. Cloud and fog droplets can have pH values ranging from 2 to 7, while aerosol particles tend to be more acidic and have a wider range, with pH values from -1 to 8.⁴⁸⁻⁵⁶ This property is dependent on their source, chemical composition, and ambient relative humidity, as shown in Figure 1.1. For example, sea spray and dust aerosols, the two largest natural emissions by mass, tend to be less acidic, with pH values from pH 3 to 8, due to the presence of nonvolatile cations and carbonates. These carbonates can react with acidic gases that partition into the particle and form salt, gaseous CO₂ and water.⁵⁷ On the other hand, sulfate-organic aerosols are quite acidic and can have a pH -1 to 5 because they typically contain organic

acids and sulfuric acid. The acidity of the aqueous phase in the atmosphere can also fluctuate due to uptake of anthropogenic emissions. Generally, sulfur dioxide (SO_2), nitrogen oxides (NO_x), and organic acids tend to increase acidity while ammonia (NH_3), nonvolatile cations, and amines are known to decrease acidity. While the partitioning of semi-volatile acidic and basic trace gases and water content can largely affect the acidity of aerosol particles, the acidity in turn affects the chemical reactions and kinetic rates within the particles.

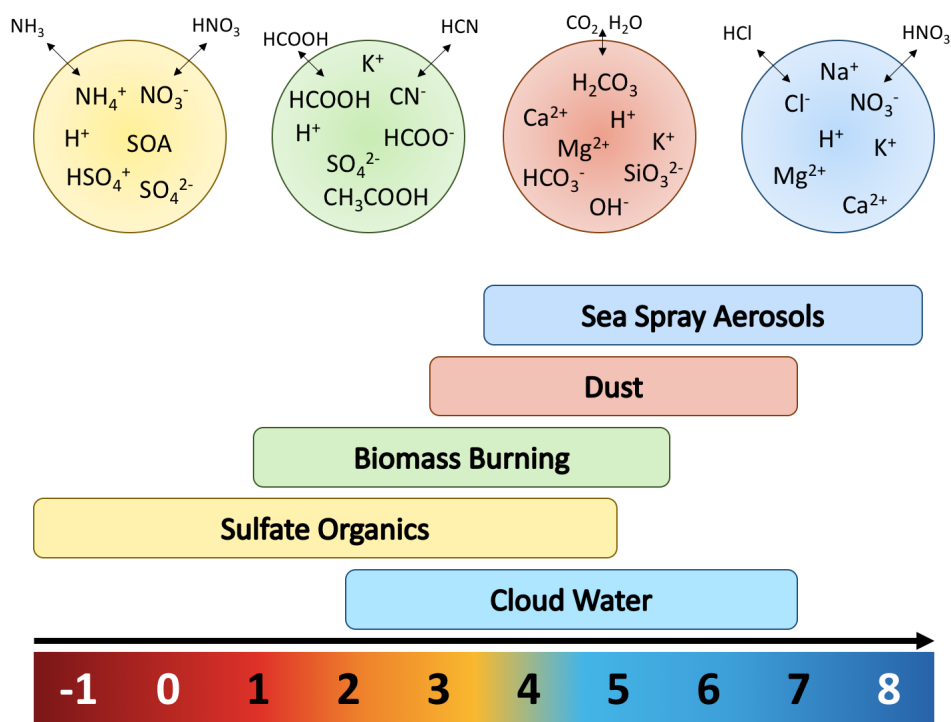


Figure 1.1: Acidity of different aerosols and cloud water in the atmosphere (Adapted from Pye et al. 2020)⁴⁷

Meteorology, changes in emissions, and particle composition can drive the variability of acidity in the atmosphere. In the summer, aerosols particles tend to be more acidic than in the winter due to availability of liquid water and variations in temperature. In general, increasing temperature and decreasing relative humidity can result in an increase in the acid-

ity of aerosols. This seasonal trend has been observed in several regions such as in United States,^{49,50} Beijing,⁵¹ Mongolia,⁵² Hong Kong,⁵³ Italy,⁵⁴ Netherlands,⁵⁵ and Canada.⁵⁶ Studies have also shown that diurnal trend in particle acidity can depend on water content and temperatures, with aerosol particles being more acidic during the day when water content is low, and temperatures are high.^{49,58-61} Different regions around the world have exhibited varying levels of acidity. For example, aerosol particles observed in Hawaii, United States and São Paulo, Brazil tend to have pH ranging between 4 to 5.^{62,63} This is likely because of the presence of non-volatile cations and nitrates from sea salts and combustion sources, which can make the particles less acidic. Moderately acidic particles (pH 2-3) have been observed Mainland China, Europe, Canada, Mexico, and the western United States.^{54-56,64-69} Highly acidic aerosols have been reported in Southeastern Asia, the eastern United States, China, and other locations, likely due to the high emissions of SO₂.^{49,55,58,61} The stratosphere has been known to be very acidic, resulting in stratospheric aerosols that can contain 40-80 wt% H₂SO₄ due to injection of SO₂ from volcanic eruptions and fewer sources of bases.^{2-4,7-10}

1.3.1 Effect of Acids on SOA Formation and Aging

Acids can play a crucial role in many chemical reactions of organic compounds, including those found in the SOA, in the atmosphere. These chemical reactions can either be acid-catalyzed or acid-driven, with the difference being that in the latter the protons from the acid are incorporated into the products formed. For instance, the formation of hemiacetal and acetal are dependent on acidic conditions. Such reactions are significant in aqueous SOA formation from carbonyl compounds such as glyoxal and methylglyoxal.⁷⁰⁻⁷⁵ The hydration of complex aldehydes, ketones and carbonyls are known to accelerate the conversion of carbonyl groups into gen-diols by the presence of acids.⁷³⁻⁷⁵ The pH sensitivity of aldol condensation is largely due to the acid catalyzed nature of the enol formation and the role of the protonated carbonyl, where studies have shown that this reaction can occur in both strongly acidic

and less conditions.⁷⁶⁻⁸⁰ Increasing the acidity can also increase the rate of esterification as the carboxyl group needs to be protonated to form a carbocation before a nucleophilic attack by an alcohol.⁸¹⁻⁸⁴ Acids can also facilitate nucleophilic addition through epoxide protonation from isoprene and monoterpene, which can lead to organosulfate formation.⁸⁵⁻⁸⁸ Therefore, understanding the effects of acidity on these organic reactions, among others, is essential to assess their impacts in multiphase models. The effects of acidity on SOA formation have also been extensively investigated. Chamber studies have shown enhanced production of SOA in the presence of acidic seed particles and can probe changes in organic aerosol chemical properties such as mass yields, oxidation state, and composition, including the formation of larger oligomers, organosulfates, and light-absorbing compounds.^{24,35,39,89-95} The reactive uptake was observed for various individual products of oxidation of biogenic VOCs onto acidified particles.^{77,87,96-98} Previous work has also focused on the reactive uptake of aldehydes and ketones into sulfuric acid solutions and particles, mimicking stratospheric aerosols.^{5,76,78,79,99} These studies have highlighted the importance of acid-catalyzed processes during SOA formation, however there is still limited understanding of role of acids in the chemical aging of organic aerosols occurring over longer timescales.

1.4 Goals of the Thesis

The acidity of aerosols is an important property that plays a crucial role in the physical and chemical processes in the atmosphere. Despite the growing literature in aerosol acidity and the advances in understanding acid-driven and acid-catalyzed chemical mechanisms in aerosol particles, there is still a large uncertainty pertaining to the role of acidity. The overarching goal of this thesis is to explore the influence of acidity, specifically sulfuric acid, on the chemical composition and optical properties of organic aerosols. The relevant background for each project will be described in depth at the beginning of each corresponding

chapter. A brief overview of the goals of each chapter is provided below.

Chapter 2 analyzes the effect of water vapor and aerosol liquid water on the molecular composition of biogenic monoterpene SOA. This work is considered a control, as it is important to understand what happens in the absence of acidity to fully comprehend its effects. SOA was generated and then aged in liquid water or water vapor and the composition was monitored with mass spectrometry. Water led to changes in the chemical composition of these aerosol particles, but the extent of these changes was small, suggesting that hydrolysis and hydration is not a major aging mechanism.

Chapter 3 explores the effect of sulfuric acid on the chemical composition and optical properties of α -pinene secondary organic aerosol. SOA was formed and then aged in various aqueous solutions of H_2SO_4 . Composition changes were analyzed using mass spectrometry, while optical properties were studied using UV-Vis and fluorescence spectroscopy. This study found that concentrated sulfuric acid is a major driver of SOA aging, resulting in a large change in the chemical composition and optical properties of aerosols in regions where high concentrations of H_2SO_4 persist (e.g., upper troposphere and lower stratosphere).

Chapter 4 identifies the mechanism and compound(s) responsible for the chromophores in Chapter 3. We aged two common monoterpene oxidation products from α -pinene, *cis*-pinonic acid and *cis*-pinoaldehyde, in highly concentrated sulfuric acid conditions. Samples were analyzed by a variety of instruments including, UV-Vis spectroscopy, HPLC-PDA-HRMS and NMR spectroscopy. It was found that under highly sulfuric acid conditions, *cis*-pinonic acid forms homoterpenyl methyl ketone and *cis*-pinonaldehyde forms 1-(4-(propan-2-ylidene)cyclopent-1-en-1-yl)ethan-1-one and two regioisomers of 1-(4-isopropylcyclopenta-1,3-dien-1-yl)ethan-1-one

Finally, Chapter 5 investigates the effect of sulfuric acid on the fluorescent properties of anthropogenic and biogenic SOA. SOA was created with different combinations of oxidants and VOC precursors, followed by the analysis of fluorescence properties. It was found that there was formation of strongly light-absorbing and fluorescent compounds at $\text{pH} = \sim -1$ suggesting that sulfuric acid is a strong driver of SOA aging.

The thesis aims to mitigate the uncertainty surrounding the chemical impacts of particle acidity in the atmosphere. The laboratory studies presented here provide a molecular level understanding of the synergistic interactions between monoterpene oxidation products and other inorganic compounds, such as H_2SO_4 . By integrating these laboratory studies along with future field measurements and model predictions, informed decisions can be made to tackle the environmental issues associated with air quality and climate change.

Chapter 2

Stability of α -Pinene and D-Limonene Ozonolysis Secondary Organic Aerosol Compounds Toward Hydrolysis and Hydration

Reprinted with permission from Wong, C.; Vite, D.; Nizkorodov, S.A., Stability of α -Pinene and D-Limonene Ozonolysis Secondary Organic Aerosol Compounds Toward Hydrolysis and Hydration, *American Chemical Society Earth and Space Chemistry*, **2021**, *5*, 2555-2564, <https://doi/10.1021/acsearthspacechem.2c00249>. Copyright 2021 American Chemical Society.

2.1 Abstract

Secondary organic aerosol (SOA), formed through the gas-phase oxidation of volatile organic compounds (VOCs), can reside in the atmosphere for several days and sometimes for weeks. The formation of SOA takes place rapidly, often within hours after VOC emissions, and SOA can then undergo much slower physical and chemical processes throughout its lifetime in the atmosphere. Water, in the form of water vapor, aerosol liquid water, and cloud and fog water, can strongly impact the composition of SOA by altering formation and short-term aging mechanisms; however, less is known about how water impacts long-term SOA aging. The goal of this work is to systematically explore the effects of water on the chemical composition of α -pinene and d-limonene SOA during long-term aging processes. SOA samples were generated in an oxidation flow reactor and collected on foil substrates. Samples were aged in the presence of water vapor at 97% relative humidity for 7-14 days or an aqueous solution for 1-2 days, then analyzed with direct infusion electrospray ionization high resolution mass spectrometry to gain insight into the chemical composition of SOA before and after aging. The patterns of peak intensities and observed molecular formulas were examined for evidence of water-driven chemistry. We found that chemical composition of the SOA did change during long-term exposure to water vapor and liquid water, but the extent of the change was surprisingly small. This indicates that the exposure to water is not a strong driver of long-term aging processes compared to other mechanisms of aging for the monoterpene SOA studied.

2.2 Introduction

Atmospheric aerosols are solid or liquid particles suspended in air that affect climate through their interactions with solar radiation and their ability to change cloud albedo. They scatter

and absorb solar radiation, diminishing visibility, and also contribute to adverse health effects as aerosol particles are small enough to penetrate deep into the lungs and other organs, causing a variety of cardio-respiratory illnesses.^{15,20} These effects are experienced on local, regional, and global scales because aerosols persist long enough to be transported hundreds of kilometers from their source.²⁰

Organic aerosols account for a dominant fraction of aerosols in the lower troposphere, with significant implications on the energy budget of the Earth and human health.²² Primary organic aerosols are directly emitted, whereas secondary organic aerosols (SOA) are formed through chemical reactions in the atmosphere involving volatile organic compounds (VOCs), which are emitted from both biogenic and anthropogenic sources.²² These reactions include the gas-phase oxidation of VOCs followed by condensation, heterogeneous oxidation of VOC oxidation products on particle surfaces, and aqueous processing in cloud or fog droplets. Atmospheric residence time for SOA can vary from minutes to weeks,¹⁹ and during this time various physical and chemical changes can occur within the particle depending on the environmental conditions.¹⁰⁰ Due to the large variability of sources, chemical constituents, and transformations, SOA formation and aging processes are one of the leading sources of uncertainty in aerosol radiative forcing in global climate models, making them one of the least understood components of atmospheric aerosols.¹⁰¹

In the atmosphere, SOA are exposed to different forms of water including water vapor, organic-phase water, aerosol liquid water, and cloud and fog droplets, which can promote reactions and result in changes in chemical composition, vapor pressure, and solubility.¹⁶ The amount of water aerosols can interact with varies in atmosphere, in which water can either act as solvent or a solute. While cloud and fog droplets typically contain liquid water with low amounts of solutes and dispersed insoluble particles, the state of water in aerosols is dependent on the relative amount of organic and inorganic compounds. Under dry con-

ditions, water is present as a thin film on particle surfaces. At higher relative humidity (typically greater than 80%), particles with soluble organics and inorganics contain concentrated aqueous solutions of inorganics and may also contain water molecules dispersed in the organics phase. For example, ammonium sulfate particles coated with SOA are known to phase separate into a deliquesced ammonium sulfate core and organic-rich shell containing water.³²

Hydrolysis, in which a water molecule is used to break a chemical bond, is one of the most common reactions that can occur in the presence of water. The hydrolysis of single bonds can result in fragmentation of larger compounds into smaller molecules.^{87,97,102,103} These compounds can lead to an increase in SOA volatility, decrease in SOA solubility, and may lead to the loss of material from organic particles by evaporation. Conversely, the hydration of compounds containing a double bond, such as carbonyls, can result in the addition of hydroxyl group and/or lead to oligomers with higher-molecular weights and lower volatility through hydrolysis, and thus do not readily evaporate from the particles.^{70,104,105}

Hydrolysis and hydration of several classes of SOA compounds has been studied from the perspective of atmospheric chemistry over the last few years. Epoxides undergo hydration, which can be catalyzed by ammonium ions and acids, leading to compounds with lower volatility and higher solubility.^{87,97,102,103} Diacyl peroxides, formed through the gas-phase $\text{RO}_2 + \text{RO}_2$ reactions, have been shown to hydrolyze in humid conditions and contribute to the formation of carboxyl and ester groups.¹⁰⁶ α -acyloxyalkyl hydroperoxides, a class of ester hydroperoxides formed through the reaction between organic acids and stabilized Criegee intermediates, were shown to undergo rapid hydrolysis in the aqueous phase.¹⁰⁷ Atmospherically relevant anhydrides can undergo hydration. For example, phthalic anhydride was found to be taken up into the particle phase and then add water to form phthalic acid.¹⁰⁸ Nucleophilic reactions can occur during the hydrolysis of lactones, resulting in ring open-

ing products.^{109,110} There have been numerous studies on organonitrates, which have been shown to hydrolyze in humid conditions, especially in the presence of acids.^{111–117} Dicarboxylic acids, such as glyoxal and methylglyoxal, can easily partition into the aqueous phase and undergo hydration, resulting in oligomer formation.^{70,104,105} Oxaloacetic acid has been shown to decarboxylate with a lifetime of 5 hours in pure water and 1 hour in ammonium sulfate aerosols.¹¹⁸ However, not all potentially hydrolysable compounds undergo hydrolysis due to kinetic limitations. For example, levoglucosan, a molecular marker for biomass combustion, can be hydrolyzed by acid catalysis to form α -D-glucose. However, levoglucosan was found to be stable with respect to hydrolysis and did not degrade over a period of 10 days.¹¹⁹

The work cited above focused on the hydrolysis and hydration of model organic compounds in the presence of atmospherically relevant acids and salts at varying pH levels. Systematic experiments on simultaneous hydrolysis and hydration of complex mixtures of compounds present in SOA have not been carried out. Previous studies of aqueous photochemistry of SOA suggested that hydrolysis of SOA compounds may occur even in the absence of catalysts,^{120–122} but studying the hydrolysis was not the primary objective of those studies. In some cases, SOA compounds appeared to decay slowly in dark conditions. However, these experiments only lasted a few hours whereas the lifetime of aerosols can be up to days and weeks.¹²¹ Additionally, understanding the chemical processes, or the lack thereof, that can occur during aging could potentially simplify future experiments. For example, the stability of SOA compounds would indicate that experimentalists can still garner reliable results even if samples were not immediately analyzed, or changes in the composition of SOA would suggest that results may be skewed if the sample was left out for a long period of time. The goal of this work is to explore the effects of water vapor and liquid water on the chemical composition of SOA compounds from the ozonolysis of monoterpenes during long-term aging processes. Based on previous results,^{120–122} we hypothesize that the composition of SOA will significantly change upon aging in water vapor and liquid water for extended period of time

(1-2 weeks and 1-2 days, respectively). Evidence of water driven chemistry was determined by monitoring changes in peak patterns and molecular formulas of lab-generated SOA before and after aging using electrospray ionization mass spectrometry (ESI-MS). This study focuses on lab generated particles and do not contain other constituents such as inorganic species. Therefore, the findings presented in this study pertains to mostly in remote locations. Our results suggest that SOA from the ozonolysis of monoterpenes remain relatively stable with respect to hydrolysis and hydration, indicating that this process is not the main aging mechanism of SOA.

2.3 Materials and Methods

2.3.1 SOA Generation

SOA samples from α -pinene and d-limonene ozonolysis were produced in a ~ 20 L continuous flow reactor under dry and dark conditions. Prior to each experiment, the reactor was purged with zero air (Parker 75-62 purge gas generator). Ozone was introduced into the reactor by flowing pure oxygen through a commercial ozone generator (OzoneTech OZ2SS-SS) at 0.5 SLM (standard liters per minute). Pure liquid α -pinene or d-limonene was evaporated into ~ 5 SLM flow of zero air using a syringe pump at a constant rate of $\sim 2 \mu\text{L min}^{-1}$. The estimated initial mixing ratios of ozone and VOC were 10 ppm and 60 ppm, respectively, so the reaction was oxidant limited. High concentrations of precursor and oxidant were used to generate enough SOA material, typically in the milligram range, for the analysis described below. Under the ozone-limited conditions, the oxidation for endocyclic double bond in d-limonene is favored, and the exocyclic double bond may survive the oxidation.¹²³ Previous studies have found that different initial concentrations of VOC and oxidant lead to different yields and ROS profiles and intensities,^{124,125} so the conclusions of this paper should only

be applied to underoxidized conditions of SOA formation. SOA was collected onto a foil substrate on Stage 7 (0.32-0.56 μm) of a micro-orifice uniform deposit impactor (MOUDI, model 110R) at a flow rate of ~ 30 SLM (5.5 SLM from the flow tube + 25 SLM make-up air) to create a uniform deposition of particles on the substrate.

2.3.2 Aging by Exposure to Water Vapor followed by Low-Resolution Mass Spectrometry Analysis

A list of experiments done to understand SOA aging by exposure to water vapor is outlined in Table 2.1. The first series of experiments was done by exposing SOA to humidified air for a prolonged period of time. A saturated slurry of K_2SO_4 (6 g salt and 50 mL of water) was prepared and added to a glass jar, serving as the relative humidity (RH) aging chamber. A segment of the foil substrate was placed on a petri dish floating on top of the saturated solution to expose the SOA sample to humid conditions, while the remaining substrate was kept frozen as a control. Based on the saturation vapor pressure of K_2SO_4 , the headspace was maintained at 97.3 ± 0.45 % RH.¹²⁶ The RH aging chamber was sealed with a ParafilmTM M film and wrapped in foil to block light exposure and left undisturbed for 1-2 weeks. The foil substrate was then removed from the aging chamber and frozen until analyzed by mass spectrometry.

SOA aged by water vapor was analyzed using a Xevo TQS quadrupole mass spectrometer with an ESI source in negative ion mode. The mass spectrometer was operated using the following parameters: source cone voltage, 50 V; cone gas flow, 150 L/h; capillary voltage, 2.21 kV; source temperature, 120 $^\circ\text{C}$; desolvation temperature, 500 $^\circ\text{C}$; desolvation gas flow 1000 L/hr. Samples were extracted using a 1:1 mixture of water and acetonitrile, placed on a shaker for ~ 10 min, and then injected into the ESI-MS by direct infusion. All samples described were in their respective solvent for up to 3 hours between extraction and analysis.

Table 2.1: Aging Experiments Summary. APIN/O₃ and LIM/O₃ refer to SOA made by ozonolysis of α -pinene and d-limonene, respectively. “Humid Air” refers to samples that were aged in a relative humidity (RH 97%) aging chamber, while “Dry Air” refers to samples that were aged in a desiccator (RH <2%). “Liquid Water” and “Acetonitrile” correspond to samples that were extracted using the respective solvent and then aged. Dashes indicate that the corresponding control samples were frozen until analysis was performed. In the initial experiments, a low-resolution mass spectrometer was used; it was replaced by a high-resolution mass spectrometer for the rest of the study. The Solvent System column describes the solution composition adjusted for the ESI-MS analysis (e.g., by adding equal volume of acetonitrile of to an aqueous solution of SOA).

SOA Type	Aging Conditions	Duration of Aging	ESI-MS Resolution	Solvent System
APIN/O ₃	-	-	Low	1:1 H ₂ O:ACN
APIN/O ₃	Humid Air	1 Week	Low	1:1 H ₂ O:ACN
APIN/O ₃	-	-	Low	1:1 H ₂ O:ACN
APIN/O ₃	Humid Air	2 Weeks	Low	1:1 H ₂ O:ACN
APIN/O ₃	-	-	High	H ₂ O
APIN/O ₃	Liquid Water	1 Day	High	H ₂ O
APIN/O ₃	Liquid Water	2 Days	High	H ₂ O
LIM/O ₃	-	-	High	H ₂ O
LIM/O ₃	Liquid Water	1 Day	High	H ₂ O
LIM/O ₃	Liquid Water	2 Days	High	H ₂ O
APIN/O ₃	-	-	High	1:1 H ₂ O:ACN
APIN/O ₃	Humid Air	1 Week	High	1:1 H ₂ O:ACN
APIN/O ₃	Humid Air	2 Weeks	High	1:1 H ₂ O:ACN
APIN/O ₃	Dry Air	1 Week	High	1:1 H ₂ O:ACN
APIN/O ₃	Dry Air	2 Weeks	High	1:1 H ₂ O:ACN
APIN/O ₃	-	-	High	1:1 H ₂ O:ACN
APIN/O ₃	Humid Air	1 Week	High	1:1 H ₂ O:ACN
APIN/O ₃	Humid Air	2 Weeks	High	1:1 H ₂ O:ACN
APIN/O ₃	Dry Air	1 Week	High	1:1 H ₂ O:ACN
APIN/O ₃	Dry Air	2 Weeks	High	1:1 H ₂ O:ACN
APIN/O ₃	-	-	High	1:1 H ₂ O:ACN
APIN/O ₃	Liquid Water	1 Day	High	1:1 H ₂ O:ACN
APIN/O ₃	Liquid Water	2 Days	High	1:1 H ₂ O:ACN
APIN/O ₃	Acetonitrile	1 Day	High	1:1 H ₂ O:ACN
APIN/O ₃	Acetonitrile	2 Days	High	1:1 H ₂ O:ACN
APIN/O ₃	-	-	High	1:1 H ₂ O:ACN
APIN/O ₃	Liquid Water	1 Day	High	1:1 H ₂ O:ACN
APIN/O ₃	Liquid Water	2 Days	High	1:1 H ₂ O:ACN
APIN/O ₃	Acetonitrile	1 Day	High	1:1 H ₂ O:ACN
APIN/O ₃	Acetonitrile	2 Days	High	1:1 H ₂ O:ACN

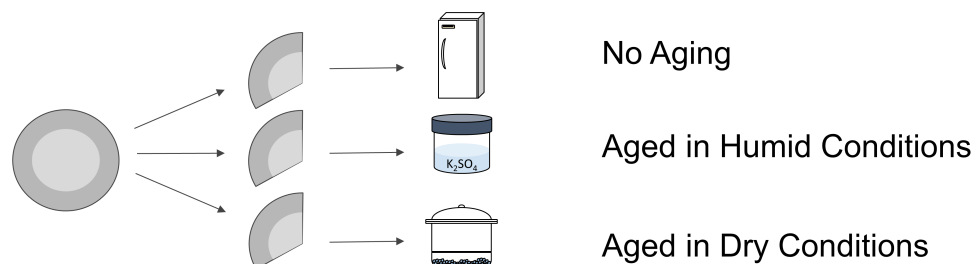
2.3.3 Aging by Exposure to Water Vapor followed by High-Resolution Mass Spectrometry Analysis

Subsequent experiments with water vapor aging relied on a modified protocol (Figure 2.1). Each SOA substrate was split into three (instead of two) equal segments. One segment was aged in a desiccator at RH <2% for 1-2 weeks; another segment was aged in the RH aging chamber for 1-2 weeks; finally, the last segment was frozen until analyzed by mass spectrometry. The goal of these additional experiments was to distinguish between hydrolysis and hydration reactions (by comparing samples aged at room temperature under dry and humid conditions) and spontaneous aging chemistry that does not require water (by comparing frozen samples with those aged at under room temperature dry conditions). Note that, very fast hydrolysis and hydration processes are difficult to study because water is ubiquitous in the atmosphere, we are primarily interested in slower processes involving water. For these and subsequent experiments, we used a high-resolution mass spectrometer equipped with a direct infusion electrospray ionization source (ESI-HRMS). Following the aging protocols, aged samples and frozen control were extracted using a 1:1 mixture of water and acetonitrile, placed on a shaker for ~10 minutes, and then promptly analyzed using high resolution mass spectrometry. The Thermo Scientific Q Exactive Plus Orbitrap mass spectrometer was operated in negative ion direct infusion mode with a spray voltage of 2.5 kV and resolving power ($m/\Delta m$) of 1.4×10^5 . A mass spectrum of the solvent was also collected to correct for the background in the spectra of SOA before and after aging.

Peak m/z values and abundances were extracted from the raw mass spectra using the Decon2LS program, (<https://omics.pnl.gov/software/decontools-decon2ls>), and then processed with in-house software. Peaks corresponding to molecules with ^{13}C atoms or obvious impurities and ion fragments, including any peaks with $m/z < 100$, were removed. Peaks with a solvent/sample ratio of more than 0.1 were also removed. The peaks were

assigned in two stages, first to internally calibrate the m/z axis with respect to the expected peaks, and then re-assigned after minor corrections (<0.001 m/z units). Mass spectra from different samples were clustered by molecular formulas of the neutral compounds, $C_cH_hO_o$, in which deprotonation was assumed to be the main ionization mechanism.

Aging by exposure to water vapor



Aging in liquid water

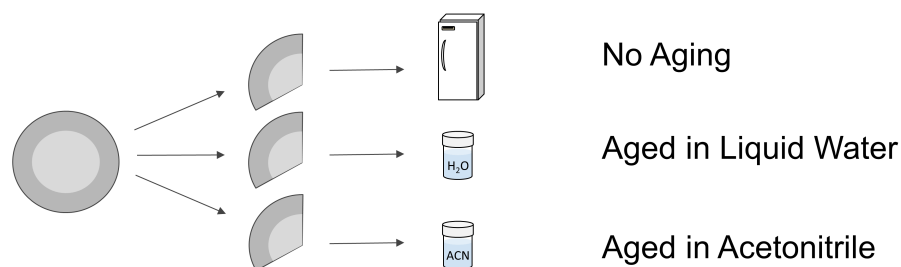


Figure 2.1: Aging Experiments Summary. SOA were first generated in a flow tube reactor and collected on a foil substrate. Foil substrates were cut into segments to age the SOA in humid conditions, dry conditions (control) or sealed and frozen (control) to understand the long-term aging of SOA by exposure to water vapor. Alternatively, the foil substrates were cut into segments to age the SOA in liquid water, acetonitrile (control) or sealed and frozen (control) to understand the long-term aging of SOA by liquid water.

2.3.4 Aging in Liquid Water followed by High-Resolution Mass Spectrometry Analysis

After observing only a limited change in the mass spectra of SOA exposed to water vapor, the next series of experiments examined water driven chemistry of SOA in liquid water. In the initial protocol, half of the foil substrate containing SOA was extracted using 10 mL

of nano-pure water, resulting in a mass concentration of 50-100 $\mu\text{g}/\text{mL}$. The solution was placed on a shaker for ~ 10 min, left undisturbed for 1-2 days, and then analyzed with high resolution mass spectrometry. The other half of the substrate was kept frozen and was dissolved before analysis.

A modified protocol was later adopted to check whether aging in solution was specific to water or could happen in an organic solvent (Figure 2.1). A SOA fraction was first separated into three equal segments. One segment was extracted and aged in 5 mL of nano-pure water, another segment was extracted and aged in 5 mL of acetonitrile, and the last segment was placed in a freezer until analysis. The appropriate amount of nano-pure water and/or acetonitrile was added to the samples so that the final solvent was a 1:1 mixture of water and acetonitrile, resulting in a mass concentration of 50-100 $\mu\text{g}/\text{mL}$. The high-resolution mass spectrometry analysis was done as described above. A detailed list of experiments done to understand SOA aging in liquid water can be found in Table 2.1.

2.4 Results

2.4.1 Composition of SOA before aging

Figure 2.2 (panels a,c) shows low-resolution mass spectra of the fresh α -pinene SOA before aging by exposure to water vapor, where peaks are normalized to the sum of the peak abundances in each spectrum. The mass spectra of the fresh α -pinene SOA are similar in the overall structure to previous mass spectra reported for α -pinene SOA.^{120,121} The monomer (<250 Da) and dimer regions (250-450 Da) are clearly evident in each spectrum, and correspond to products containing one and two oxygenated α -pinene units, respectively. The five most abundant monomer peaks have molecular weights of 170, 172, 184, 186, and 200 Da,

which most likely correspond to pinalic acid, terpenylic acid, pinonic acid, pinic acid, and 10-hydroxypinonic acid, respectively.^{127,128} The most abundant dimer peaks have molecular weights of 326, 338, 354, 368 and 370 Da, all of which were observed in previous studies, including a recent study that investigated high-molecular weight dimers esters in α -pinene ozonolysis and the boreal forest field studies in Hyytiälä, Finland.^{129,130} Repeated α -pinene SOA experiments were done and analyzed using ESI-HRMS to confirm these results. The HRMS mass spectra showed similar patterns and abundant monomer and dimer peaks, so they are not shown here.

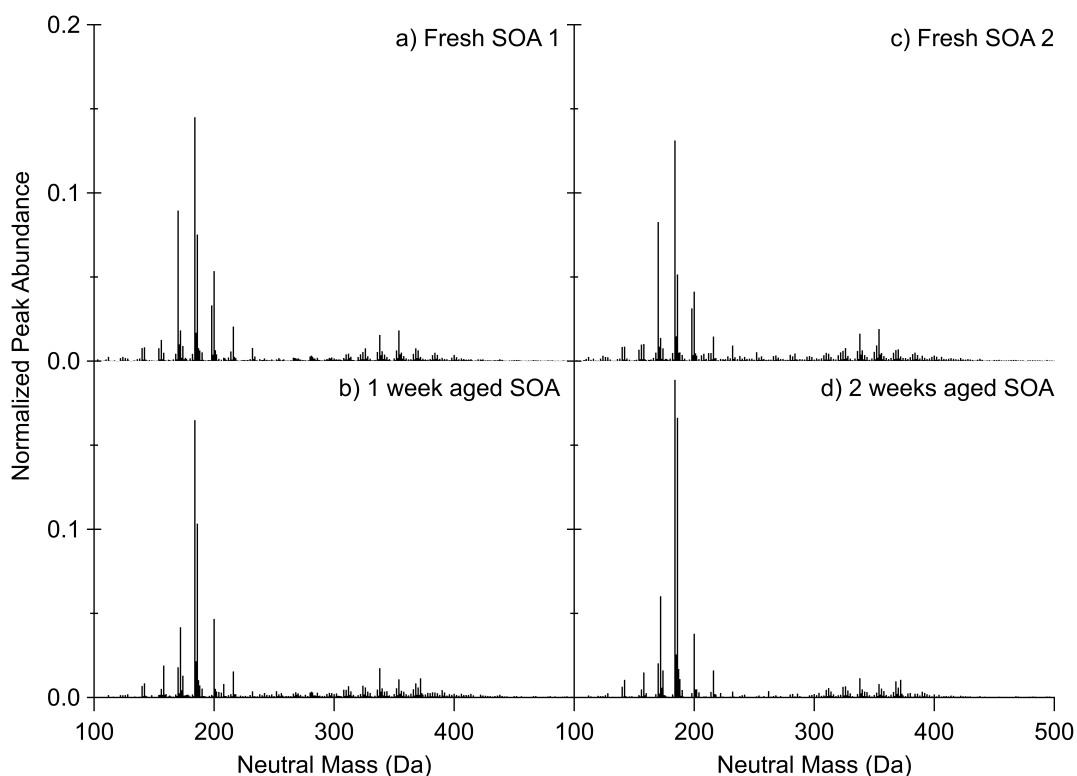


Figure 2.2: ESI-MS mass spectra of fresh α -pinene SOA (a,c) and α -pinene SOA in the presence of water vapor for 1 (b) and 2 (d) weeks. Peaks were normalized to the combined peak abundance.

Figure 2.3 shows high-resolution mass spectra of the fresh α -pinene and d-limonene SOA before aging in liquid water, where peaks are normalized to the combined peak abundance. The mass spectra of the fresh α -pinene and d-limonene SOA were similar to the previous results reported for α -pinene and d-limonene ozonolysis with distinct distribution of peaks

in the monomer and dimer region in each spectrum. The high resolution of the mass spectrometer makes it possible to unambiguously determine molecular formulas but makes no distinction between isobaric compounds. Formulas corresponding to $C_9H_{14}O_3$ (pinalic and limonic acid), $C_{10}H_{16}O_3$ (pinonic and limononic acid), $C_9H_{14}O_4$ (pinic and limononic acid), and $C_{10}H_{16}O_4$ (10-hydroxypinonic and 7OH-limononic acid) are the most abundant peaks in the monomer range, as seen in previous studies.^{129–132} The most likely identities for these products appear in parenthesis next to the formulas. The three strongest peaks in the dimer range are $C_{19}H_{30}O_6$ (MW of 354), $C_{19}H_{30}O_5$ (MW of 338), and $C_{19}H_{28}O_7$ (MW of 368) for α -pinene SOA and $C_{19}H_{30}O_7$ (MW of 370), $C_{19}H_{30}O_8$ (MW of 386), and $C_{20}H_{32}O_8$ (MW of 400) for d-limonene SOA. These peaks in the dimer range have also been observed in the fresh α -pinene SOA and d-limonene SOA in previous studies.^{129–131}

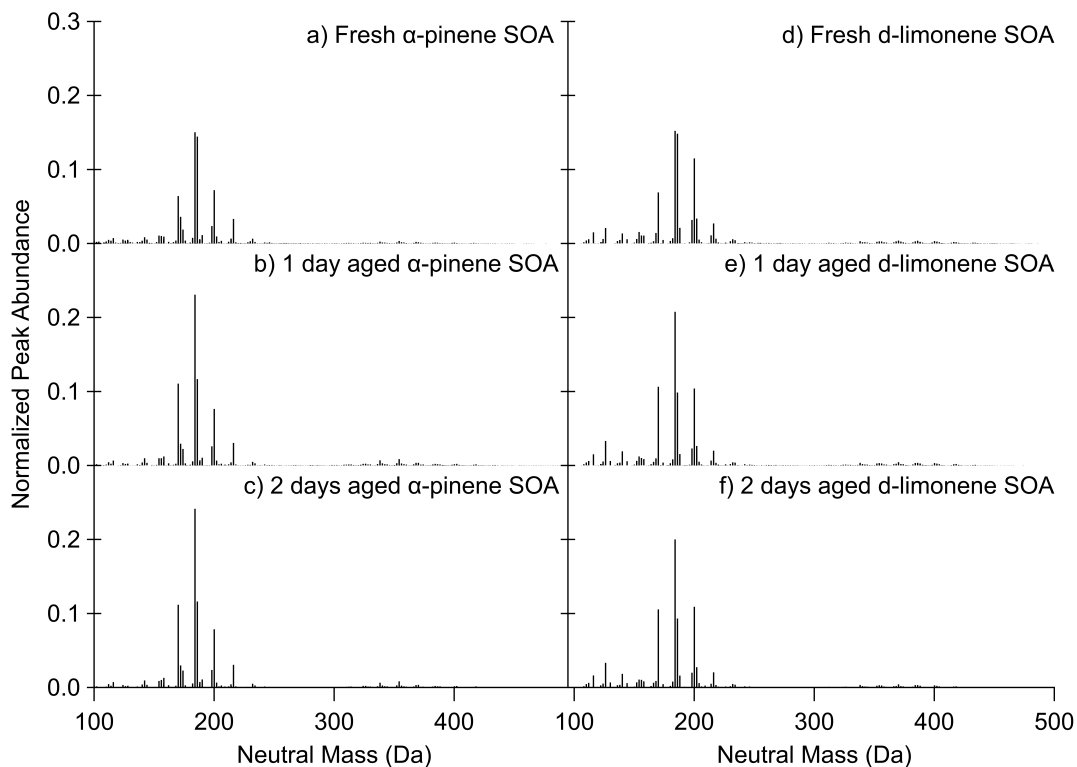


Figure 2.3: ESI-HRMS mass spectra of fresh α -pinene (a) and d-limonene (d) SOA and α -pinene and d-limonene SOA after aging in liquid water for 1 (b,e) and 2 (c,f) days. Peaks were normalized to the combined peak abundance.

2.4.2 Aging by exposure to water vapor

Comparing the fresh α -pinene SOA and aged α -pinene SOA in Figure 2.2 shows there are only subtle changes in the peak pattern indicating that water driven chemistry does not result in large changes in the chemical composition in α -pinene SOA, even after 2 weeks of exposure. To take a closer look at the changes in the peak patterns, difference spectra were created by subtracting the spectra of SOA before aging from the spectra of SOA after aging. The resulting difference spectra in Figure 2.4 confirm that aging α -pinene SOA by exposure to water vapor for 1 week and 2 weeks did not produce drastic changes in chemical composition. None of the major peaks disappeared completely, and no new major peaks appeared after aging. There is no evidence for effective hydrolysis of dimers into monomers which would have resulted in systematically negative differences in the dimer region. The peak abundances did change with a good level of reproducibility between the independently prepared 1-week and 2-week samples (panels 1 and b in Figure 2.4). Peaks that increased after aging had molecular weights of 172, 184, and 186 Da, which most likely correspond to terpenylic acid, pinonic acid, and pinic acid, respectively. On the other hand, peaks at 170 and 198 Da showed slight decreases after aging for 1 and 2 weeks. A list of the major peaks that changed after aging by exposure to water vapor can be found in Table 2.2.

In follow up experiments, α -pinene SOA samples were also aged in dry room-temperature conditions to serve as a comparison to aging under humid conditions. The difference high-resolution mass spectra of the fresh α -pinene SOA and aged α -pinene SOA in dry conditions (Figure 2.5 and Figure 2.6) also indicate that the changes in peak patterns are subtle. Furthermore, peak abundances appeared to change regardless of the presence of water. For example, peaks with molecular weights of 172.074 Da ($C_9H_{14}O_3$, pinalic acid), 184.109 Da ($C_{10}H_{16}O_3$, pinonic acid), and 186.089 Da ($C_9H_{14}O_4$, pinic acid), increased by similar amounts after both dry and humid air aging. Peaks with molecular weights of 170.094 Da ($C_8H_{12}O_4$, terpenylic acid) and 198.089 Da ($C_{10}H_{14}O_4$, oxopinonic acid) decreased under

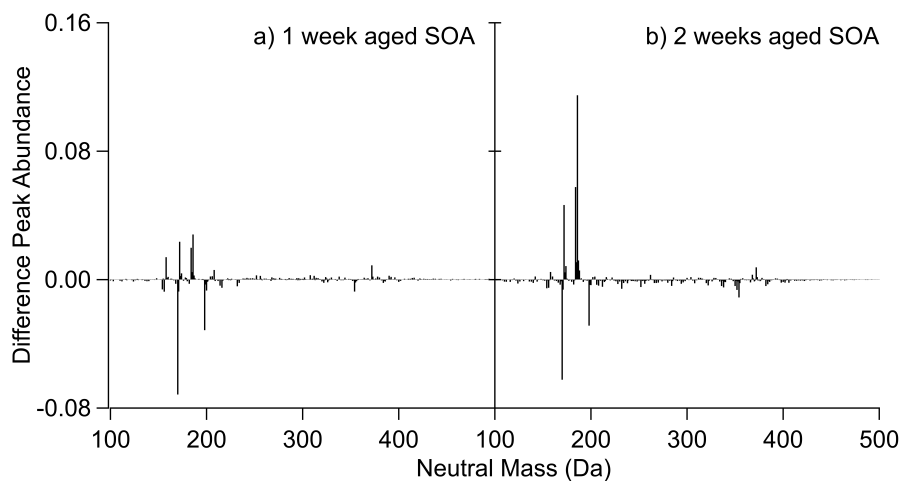


Figure 2.4: Difference low-resolution mass spectra of α -pinene SOA aged for 1 and 2 weeks by exposure to water vapor. Positive and negative peaks represent compounds that increased and decreased after aging by exposure to water vapor, respectively.

Table 2.2: Major compounds in α -pinene SOA that changed after aging by exposure to water vapor. Ratios 1 indicate that the corresponding peak increased with aging while ratios <1 suggest that the peak decreased after aging.

Observed MW (Da)	Likely Structure	Aged:Fresh Ratios	
		Aged for 1 Week	Aged for 2 weeks
170	<p>Pinalic Acid</p>	0.20	0.25
172	<p>Terpenylic acid</p>	2.30	4.38
184	<p>Pinonic Acid</p>	1.14	1.44
186	<p>Pinic Acid</p>	1.37	3.23
198	<p>Oxopinonic acid</p>	0.05	0.08

both dry and humid conditions. A list of the major peaks that changed after aging in dry and humid conditions can be found in Table 2.3 and Table 2.4. The oxopinonic acid peak is notable as it exhibited one of the largest changes in relative abundance decreasing by a factor of three after aging in dry air and by more than an order of magnitude after aging in humid air. The rest of the aged:fresh ratios ranged from ~ 0.2 to ~ 4 , i.e., within one order of magnitude.

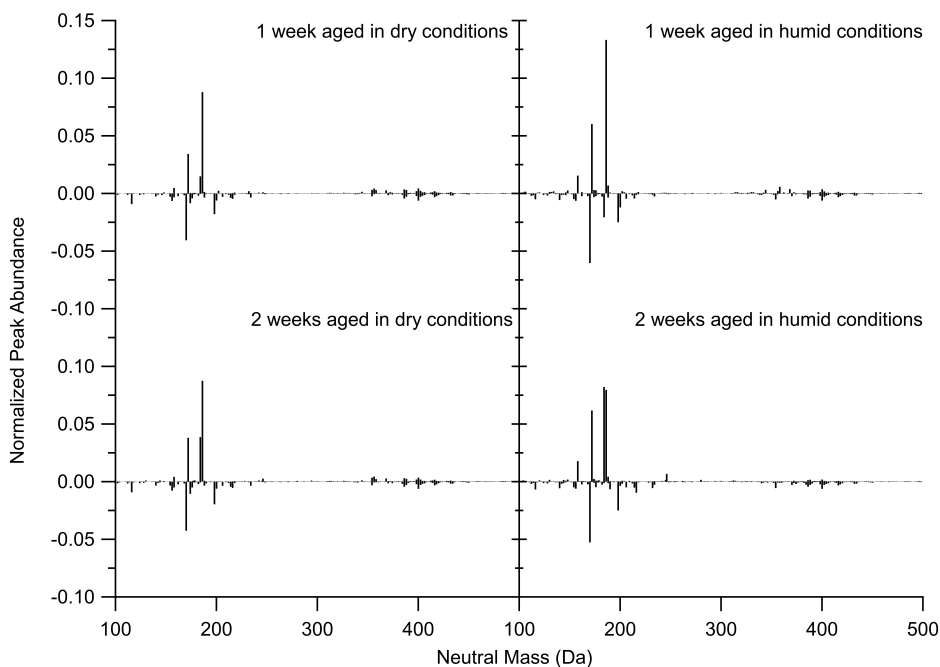
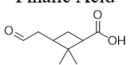
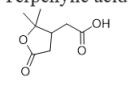
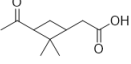
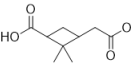
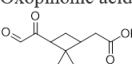


Figure 2.5: Difference high-resolution mass spectra of α -pinene SOA aged for 1 and 2 weeks in dry and humid conditions. Positive and negative peaks represent compounds that increased and decreased after aging by exposure to water vapor, respectively. (Trial 2)

2.4.3 Aging in liquid water

Figure 2.3 shows the high-resolution mass spectra of fresh α -pinene and d-limonene SOA and the corresponding mass spectra of SOA aged in liquid water for 1 and 2 days. The aged SOA still had a distinct distribution of peaks in the monomer and dimer regions in each spectrum. Comparing the fresh SOA to the aged SOA in Figure 2.3, the composition of the SOA did change, but the extent of the change was again relatively small. For example, the

Table 2.3: Major compounds in α -pinene SOA that changed after aging by exposure to water vapor (humid conditions) or desiccant (dry conditions). Ratios >1 indicate that the correspond peak increased with aging while ratios <1 suggest that the peak decreased after aging. (Trial 2)

Observed MW (Da)	Molecular Formula	Suggested Structure	Aged:Fresh Ratios			
			1 week aged in dry conditions	2 weeks aged in dry conditions	1 week aged in humid conditions	2 weeks aged in humid conditions
170.094	C ₉ H ₁₄ O ₃	<p>Pinalic Acid</p> 	0.46	0.44	0.20	0.30
172.074	C ₈ H ₁₂ O ₄	<p>Terpenylic acid</p> 	2.12	2.25	2.97	3.02
184.109	C ₁₀ H ₁₆ O ₃	<p>Pinonic Acid</p> 	1.11	1.28	0.85	1.59
186.089	C ₉ H ₁₄ O ₄	<p>Pinic Acid</p> 	1.66	1.65	2.00	1.59
198.089	C ₁₀ H ₁₄ O ₄	<p>Oxopinonic acid</p> 	0.35	0.30	0.09	0.09

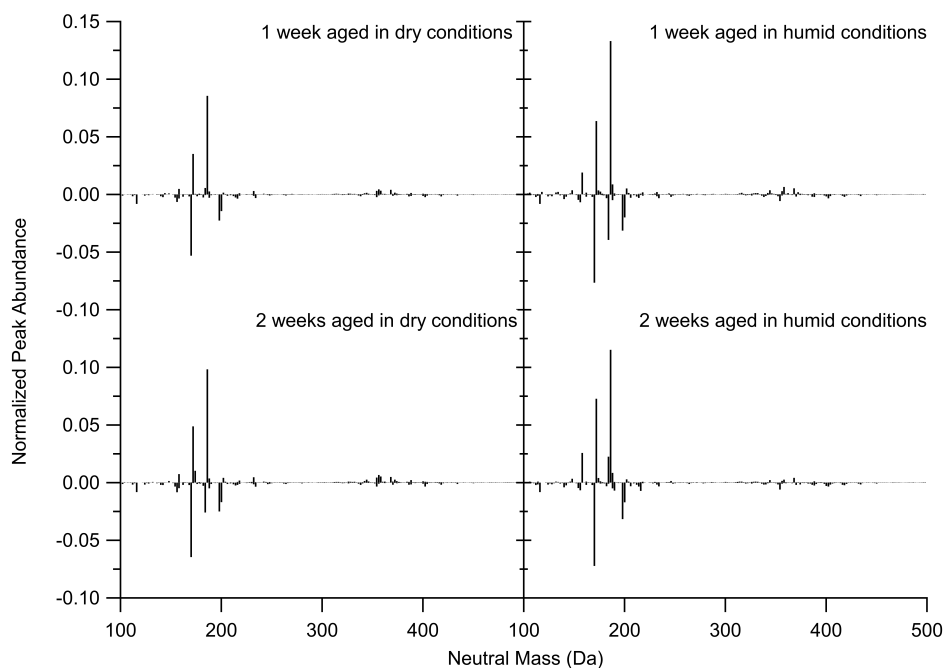
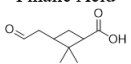
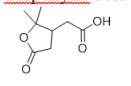
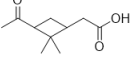
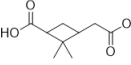
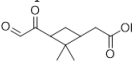


Figure 2.6: Difference high-resolution mass spectra of α -pinene SOA aged for 1 and 2 weeks in dry and humid conditions. Positive and negative peaks represent compounds that increased and decreased after aging by exposure to water vapor, respectively. (Trial 3)

Table 2.4: Major compounds in α -pinene SOA that changed after aging by exposure to water vapor (humid conditions) or desiccant (dry conditions). Ratios >1 indicate that the correspond peak increased with aging while ratios <1 suggest that the peak decreased after aging. (Trial 3)

Observed MW (Da)	Molecular Formula	Suggested Structure	Aged:Fresh Ratios			
			1 week aged in dry conditions	2 weeks aged in dry conditions	1 week aged in humid conditions	2 weeks aged in humid conditions
170.094	C ₉ H ₁₄ O ₃	Pinalic Acid 	0.42	0.29	0.16	0.21
172.074	C ₈ H ₁₂ O ₄	Terpenylic acid 	2.29	2.79	3.34	3.67
184.109	C ₁₀ H ₁₆ O ₃	Pinonic Acid 	1.03	0.84	0.76	1.14
186.089	C ₉ H ₁₄ O ₄	Pinic Acid 	1.68	1.78	2.05	1.92
198.089	C ₁₀ H ₁₄ O ₄	Oxopinonic acid 	0.33	0.27	0.08	0.07

dimer region was still clearly discernable in the mass spectra. Similar to the results with the water vapor aging described above, this indicates that liquid water does not produce large chemical composition changes in dissolved SOA.

The α -pinene and d-limonene SOA products before and after aging in liquid water are compared using difference mass spectra in Figure 2.7. Similar to the SOA aged by exposure to water vapor, there are no drastic changes in a majority of the relative peak abundances indicating that a change in phase state of water does not result in large changes in the chemical composition of SOA. Table 5 lists the major peaks that changed after aging in liquid water for 1-2 days. C₉H₁₄O₃ (pinalic and limonic acid), C₁₀H₁₆O₃ (pinonic and limonic acid) increased after aging in liquid water while C₉H₁₄O₄ (pinic and limonic acid) acid shows a slight decrease after 1-2 days. The aged:fresh relative peak abundance ratios range from 0.6 to 1.7, i.e., less than a factor of two difference. C₈H₁₂O₄ (terpenylic acid) decreased after aging in liquid water, but C₈H₁₂O₄ (limonic acid) increased after aging in liquid wa-

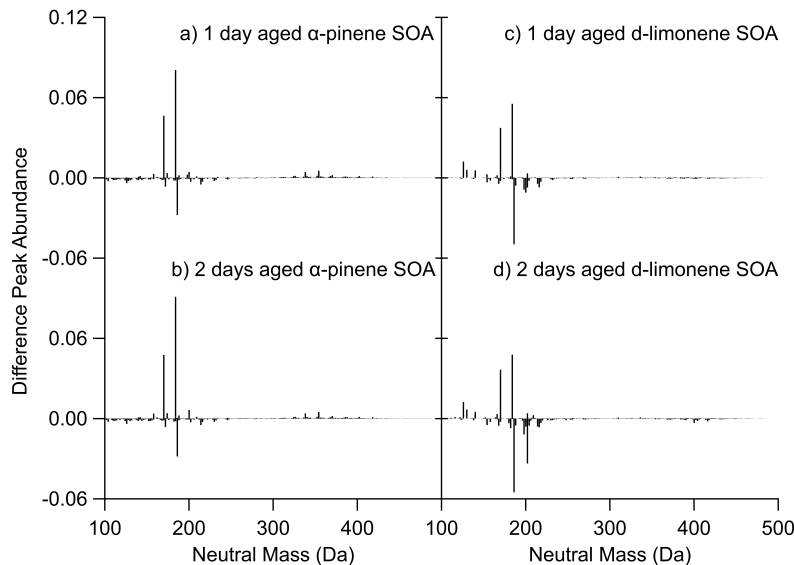
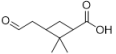
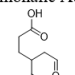
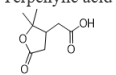
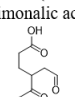
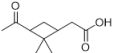
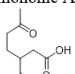
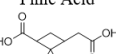
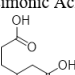
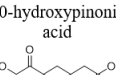
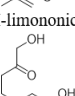


Figure 2.7: Difference high-resolution mass spectra of α -pinene and d-limonene ozonolysis SOA aged in liquid water for 1 and 2 days. Positive peaks represent compounds that increased after aging in water and negative peaks presents compounds that decreased after aging in water.

ter. Similarly, $C_{10}H_{16}O_4$ (10-hydroxypinonic acid) increased after aging in liquid water, but $C_{10}H_{16}O_4$ (7OH-limononic acid) decreased after aging in liquid water. However, the extent of these are relative small as the relative peak abundance ratios ranged from ~ 0.8 -1.8.

Figure 2.8 and Figure 2.9 contrasts difference mass spectra that compare the effect of α -pinene SOA aging in acetonitrile and water. Again, the changes in peak patterns are subtle. The peak corresponding to 170.094 Da ($C_9H_{14}O_3$, pinalic acid) increased after aging in acetonitrile and compounds that had molecular weights of 184.109 Da ($C_{10}H_{16}O_3$, pinonic acid) and 186.089 Da ($C_9H_{14}O_4$, pinic acid). A list of the major peaks that changed after aging in dry conditions can be found in Table 2.6 and Table 2.7, with the aged:fresh relative peak abundance ratios range from 0.6 to 1.3. Of the compounds listed, pinonic acid is the most interesting one as it showed opposite effects in acetonitrile (slight decrease) and water (slight increase).

Table 2.5: Major compounds in α -pinene and d-limonene SOA that changed after aging in liquid water. Ratios >1 indicate that the correspond peak increased with aging while ratios <1 suggest that the peak decreased after aging.

Observed MW (Da)	Molecular Formula	Suggested Structures		Aged:Fresh Ratios			
		α -pinene SOA	d-limonene SOA	α -pinene SOA 1 day aged	α -pinene SOA 2 days aged	d-limonene SOA 1 day aged	d-limonene SOA 2 days aged
170.094	C ₉ H ₁₄ O ₃	Pinalic Acid 	Limonalic Acid 	1.72	1.74	1.54	1.52
172.074	C ₈ H ₁₂ O ₄	Terpenylic acid 	Limonalic acid 	0.81	0.82	1.41	1.89
184.109	C ₁₀ H ₁₆ O ₃	Pinonic Acid 	Limononic Acid 	1.54	1.61	1.36	1.31
186.089	C ₉ H ₁₄ O ₄	Pinic Acid 	Limonic Acid 	0.81	0.80	0.66	0.63
200.105	C ₁₀ H ₁₆ O ₄	10-hydroxypinonic acid 	7OH-limononic acid 	1.06	1.09	0.90	0.95

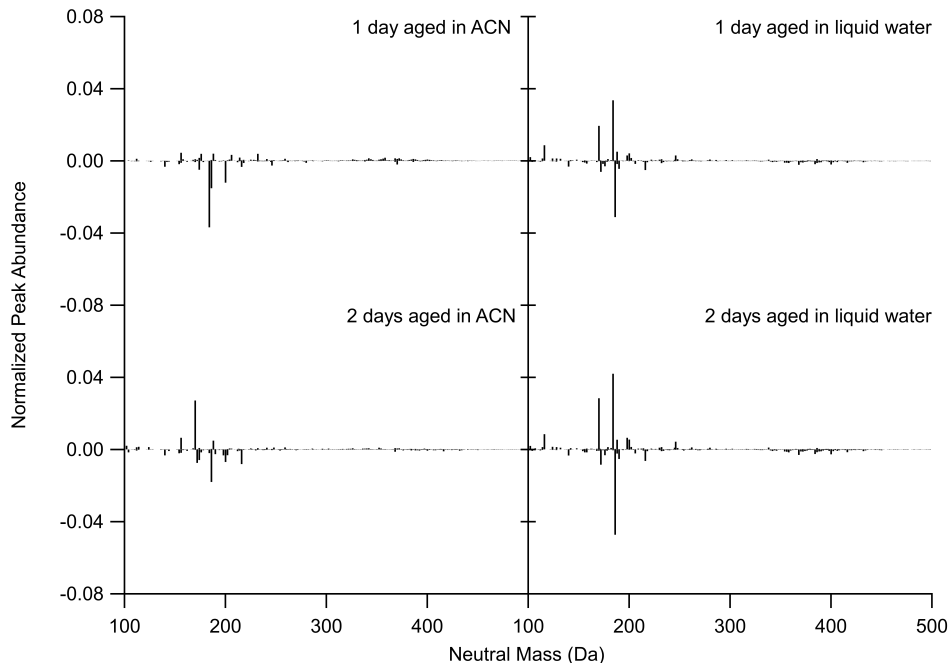
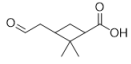
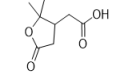
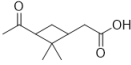
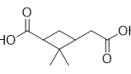
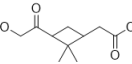


Figure 2.8: Difference high-resolution mass spectra of α -pinene SOA aged in acetonitrile and liquid water for 1 and 2 days. Positive peaks represent compounds that increased after aging in water and negative peaks presents compounds that decreased after aging in water. (Trial 2)

Table 2.6: Major compounds in α -pinene that changed after aging in acetonitrile and liquid water. Ratios >1 indicate that the correspond peak increased with aging while ratios <1 suggest that the peak decreased after aging. (Trial 2)

Observed MW (Da)	Molecular Formula	Suggested Structure	Aged:Fresh Ratio			
			1 day aged in ACN	2 days aged in ACN	1 day aged in liquid water	2 days aged in liquid water
170.094	C ₉ H ₁₄ O ₃	<p>Pinalic Acid</p> 	1.01	1.39	1.26	1.39
172.074	C ₈ H ₁₂ O ₄	<p>Terpenylic acid</p> 	1.02	0.80	0.83	0.77
184.109	C ₁₀ H ₁₆ O ₃	<p>Pinonic Acid</p> 	0.76	0.99	1.22	1.28
186.089	C ₉ H ₁₄ O ₄	<p>Pinic Acid</p> 	0.91	0.90	0.82	0.73
200.105	C ₁₀ H ₁₆ O ₄	<p>10-hydroxypinonic</p> 	0.79	0.88	1.07	1.10

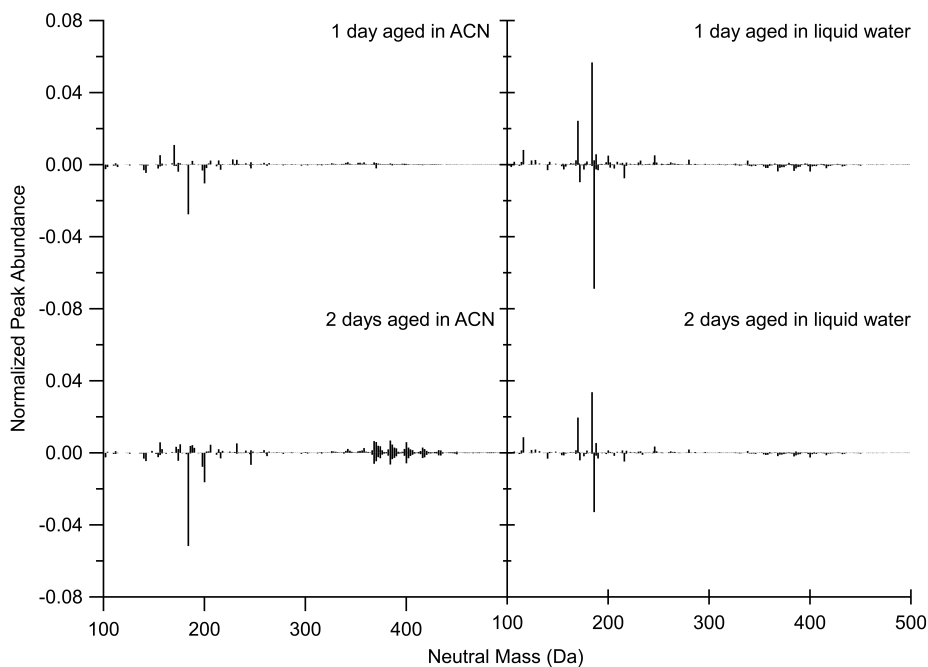
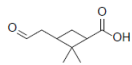
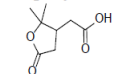
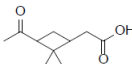
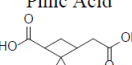
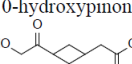


Figure 2.9: Difference high-resolution mass spectra of α -pinene SOA aged in acetonitrile and liquid water for 1 and 2 days. Positive peaks represent compounds that increased after aging in water and negative peaks presents compounds that decreased after aging in water. (Trial 3)

Table 2.7: Major compounds in α -pinene that changed after aging in acetonitrile and liquid water. Ratios >1 indicate that the correspond peak increased with aging while ratios <1 suggest that the peak decreased after aging. (Trial 3)

Observed MW (Da)	Molecular Formula	Suggested Structure	Aged:Fresh Ratio			
			1 day aged in ACN	2 days aged in ACN	1 day aged in liquid water	2 days aged in liquid water
170.094	C ₉ H ₁₄ O ₃	<p>Pinalic Acid</p> 	1.14	0.99	1.30	1.24
172.074	C ₈ H ₁₂ O ₄	<p>Terpenylic acid</p> 	0.98	1.09	0.72	0.88
184.109	C ₁₀ H ₁₆ O ₃	<p>Pinonic Acid</p> 	0.84	0.70	1.33	1.19
186.089	C ₉ H ₁₄ O ₄	<p>Pinic Acid</p> 	0.99	1.02	0.58	0.80
200.105	C ₁₀ H ₁₆ O ₄	<p>10-hydroxypinonic</p> 	0.83	0.73	1.08	1.02

2.5 Discussion

While direct infusion ESI mass spectrometric techniques are not quantitative, the absence and presence of peaks and changes in peak abundances between samples are suitable indicators of the differences in composition. The subtle changes in the mass spectra in both the SOA aged by exposure to water vapor and the SOA aged in liquid water imply that most of the compounds remained stable with respect to hydrolysis and hydration. None of the peaks were completely removed by hydrolysis and hydration, and no new major peaks appeared after aging, indicating that the distribution of compounds in the SOA stayed approximately the same between the fresh and aged samples. Major peaks in both low and high-resolution mass spectra did change as the aged SOA to fresh SOA ratio ranged between ~ 0.05 -4. As the samples were analyzed in triplicate and the mass spectra of the replicates were reproducible, this allows relative certainty that the differences between the fresh and aged samples were due to measurable differences in the composition of the samples after aging.¹³³

The mass spectra of the controls helped determine whether the changes resulted due to the presence of water vapor or liquid water or whether the changes in the mass spectra resulted from chemistry that did not need water to occur. The major peaks that changed in the SOA aged by exposure to water vapor and the SOA aged in dry air were similar. For example, compounds that had molecular weights of 172.074 Da ($C_9H_{14}O_3$), 184.109 Da ($C_{10}H_{16}O_3$), and 186.089 Da ($C_9H_{14}O_4$) increased after aging, while compounds that decreased after aging had molecular weights of 170.094 ($C_8H_{12}O_4$) and 198.089 ($C_{10}H_{14}O_4$). However, the extent of change was larger in the SOA aged by exposure to water vapor as noted by the aged:fresh ratios. The changes in the mass spectra after SOA aged in liquid water and in acetonitrile were also slightly different. For example, pinic acid ($C_9H_{14}O_4$) decreased slightly after aging in liquid water, but remained essentially unchanged after aging in acetonitrile. Additionally, the peak that corresponds to pinonic acid ($C_{10}H_{16}O_3$) increased after in liquid water but decreased after aging in acetonitrile. This indicates that some of the differences in the fresh SOA and aged SOA in liquid water were likely due to the presence of a water. Overall, the difference mass spectra for the controls and the SOA aged by exposure to water vapor and in liquid water were relatively subtle.

Our initial hypothesis that the long term aging of SOA would lead to significant changes in the chemical composition was prompted by the findings by Romonosky et al. (2017).¹²¹ Using direct-infusion ESI-MS, they observed that the SOA dimer region decreased by $\sim 30\%$ and some peaks in the monomer peaks increased by $\sim 20\text{-}50\%$ in the mass spectrum when leaving α -pinene SOA from ozonolysis in water undisturbed for 4 h in the dark as a control.¹²¹ Additionally, aging the SOA in water led to a decrease in the average O:C ratio and average molecular weight, which made the SOA compounds more volatile.¹²¹ Based on the observations of Romonosky et al. (2017), we fully expected that aging the SOA in liquid water for as long as two days should have led to a large change in the dimer and trimer region

in the mass spectrum. However, in this study there were only subtle changes in the mass spectrum with the most notable changes from the monomeric compounds. The SOA generations methods from this study and the Romonosky et al. (2017) paper could potentially be responsible for the differences in results. SOA in Romonosky et al. (2017) was generated in a 5 m³ chamber, in which ozone was in excess. In this study, SOA was generated in a flow tube reactor, in which VOC precursor was in excess. As previously mentioned, the oxidant:VOC ratio used in experiments can lead to different SOA composition with diverse physical and chemical properties. For example, in the case of d-limonene, experiments with excess d-limonene would favor a selective oxidation of the endocyclic double bond whereas experiments with excess ozone would completely oxidize both the endocyclic and exocyclic double bonds.¹²³ Figure 2.10 shows a Van Krevelen diagram of fresh α -pinene SOA from Romonosky et al. (2017) compared to this study. The size of the markers in each plot is scaled to the normalized intensity. The compounds between the two studies share similar compounds that have comparable O:C and H:C ratios. However, the main difference between the fresh α -pinene SOA is that there are higher intensities of compounds with a larger O:C in Romonosky et al. compared to this study indicating that the sample was more oxygenated. Again, this likely due to initial conditions used in SOA formation, in which VOC was in excess in this study and ozone was in excess in the Romonosky et al. rather than aging in the presence of ozone as the composition of α -pinene ozonolysis SOA remains pretty stable after oxidative aging.^{134,135} Many reactions are accelerated in acidic environments. For example, aldol condensation, polymerization, gem-diol reactions, dehydration, and esterification are catalyzed by acids and results in oligomers and dimers. Due to the nature of the excess oxidant environment in which the chamber was ran, the SOA that was collected most likely had higher fraction of carboxylic acids, which would explain the higher of compounds with a larger O:C illustrated in Figure 2.10. Thus, the high fraction of carboxylic acids would lower the pH when the sample was dissolved in water and therefore promoting acid catalyzed reactions leading differences in the mass spectra when aged in water. Additionally, other

studies have shown the initial concentration of oxidant and VOC can lead to disparities in mass concentrations and ROS profiles, which could indicate that the SOA compositions are not the same.^{124,125} Both studies are atmospherically relevant. Romonosky et al. (2017) is more applicable to the outdoor atmosphere, in which SOA is formed in a VOC-limited environment. This study, on the other hand, pertains mostly to the indoor atmosphere. The off gassing by wood products as well as the increase use of terpenoids in cleaning products and air fresheners would results in elevated concentrations of these compounds that exceeds the concentration of ozone.¹³⁶⁻¹³⁸ Due to differences in initial conditions, it likely that the composition of SOA used in this study and the Romonosky et al. (2017) differ, which could results in varying degrees of hydrolysis and hydration.

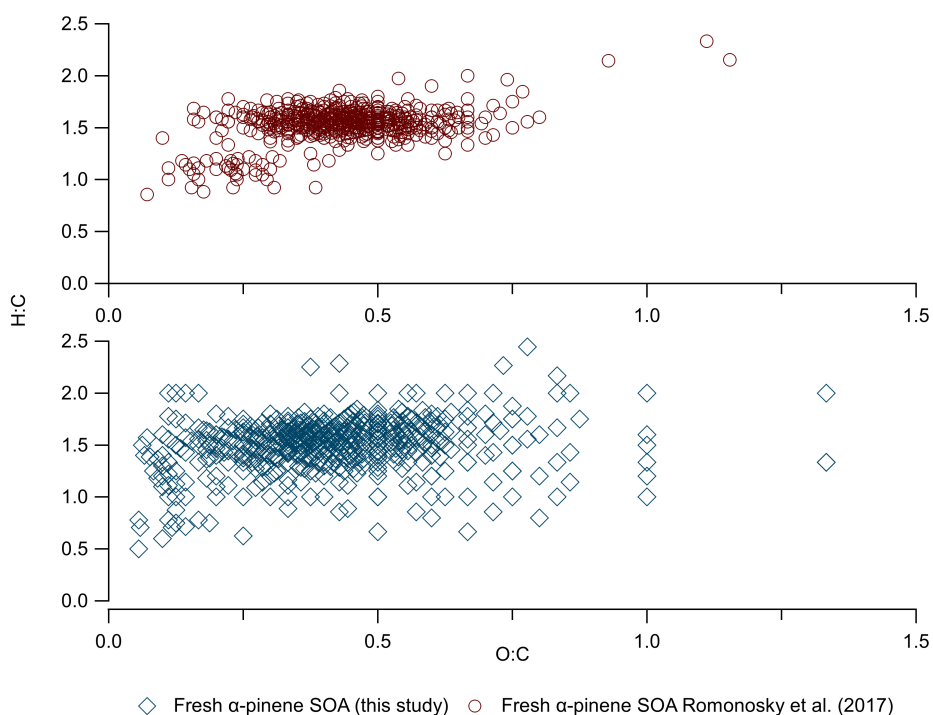


Figure 2.10: Van Krevelen diagram of fresh α -pinene SOA from Romonosky et al. (2017) compared to this study. Size of the markers are scaled to the normalized intensity.

D'Ambro et al. (2018), examined isothermal evaporation of α -pinene ozonolysis SOA by collecting a spot of SOA material on a filter, leaving the material exposed to a flow of humidified nitrogen at room temperature for up to 28 h, and then examining the chemical

composition of the remaining material by thermal desorption mass spectrometry.¹³⁹ They observed significant loss of SOA compounds from the filter, with 50-70% of organics lost after 24 hours. Unlike previous studies of SOA particle evaporation rates, which were shown to be strongly affected by RH, D'Ambro et al. (2018) observed only a weak dependence of the SOA material loss rate on RH, which could be specific to filter-based aging experiments because it takes longer for collected SOA on the filter to take up water.¹³⁹ While most of their observations could be explained by evaporation, they had to assume that oligomers in SOA can reversibly decompose with decompaction rates ranging from 10^{-5} to 10^{-4} s⁻¹ depending on the method of SOA preparation. Our aging experiments were carried out in small sealed volumes to help suppress evaporation, but it is likely that some evaporative loss took place in our vapor aging experiments. To account for that, we normalized the mass spectra to highlight relative changes in composition after aging. Our observations support the general conclusions of D'Ambro et al. (2018) that exposure to water vapor does not have a strong effect on the composition of the SOA (evaporative loss is more important). The control experiments, in which SOA was exposed to dry instead of humid air, produced comparable changes in mass spectra to those under humid conditions.

2.6 Summary and Implications

Different forms of water including water vapor, aerosol liquid water, organic-phase water, and cloud and fog water can promote reactions that result in changes in chemical properties within SOA. This environment is particularly important when understanding the aging of compounds in aerosols which spend days to weeks in the atmosphere. We analyzed the effect long-term aging has on the chemical composition of model SOA prepared by ozonolysis of α -pinene and d-limonene. Our initial expectation was that aging SOA derived from ozonolysis by exposure to water vapor and liquid water would result in changes in the monomeric and

dimeric compounds through hydrolysis and hydration of oligomeric compounds. While the presence of water lead to changes in the chemical composition of these aerosols, the extent of these changes was relatively small, suggesting that hydrolysis and hydration is not a major aging mechanism in the atmosphere (at least for these types of SOA). Further investigation on the pH dependence of hydrolysis and hydration reactions in SOA are next logical step in the study.

Chapter 3

Highly acidic conditions drastically alter chemical composition and absorption coefficient of α -pinene secondary organic aerosol

Reprinted with permission from Wong, C.; Liu, S.; Nizkorodov, S.A., Highly Acidic Conditions Drastically Alter the Chemical Composition and Absorption Coefficient of α -Pinene Secondary Organic Aerosol, *American Chemical Society Earth and Space Chemistry*, **2022**, 6(12), 2983–2994, doi/10.1021/acsearthspacechem.2c00249. Copyright 2022 American Chemical Society.

3.1 Abstract

Secondary organic aerosol (SOA), formed through the gas-phase oxidation of volatile organic compounds (VOCs), can reside in the atmosphere for many days. The formation of SOA takes place rapidly within hours after VOCs emissions, but SOA can undergo much slower physical and chemical processes throughout its lifetime in the atmosphere. The acidity of atmospheric aerosols spans a wide range, with the most acidic particles having negative pH values, which can promote acid-catalyzed reactions. The goal of this work is to elucidate poorly understood mechanisms and rates of acid-catalyzed aging of mixtures of representative SOA compounds. SOA was generated by ozonolysis of α -pinene in a continuous flow reactor and then collected using a foil substrate. SOA samples were extracted and aged by exposure to varying concentrations of aqueous H_2SO_4 for 1-2 days. Chemical analysis of fresh and aged samples was conducted using ultra-performance liquid chromatography coupled with a photodiode array spectrophotometer and a high-resolution mass spectrometer. In addition, UV-Vis spectrophotometer, and fluorescence spectrophotometer were used to examine the change in optical properties before and after aging. We observed that SOA aged in moderately acidic conditions (pH from 0 to 4) experienced small changes in the composition, while SOA aged in a highly acidic environment (pH from -1 to 0) saw more dramatic changes in composition, including the formation of compounds containing sulfur. Additionally, at highly acidic conditions, light-absorbing and weakly-fluorescent compounds appeared, but their identities could not be ascertained due to their small relative abundance. This study shows that acidity is a major driver of SOA aging, resulting in a large change in the chemical composition and optical properties of aerosols in region where high concentrations of H_2SO_4 persist, such as upper troposphere and lower stratosphere.

3.2 Introduction

Aerosols play an important role in the atmosphere directly by absorbing and scattering radiant energy and indirectly by acting as cloud condensation nuclei and ice nucleating particles.²³ They can contribute to poor air quality, causing decreased visibility and adverse health effects.^{15,20} Organic aerosols are ubiquitous and account for the dominant fraction of aerosols in the atmosphere.²² Secondary organic aerosol (SOA), which are primarily formed through either nucleation, condensation, or multiphase chemical processing of oxidation products of volatile organic compounds (VOCs), has highly complex composition and a wide range of physical and chemical characteristics. The lifetimes of SOA can be as long as several days or even weeks, with SOA in the upper troposphere having longer lifetimes because removal mechanisms for particles at this altitude are inefficient.¹⁹

The acidity of atmospheric aqueous phase (i.e., aerosols particles, cloud droplets, and fog droplets) is an important factor that can influence physical and chemical processes. There is a wide range of acidities in the atmosphere. Cloud and fog droplets can have pH values ranging from +2 to +7, while aerosol particles tend to be more acidic and have a wider range with pH values from -1 to +8, depending on their source, chemical composition and ambient relative humidity (RH).^{47,81}

Organic reactions in the atmosphere can either be acid catalyzed or acid driven, the difference being that in the latter the protons from the acid are incorporated into the products formed. Hemiacetal and acetal formation are dependent on acidic conditions in which a compound containing a hydroxyl group is added to a carbonyl compound after the protonation of the carbonyl, followed by the addition of an alcohol. This reaction have been shown to be significant for aqueous SOA formation from carbonyl compounds such as glyoxal and methylglyoxal.^{70,72,140} The rates of hydration of complex aldehydes, ketones, and carbonyls

have been shown to be strongly influenced by the presence of acids once partitioned into the aqueous phase in which the carbonyl group is converted into gem-diols.⁷³⁻⁷⁵ Aldol condensation can be highly pH sensitive due to the acid catalyzed nature of the enol formation and the role of the protonated carbonyl. Several studies of atmospherically-relevant carbonyls have reported that this reaction is favorable under strongly acidic condition $\text{pH} < 2$,⁷⁶⁻⁸⁰ while another study reported that this aldol condensation can occur at pH as high as +4 to +5.⁷¹ Multiple studies have shown that rate of esterification will increase with increasing acidity because the carboxyl group needs to be protonated to form a carbocation before a nucleophilic attack by an alcohol.⁸¹⁻⁸⁴ Finally, acids can also facilitate nucleophilic addition through isoprene and monoterpene epoxide protonation, which can lead to organosulfate formation.⁸⁵⁻⁸⁸

The effects of seed particle acidity on the growth of SOA have been extensively investigated. Chamber studies have shown enhanced production of SOA in presence of acidic seed particles suggesting the importance of acid-catalyzed processes^{24,35,39,89-95} The presence of acidic sulfate seeds in the formation of SOA from various combinations of VOC precursors (i.e., isoprene, α -pinene, d-limonene, m-xylene, toluene, benzene, etc.) and oxidants (i.e., O_3 , OH) can probe changes in organic aerosol chemical properties such as mass yields, oxidation state, and composition, including the formation of larger oligomers, organosulfates, and light absorbing compounds.^{24,35,39,89-95} Studies have shown that the reactive uptake was observed for various individual products of oxidation of biogenic volatile organic compounds onto acidified particles. For example, pinonaldehyde uptake on inorganic sulfate seeds aerosols resulted in oligomer and organosulfate formation.^{77,96} The uptake of isoprene-derived epoxy-diols in solutions of sulfates (i.e., H_2SO_4 , Na_2SO_4 , $(\text{NH}_4)_2\text{SO}_4$, $(\text{NH}_4)\text{HSO}_4$), leads to the formation of polyols and sulfate esters as well as light absorbing compounds, with the rate of formation being dependent on the acidity of the solution.^{87,97,98} Additionally, previous work has also focused on the reactive uptake of aldehydes and ketones into sulfuric acid solutions and particles, mimicking stratospheric aerosols.^{5,76,78,79,141} It was found that the rate con-

stant was dependent on chain length and acidity and acidities also facilitated the formation of light absorbing compounds and oligomers.^{5,76,78,79,99}

While the effects of acidity on the initial SOA formation is well understood, less is known about role of acids in the chemical aging of organic aerosols occurring over longer time scales. Previous work in our group found that the evaporation of bulk biogenic and anthropogenic SOA solutions in the presence of sulfuric acid enhanced absorbance at visible wavelengths and resulted in a significant changes in the chemical composition, including organosulfate formation.^{141,142} However, the pH was difficult to measure during the evaporation and it was not clear at what specific pH values these changes took place. Additionally, other studies focused either on a limited range of acidity, limited number of organic compounds, or were conducted on a short time scale. We hypothesize that aging SOA in acid for an extended period of time (days) would probe acid-catalyzed and acid-driven chemical reactions leading to significant changes in the composition. The goal of this work is to elucidate mechanisms and rates of aging processes of mixtures of representative SOA compounds in presence of increasing levels of acidity. Our results suggest that SOA aging processes are accelerated in sulfuric acid solutions at atmospherically relevant pH with organosulfates and light-absorbing products forming under highly acidic conditions.

3.3 Experimental Methods

3.3.1 Secondary Organic Aerosol Generation

SOA samples were generated in a $\sim 20\text{L}$ continuous flow reactor under dry and dark conditions. The reaction reactor was purged with zero air (Parker 75-62 purge gas generator) prior to each experiment and ozone was introduced into the reactor by flowing pure oxygen through a commercial ozone generator (OzoneTech OZ2SS-SS) at 0.5 slm (standard liters per minute). Liquid α -pinene (Fisher Scientific, 98% purity) was injected into ~ 5 slm flow of zero air using a syringe pump at a constant rate of $\sim 25 \mu\text{L h}^{-1}$. The estimated initial mixing ratios of ozone and VOC were 14 ppm and 10 ppm, respectively. This high loading was used to generate enough SOA material for the analysis described below, which favors RO_2+RO_2 reactions and prompts higher volatile higher volatility compounds to partition in the particles. The SOA compounds that are generated through this method are still observed in fields studies, however, future studies should focus on reducing the loading to increase the relevance of the work.

SOA was collected onto a foil substrate on stage 7 (0.32-0.56 μm) of a micro-orifice uniform deposit impactor (MOUDI, model 110R) at a flow rate of ~ 30 slm to create a uniform deposition of particles on the substrate (with 5.5 slm coming from the cell and the rest coming from a filtered lab air). This method removes most volatile compounds from particles, and thus collecting the majority of low volatile compounds in the SOA, which more atmospherically relevant. The mass on the foil substrate was typically ~ 2 mg. Some samples were vacuum-sealed and frozen, while other samples were aged in acidic conditions until mass spectrometry analysis was performed.

3.3.2 Aging in Sulfuric Acid

Each SOA substrate was cut into three approximately equal segments. SOA from the first segment was extracted and then aged in a solution of sulfuric acid to monitor the change in chemical composition by mass spectrometry, SOA from the second segment was similarly aged in a sulfuric acid solution to detect light-absorbing compounds by spectrophotometry, and finally, the last segment was sealed with a food-sealer and frozen for control mass spectrometry experiments. The protocol used for these experiments is illustrated in Figure 3.1. Two segments containing SOA were first extracted using ~ 4 mL of acetonitrile into a scintillation vial by shaking it for ~ 10 minutes. The solvent was then removed from the vial using a rotary evaporator at $\sim 25^\circ\text{C}$. This process may have removed semivolatile compounds that have partitioned into the particle, however, we were mostly concerned about low volatile compounds in the SOA as they are more atmospherically relevant. A volume of ~ 4 mL of dilute aqueous solution sulfuric acid (Fisher Scientific, 96% purity) as described in Table 3.1 was added to the vials, resulting in a mass concentration of 180-200 $\mu\text{g}/\text{mL}$. Note that the dilute aqueous solutions of sulfuric acid were prepared and cooled to room temperature before their addition to the SOA extract. When appropriate ($\text{pH} > 0$), a pH meter (Mettler Toledo SevenEasy S20) was used determine the acidity of the SOA and sulfuric acid solution. One sample was immediately placed in the spectrophotometer (Shimadzu UV-2450) to monitor the absorption spectrum as a function of time, and the other solution was left undisturbed in darkness for 2 days until mass spectrometric analysis. The SOA on the frozen control was extracted immediately before the analysis using the same method as described above, however $\sim 4\text{mL}$ of nanopure water was added to the scintillation vial as the solvent.

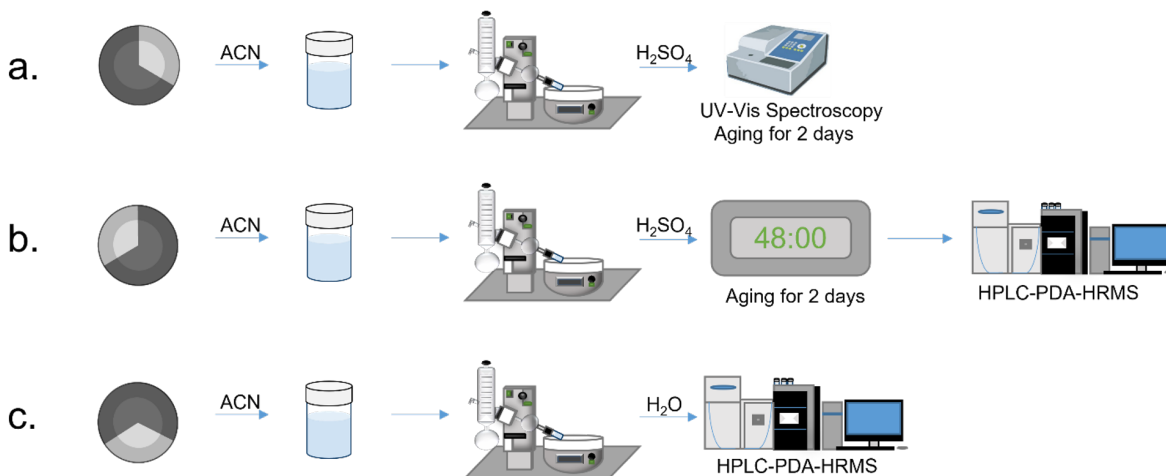


Figure 3.1: Aging Experiments Summary. SOA were first generated in a flow tube reactor and collected on a foil substrate. Foil substrates were cut into three segments, extracted using acetonitrile, and acetonitrile was removed using a rotary evaporator. The corresponding acid was added to Sample A and Sample B. Sample C was extracted using the same method and dissolved in water for our control group.

3.3.3 Measurements and Modeling of pH

A pH meter (Mettler Toledo SevenEasy S20) was used to determine the acidity of the sulfuric acid solution and the SOA and sulfuric acid sample ($\text{pH} > 0$). However, determining the pH for highly acidic ($\text{pH} < 0$) conditions is difficult due to the limited range of the pH probe (pH 0.00-14.0). Therefore, Extended Aerosol Inorganic Model I (E-AIM) was utilized to estimate the pH of the sulfuric acid solution.¹⁴³⁻¹⁴⁵ By inputting the starting moles of H^+ and SO_4^{2-} present and ambient conditions of the solution, the aqueous molality and mole fractions of H^+ can be determined and used to calculate the effective pH of the solution:

$$\text{pH} = -\log_{10}[\text{H}^+] \quad (3.1)$$

where $[\text{H}^+]$ is the molality of protons. The resulting effective pH values ranged from -1 to +3, with the exact values for each trial listed in Table 3.1. It is noted that for the positive pH values, the pH meter readings and the E-AIM output agreed reasonably well, with small deviations. E-AIM model also provided activity coefficients for H^+ , which are included in

Table 3.1 and can be used to calculate the pH corrected for the activity. For the remainder of this paper, we will refer to the solutions by their effective pH calculated from Eq. (3.1).

Table 3.1: Solution Acidity in Aging Experiments. The first column lists the molar concentration of H_2SO_4 added to the solution. The molalities of $[\text{H}^+]$ and other ions were calculated using the Extended Aerosol Inorganics Model (E-AIM, <http://www.aim.env.uea.ac.uk/aim/aim.php>). The effective pH values listed in the last column and quoted in the paper represent the negative logarithm of molality of $[\text{H}^+]$.

Estimated Concentration of H_2SO_4	pH Meter Reading	E-AIM Output				
		$[\text{HSO}_4^-]$ (mol/kg)	$[\text{SO}_4^{-2}]$ (mol/kg)	$[\text{H}^+]$ (mol/kg)	Activity Coefficient of H^+	Effective pH = $-\log[\text{H}^+]$
0 M	4.3	-	-	-	-	Control
0.52 mM	2.7	0.0000386	0.000481	0.00100	0.96	3.00
6.4 mM	1.9	0.00240	0.00402	0.0105	0.88	1.98
90 mM	1.1	0.0654	0.0249	0.115	0.76	0.94
1.0 M	-	0.754	0.249	1.25	0.78	-0.01
1.8 M	-	1.26	0.508	2.28	0.92	-0.36
3.2 M	-	2.15	1.01	4.17	1.4	-0.62
5.6 M	-	3.96	1.67	7.30	3.7	-0.86
10 M	-	8.10	1.93	12.0	20	-1.08

3.3.4 Mass Spectrometry Analysis

Analysis of fresh and aged samples was conducted using a Thermo Scientific Vanquish Horizon ultra-performance liquid chromatography (UPLC) coupled with a Vanquish Horizon photodiode array (PDA) spectrophotometer and a Thermo Scientific Q Exactive Plus Orbitrap high resolution mass spectrometer to examine the chemical composition of SOA before and after aging. UPLC separation was carried out on a Phenomenex Luna Omega Polar C18 column, 150×2.1 mm, with $1.6 \mu\text{m}$ particles and 100\AA pores, with the temperature set to 30°C and a flow rate of 0.3 mL/min . The mobile phase consisted of water (eluent A) and acetonitrile (eluent B), each containing 0.1% formic acid. The gradient elution was programmed as follows: 0-3 min 95% eluent A; 3-14 min linear ramp to 95% eluent B; 14-16 min hold at 95% eluent B, 16-22 min return to 95% eluent A. The mass spectrometer was

operated in negative ion mode with a spray voltage of 2.5 kV and a resolving power of $m/\Delta m = 1.4 \times 10^5$. Most of the analysis was done with negative ion mode data to observe presence of organosulfur compounds, however, positive ion mode data sets were also acquired SOA aged in pH -1.08 to analyze potential chromophores.

Peaks were imported to Thermo Scientific program FreeStyle 1.6 and integrated between 2-16 minutes, which corresponds to the elution of the majority of the SOA compounds in the chromatogram. Peak m/z values and abundances were extracted from the raw mass spectra using the Decon2LS program (<https://omics.pnl.gov/software/decontools-decon2ls>), and then processed with in-house software. Peaks corresponding to molecules with ^{13}C atoms or obvious impurities and ion fragments, signified by anomalous full width at half maximum and mass defects were removed from the peak table. Additionally, peaks with a solvent/sample ratio of more than 1 were considered impurities and was excluded from further analysis. The solvent peak abundances were then subtracted from the peak abundances in the samples. The peaks were assigned to formulas in two stages, first to internally calibrate the m/z axis with respect to the expected peaks for α -pinene ozonolysis, and then reassigned after a minor (<0.001 m/z units) adjustment to the m/z values. Mass spectra from different samples were clustered by molecular formulas of the neutral compounds CHO and CHOS for fresh and aged SOA, respectively. Deprotonation was assumed to be the main ionization mechanism for negative ion mass spectra.

3.3.5 Spectroscopic Measurements

UV-Vis spectrophotometer (Shimadzu UV-2450) was used to monitor the formation of light-absorbing compounds over time. The spectrophotometer was programmed to collect a spectrum every 15 minutes for 24 hours and one more spectrum was then collected at the 48-hour time point. Mass absorption coefficients (MAC), in units of $\text{cm}^2 \text{g}^{-1}$, were calculated using

the following equation where A_{10} is the base-10 absorbance, C_{mass} (g cm^{-3}) is the concentration of the SOA in solution and was estimated by measuring the mass of the foil segment before and after extraction, and b (cm) is the path length (standard 10 mm cuvettes were used in these experiments):

$$MAC(\lambda) = \frac{A_{10}(\lambda) \times \ln(10)}{b \times C_{\text{mass}}} \quad (3.2)$$

Aliquots of some samples were also examined using Cary Eclipse Fluorescence Spectrometer to investigate the presence of fluorescence molecules. The parameters used for these experiments mimic past studies in our group.¹⁴⁶ The background for the fluorescence spectrum was deionized water and the samples analyzed were the SOA aged in H_2SO_4 after 2 days. The excitation wavelength varied over the 200-500 nm range in 5 nm steps, and the emitted fluorescence was recorded over the 300-600 nm range in 2 nm steps for the excitation-emission spectra.

3.4 Results and Discussion

3.4.1 Chemical Composition of Fresh α -pinene SOA

Figure 3.2 shows a representative high-resolution mass spectrum of the fresh α -pinene ozonolysis SOA, where the peaks are normalized to the sum of peak abundances. The mass spectrum is similar to the previous ESI mass spectra reported for α -pinene ozonolysis SOA with distinct monomer (<250 Da) and dimer (250-450 Da) regions, which correspond to products with one and two oxygenated α -pinene units. The five most abundant monomer peaks have monoisotopic molecular masses of 186.089 Da ($\text{C}_9\text{H}_{14}\text{O}_4$, pinic acid), 172.074 Da ($\text{C}_8\text{H}_{12}\text{O}_4$, terpenylic acid), 198.089 Da ($\text{C}_{10}\text{H}_{14}\text{O}_4$, oxopinonic acid), 200.105 Da ($\text{C}_{10}\text{H}_{16}\text{O}_4$, 10-hydroxypinonic acid), and 216.100 Da ($\text{C}_{10}\text{H}_{16}\text{O}_5$). The molecular formulas and most

likely identities for these products appear in parentheses.^{127,128} The five most abundant dimer peaks have monoisotopic molecular masses of 354.204 Da ($C_{19}H_{30}O_6$), 368.184 Da ($C_{19}H_{28}O_7$), 338.209 Da ($C_{19}H_{30}O_5$), 358.163 Da ($C_{17}H_{26}O_8$), and 370.199 Da ($C_{19}H_{30}O_7$). These most abundant monomers and dimers has been commonly observed in both lab-generated and ambient SOA samples, confirming that our starting SOA material is representative of typical α -pinene SOA.^{120,128,129,147,148}

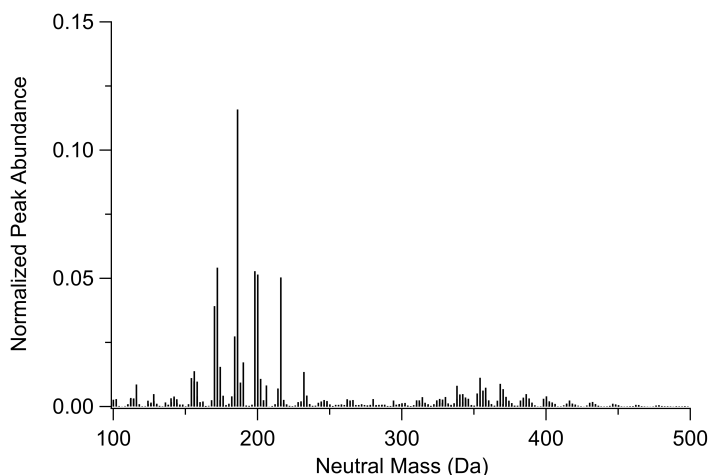


Figure 3.2: Retention time integrated mass spectra of fresh α -pinene ozonolysis SOA. Peaks were normalized to the combined peak abundance.

3.4.2 Chemical Composition of Aged α -pinene SOA

Figure 3.3 shows mass spectra of SOA α -pinene ozonolysis samples aged for 2 days in various concentrations of sulfuric acid. Specific details of the aging conditions are outlined in Table 3.1. The mass spectra of the SOA aged in moderately acidic conditions (Fig. 3.3a-c) are very similar to the mass spectrum of fresh SOA (Fig. 3.2). The mass spectra have similarly well-defined monomer (<250 Da) and dimer regions (250-450 Da). The dominant peaks in the monomer and dimer regions are also similar. The top 5 monomer peaks correspond to 186.089 Da ($C_9H_{14}O_4$, pinic acid), 172.074 Da ($C_8H_{12}O_4$, terpenylic acid), 198.089 Da ($C_{10}H_{14}O_4$, oxopinonic acid), 200.105 Da ($C_{10}H_{16}O_4$, 10-hydroxypinonic acid), and 216.100

Da ($C_{10}H_{16}O_5$). The most prominent dimer peaks correspond to 338.2093 Da ($C_{19}H_{30}O_5$) and 368.184 Da ($C_{19}H_{28}O_7$). Additionally, peaks of organosulfur compounds are small in number and abundance. This implies that there is little to no evidence of acid catalyzed aging processes occurring under these moderately acidic conditions. This observation is consistent with previous work that showed that preexisting seeds and aerosol acidity did not result in significant increases in the intensities in oligomers, likely due to the relatively low acidity of the seeds.^{34,128}

In stark contrast, the mass spectrum of the SOA aged under the most acidic conditions of pH -1.08 (Fig. 3.3i) is notably different. There is no distinct monomer or dimer region, and organosulfur compounds have prominent peak abundances. The top 5 peaks corresponding to CHO compounds are 186.089 Da ($C_9H_{14}O_4$, pinic acid), 172.074 Da ($C_8H_{12}O_4$, terpenylic acid), 166.099 Da ($C_{10}H_{14}O_2$), 198.089 Da ($C_{10}H_{14}O_4$), and 158.058 Da ($C_7H_{10}O_4$). Additionally, the five strongest peaks corresponding to CHOS compounds are 238.051 Da ($C_9H_{14}SO_4$), 224.036 ($C_7H_{12}SO_6$), 280.062 Da ($C_{10}H_{16}SO_7$), 264.067 Da ($C_{10}H_{16}SO_6$), and 284.093 Da ($C_{10}H_{20}SO_7$). These compounds have been detected in both experimental studies^{39,149–151} as well as field studies all over the world including, the southeast US, Denmark, China, Finland, Germany, Greenland, and Norway^{152–161}. A more detailed list of peaks of interest can be found in Table 3.2.

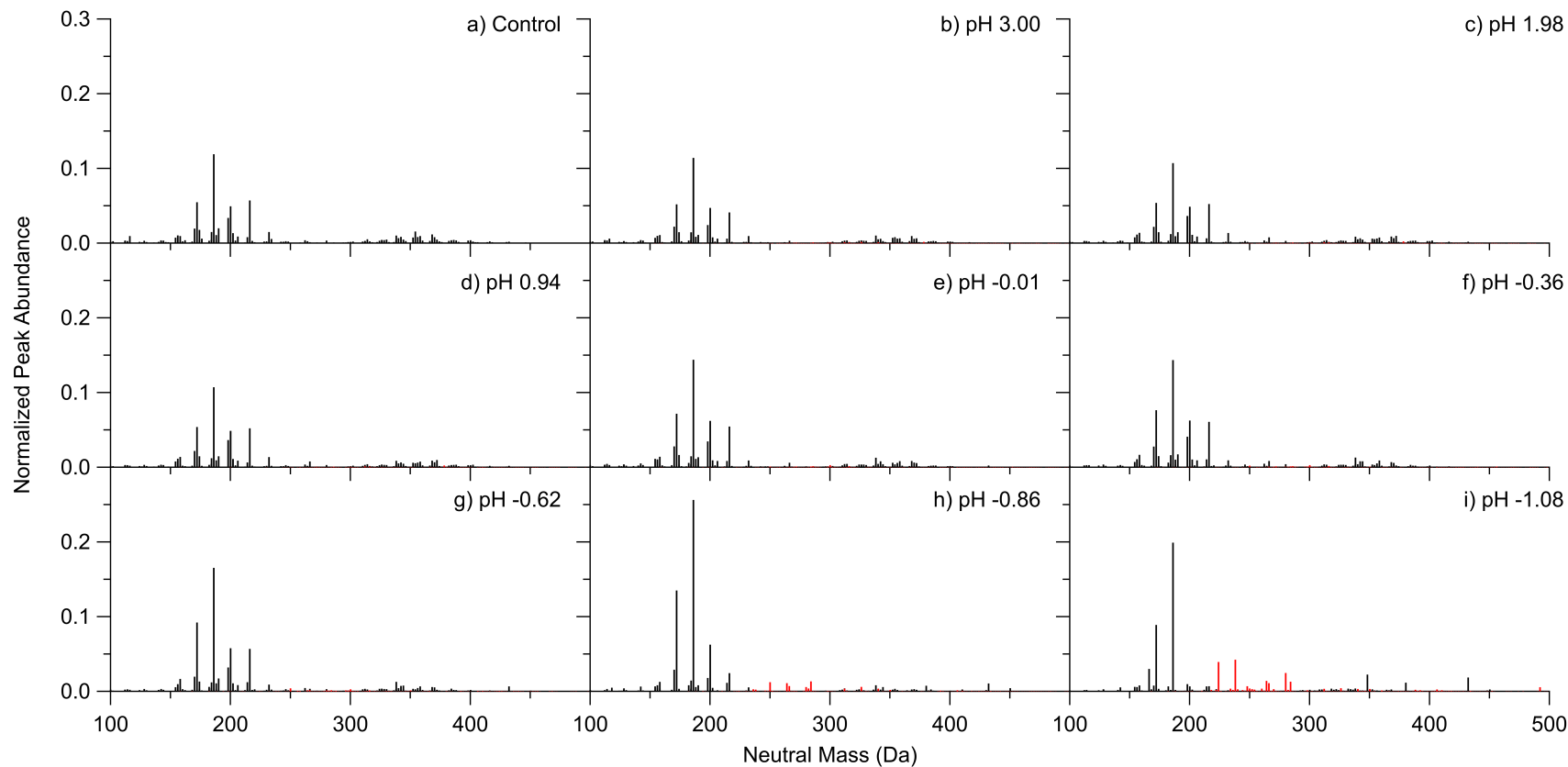
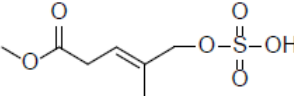
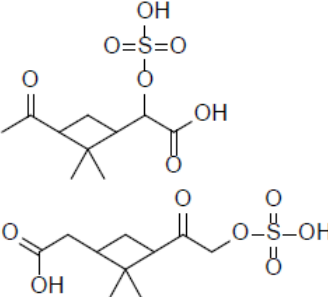
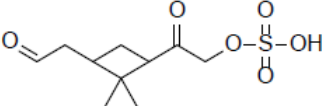


Figure 3.3: Mass spectra of α -pinene ozonolysis SOA samples aged for 2 days in (a) 0 M (control), (b) 0.52 mM (pH 3.00), (c) 6.4 mM (pH 1.98), (d) 90 mM (pH 0.94), (e) 1.0 M (pH -0.01), (f) 1.8 M (pH -0.36), (g) 3.2 M (pH -0.62), (h) 5.6 M (pH -0.86), and (i) 10 M (pH -1.08) of H_2SO_4 . Black traces correspond to CHO compounds, while red traces correspond to CHOS compounds. Mass spectra were derived by integrating over 2-16 min for each of the LC run and normalizing by the combined peak abundance.

Table 3.2: Some of the major CHOS compounds detected in Aged APIN SOA in pH -1.08 by Mass Spectrometry

Observed Molecular Weight (Da)	Compound Formulas and Suggested Structure	References
238.051	$C_8H_{14}SO_6$	Ma et al., 2014 Meade et al., 2016 Hettiyadura et al., 2019
224.036	 $C_7H_{12}SO_6$	Deng et al., 2021 Ma et al., 2014
280.062	 $C_{10}H_{16}SO_7$	Deng et al., 2021 Hallquist et al., 2009 Yttri et al., 2011 Kristensen et al., 2016 Nguyen et al., 2014 Brüggemann et al., 2019 Ma et al., 2014 Kristensen et al., 2011 Hansen et al., 2014 Meade et al., 2016
264.067	 $C_{10}H_{16}SO_6$	Ma et al., 2014
284.093	$C_{10}H_{20}SO_7$	Brüggemann et al., 2019 Ma et al., 2014

Most of our experiments in Figure 3.3 were for pH between 0 and -1 to determine whether the extent of chemical change in SOA was gradual or abrupt as a function of pH. The mass spectra of the SOA aged in pH 0.94 (Fig. 3.3d), pH -0.01 (Fig. 3.3e), pH -0.36 (Fig. 3.3f) and pH -0.62 (Fig. 3.3g) conditions are still fairly similar to the fresh SOA, in that the mass spectra have similar peak patterns in the monomer (<250 Da) and dimer (250-450 Da) regions. However, the mass spectrum of the SOA aged in pH -0.86 (Fig. 3.3h) has many

notable differences in comparison to the fresh SOA and is resembling the pH -1.08 mass spectrum (Fig. 3.3i). These differences include changes in the peak pattern in the monomer region (<250 Da) as well as evidence in peaks of organosulfur compounds colored in red in Figure 3.3. The top 5 monomer peaks SOA aged in pH -0.86 sample include 186.089 Da ($C_9H_{14}O_4$, pinic acid), 172.074 Da ($C_8H_{12}O_4$, terpenylic acid), 200.105 Da ($C_{10}H_{16}O_4$, 10-hydroxypinonic acid), 170.093 Da ($C_9H_{14}O_3$, pinalic acid), and 216.100 Da ($C_{10}H_{16}O_5$). Some of these peaks are the same as the strongest peaks in the fresh SOA, however the peaks vary in intensity compared to the fresh SOA. The major CHOS compounds correspond to 284.093 ($C_{10}H_{20}SO_7$), 250.087 ($C_{10}H_{18}SO_5$), 264.067 ($C_{10}H_{16}SO_6$), 266.082 ($C_{10}H_{18}SO_6$), and 326.019 ($C_{18}H_{30}SO_3$). In comparison to the SOA aged in pH -1.08 mass spectra, the pH -0.86 mass spectra have some key differences. These discrepancies include larger intensities of 200.105 Da ($C_{10}H_{16}O_4$, 10-hydroxypinonic acid), 170.093 Da ($C_9H_{14}O_3$, pinalic acid), and 216.100 Da ($C_{10}H_{16}O_5$) and missing some larger CHOS compounds (e.g., 238.051 ($C_8H_{14}SO_6$), 224.036 ($C_7H_{12}SO_6$)). This implies that even a relatively small change in pH (by 0.25 units) can have a strong effect on the disappearance of specific CHO and formation of CHOS compounds. The mass spectrometric analysis suggests that aging aerosols in highly concentrated sulfuric acid leads to significant changes in chemical composition, for example, the formation of organosulfur compounds. This is further illustrated by Figure 3.4, which shows the relative intensity of CHO and CHOS compounds for each sample. As the pH decrease, there is an increase in the relative abundance of organosulfur compounds, especially at the lowest pH values probed here. Specifically, when SOA α -pinene ozonolysis samples were aged in pH -0.86 and pH -1.08 conditions, the fraction of the observed organosulfur compounds was \sim 12% and 30%, respectively. Note that the concentration of sulfate varies in each experiment, however, the formation of organosulfur compounds is assumed to be probed by the change in pH rather than the increase in sulfate concentration as these reactions has shown to be pH dependent.

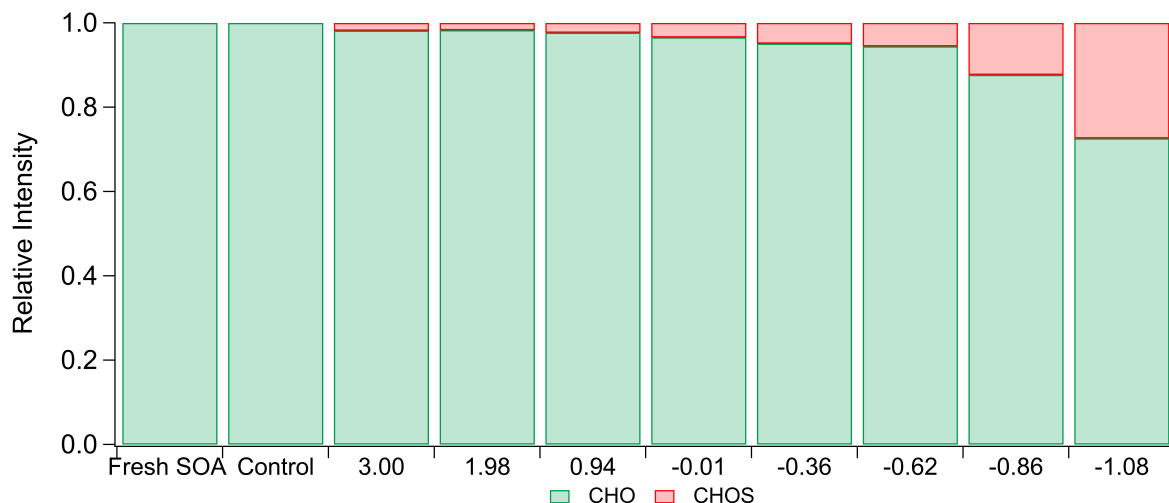


Figure 3.4: Overall Amounts of CHO and CHOS Compounds. Relative ion abundance of the CHO (green) and CHOS (red) compounds present in fresh and aged α -pinene ozonolysis SOA samples. The labels on the x-axis represent pH values from the E-AIM model (Table 3.1), except for pH 4.3 sample, which corresponds to the pH meter reading. The ion peak abundances for all observed CHO and CHOS compounds were added. CHOS compounds may be overestimated in this approach as they have higher ionization efficiencies in ESI.

3.4.3 Optical Properties and Kinetics of Aged α -pinene SOA

Wavelength dependent MACs for aged α -pinene SOA at various concentrations of sulfuric acid at 3 different time points of aging are summarized in Figure 3.5. The details of the aging conditions used for these experiments are explained in Table 3.1. The MAC spectra of the SOA aged in moderately acidic conditions (Fig, 2a-c) are very similar to the absorption spectra collected in a previous study.^{146,162,163} The shapes of the observed spectra of unaged SOA are consistent with the weak $n \rightarrow \pi^*$ transition in carbonyls superimposed on the smooth absorption band from peroxides.¹⁶⁴ Both peroxide and carbonyl functional groups are common in α -pinene ozonolysis SOA.^{127,128,165}

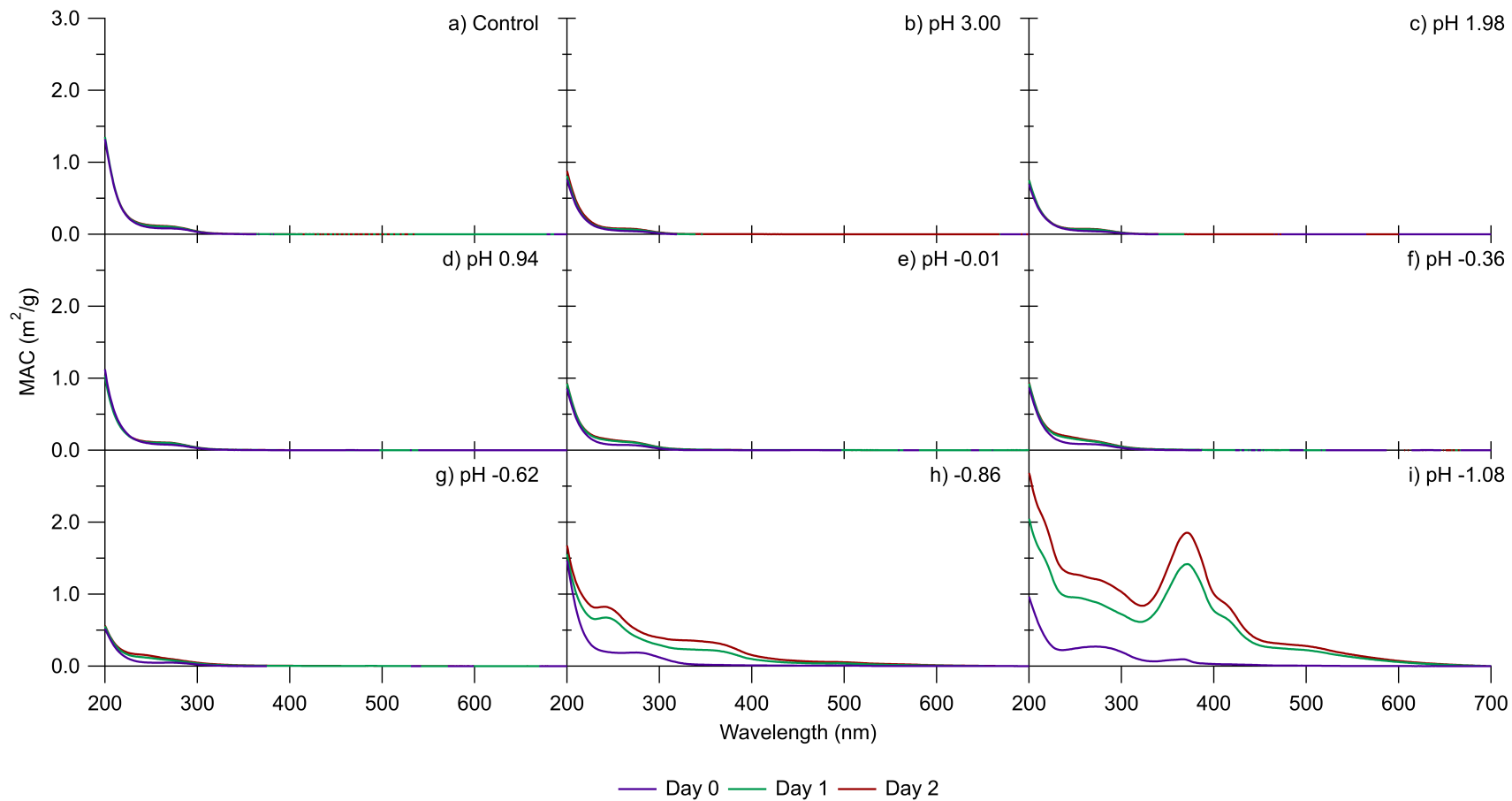


Figure 3.5: MAC spectra of α -pinene ozonolysis SOA samples aged for 0, 1, and 2 days in (a) 0 M (control), (b) 5.2×10^{-4} M (pH 3.00), (c) 6.4×10^{-3} M (pH 1.98), (d) 9.0×10^{-2} M (pH 0.94), (e) 1.0 M (pH -0.01), (f) 1.8 M (pH -0.36), (g) 3.2 M (pH -0.62), (h) 5.6 M (pH -0.86), and (i) 10 M (pH -1.08) solutions of H_2SO_4 .

As the concentration of sulfuric acid increases, the shape of the spectra changes when the pH reaches -0.86 and -1.08. At pH -0.86, two dominant peaks appear at 239 nm and 351 nm after one day of aging, can continue to increase during the second day of aging. The MAC spectrum of SOA aged in pH -1.08 (Fig. 3.5f) at Day 0 has a different shape from the MAC of unacidified SOA, with a small peak at 370 nm and 250 nm indicating that some chemistry happens already during 1-2 min between mixing the solution and taking the first spectrum. The spectra at Day 1 and Day 2 have 3 dominate peaks present at 254 nm, 370 nm, and 418 nm.

There have been reports of acid-catalyzed formation of chromophores from monoterpene ozonolysis SOA.^{93,141,142} Evaporation of SOA solutions the presence of sulfuric acid was found to enhance the absorbance, with the largest effect observed for d-limonene ozonolysis SOA. The authors attributed to this observation to acid catalyzed dehydration resulting in higher unsaturation (e.g., as a result of adol condensation).^{141,142} Song et al. (2013) did not observe brown carbon formation for α -pinene O₃ system in the presence of neutral or acidic seeds, therefore it is likely the pH of these seeds were not as acidic as the samples used in this study.⁹³

Figure 3.6a shows the UV-Vis spectra of α -pinene ozonolysis SOA samples aged in 5.6M (pH -0.86) taken with a higher time resolution, where each spectrum was collected every 15 min over 24 h. Again, two dominate peaks at 239 nm and 351 nm were observed. Assuming first order kinetics, the lifetime of browning for the peaks of interest were relatively slow as indicated in Table 3.3. The times series plots for each peak, in which the lifetimes of browning were calculated, are shown in Figure 3.7. The color change after 24 h of aging for pH -0.86 sample is relatively small (see the photograph in Fig. 3.6). On the other hand, there is a large color change in the α -pinene ozonolysis SOA samples aged at pH -1.08, where after 24 h of aging, the sample has a dark orange, brown tint (Fig. 3.6). The spectra (SOA

samples aged at pH -1.08 (Fig. 2.6b) show that five distinct absorption peaks at 254 nm, 273 nm, 370 nm, 418 nm, and 500 nm, all of which have a much faster lifetime of browning (Table 3.3) than for the pH -1.08 sample. These observations of the formation of light absorbing compounds for α -pinene ozonolysis SOA samples aged at pH -0.86 and pH -1.08, are consistent with the change in chemical composition indicated by its respective mass spectra.

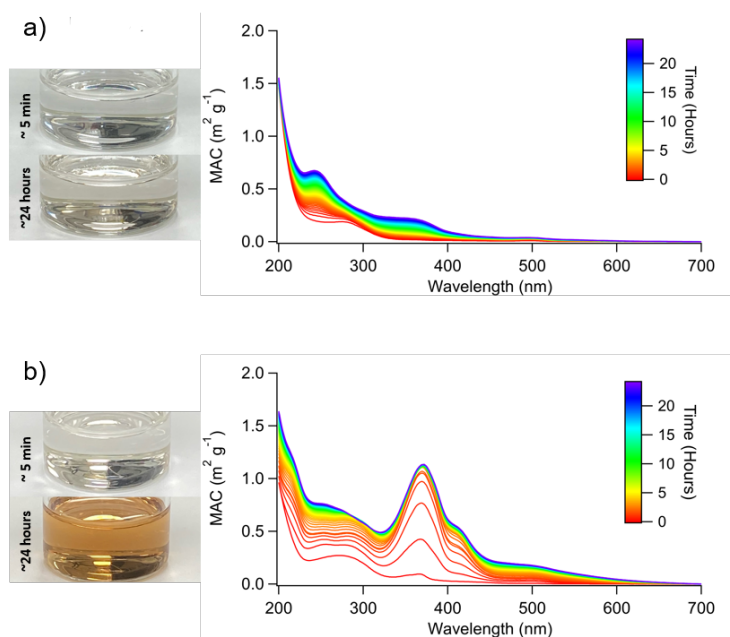


Figure 3.6: MAC absorption spectra of α -pinene ozonolysis SOA samples aged in (a) 5.6 M (pH -0.86) and (b) 10 M (pH -1.08) of H_2SO_4 collected every 15 min over 24 h. Photographs of SOA and acid solution after ~ 5 min and ~ 24 h of aging

SOA samples aged at pH -1.08 were also analyzed using fluorescence spectroscopy (Figure 3.8). A relatively fluorescence band appeared at $\lambda_{\text{ex}} \approx 450 \text{ nm} / \lambda_{\text{em}} \approx 520 \text{ nm}$. The presence of this band is indicative of the formation of strongly conjugated products.

3.4.4 HPLC Analysis of the Chromophores

Figure 4 shows the HPLC-PDA chromatograms for α -pinene ozonolysis SOA samples aged in (a) 5.6 M (pH -0.86), and (b) 10 M (pH -1.08) solutions of H_2SO_4 . The chromatograms

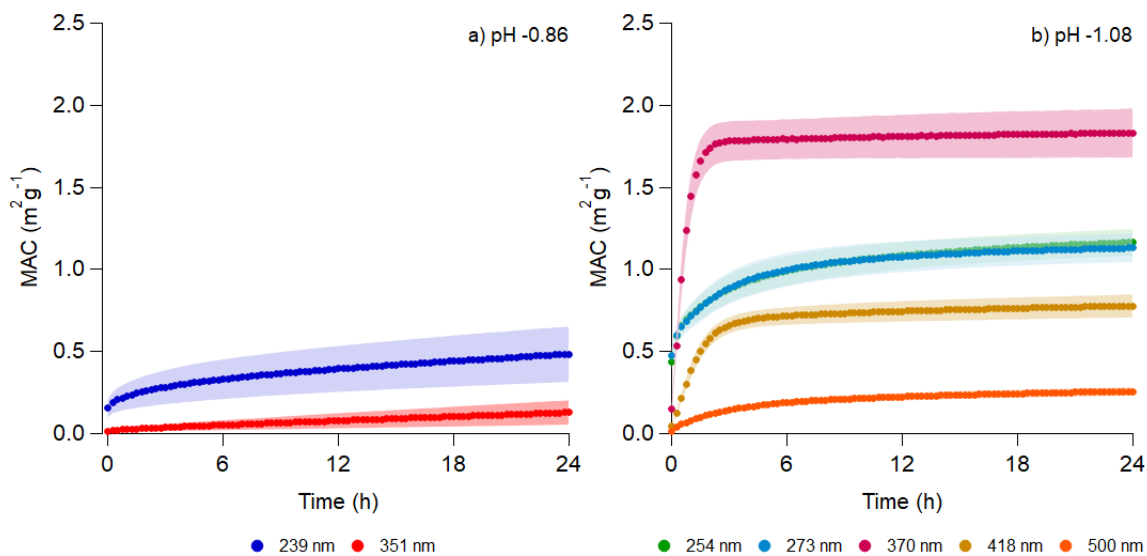


Figure 3.7: Time Dependent MAC for peaks of interest in SOA samples aged in pH -0.86 and pH -1.08

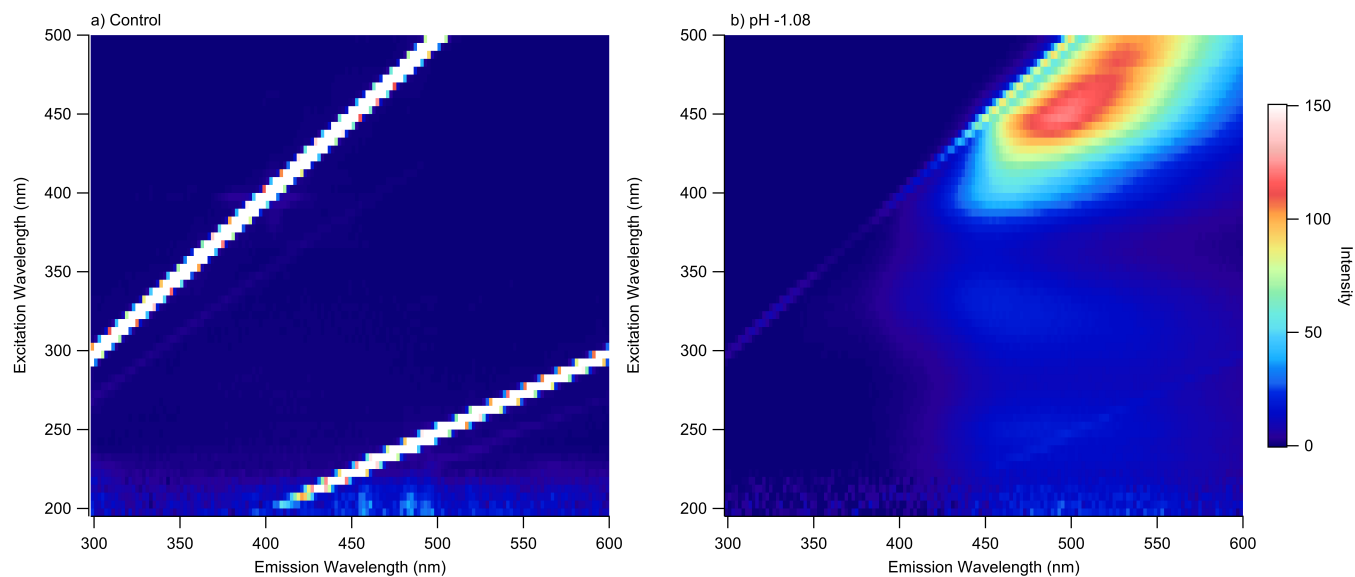


Figure 3.8: Fluorescence of APIN SOA Excitation-emission matrix plot for water (a), pH -1.08 solution (b), and SOA aged at pH -1.08. There is no visible fluorescence in the controls, however a relatively weak fluorescence band appeared at $\lambda_{\text{ex}} \approx 450 \text{ nm} / \lambda_{\text{em}} \approx 520 \text{ nm}$ in the aged SOA sample.

Table 3.3: Lifetime of browning for several peaks on interest in α -pinene ozonolysis SOA samples aged in 5.6M (pH -0.86), and 10 M (pH -1.08) H_2SO_4 . Lifetimes were calculated by assuming pseudo first order reactions in the times series fits for each peak.

Sample	Peaks of Interest (nm)	Lifetime of Browning (h)
pH -0.86	239	13 ± 2
pH -0.86	351	49 ± 3
pH -1.08	254	4.6 ± 0.6
pH -1.08	273	3.8 ± 0.6
pH -1.08	370	0.68 ± 0.06
pH -1.08	418	1.51 ± 0.07
pH -1.08	500	5.0 ± 0.3

have well defined peaks, which we attempted to identify by correlating PDA and TIC chromatograms. Due to a very large number of co-eluting compounds, it was difficult to definitively associate the molecular formulas in the HRMS chromatograms with the peaks appearing in the PDA chromatograms. Therefore, additional SOA samples were prepared and aged, and the positive ion mode data were acquired. Figure 3.10 shows the HPLC chromatograms associated with the PDA and positive ion mode HRMS for α -pinene ozonolysis SOA samples aged in 10 M (pH -1.08) of H_2SO_4 . The peak at 11.39 min in the PDA chromatogram corresponds to the peak at 11.46 min in the MS chromatogram (there is a 0.06 min time delay between the PDA and the HRMS analyzers). The best match was with an ion at m/z 151.112 ($\text{C}_{10}\text{H}_{15}\text{O}^+$), which had a strikingly similar single-ion chromatogram to the PDA chromatogram (triplet peaks at 11.39 min, 11.59 min, and 11.71 min). Efficient chromophores tend to have either a heteroatom or high level of aromaticity. However, the $\text{C}_{10}\text{H}_{14}\text{O}$ compound corresponding to this ion does not have a heteroatom and has a low aromaticity index¹⁶⁶ of 0.33, suggesting that this may have been a fragment of the original chromophore rather than the chromophore itself. Other coeluting ions either do not have similar chromatograms as the PDA and higher weight oligomers MS/MS spectra do not have m/z 151.112 ($\text{C}_{10}\text{H}_{15}\text{O}^+$) as a corresponding fragment. At this time, we do not have conclusive information about the molecular formulas of the chromophores in the aged SOA,

but we are currently testing select α -pinene oxidation compounds (such as pinonic acid and pinonaldehyde) to obtain more information.

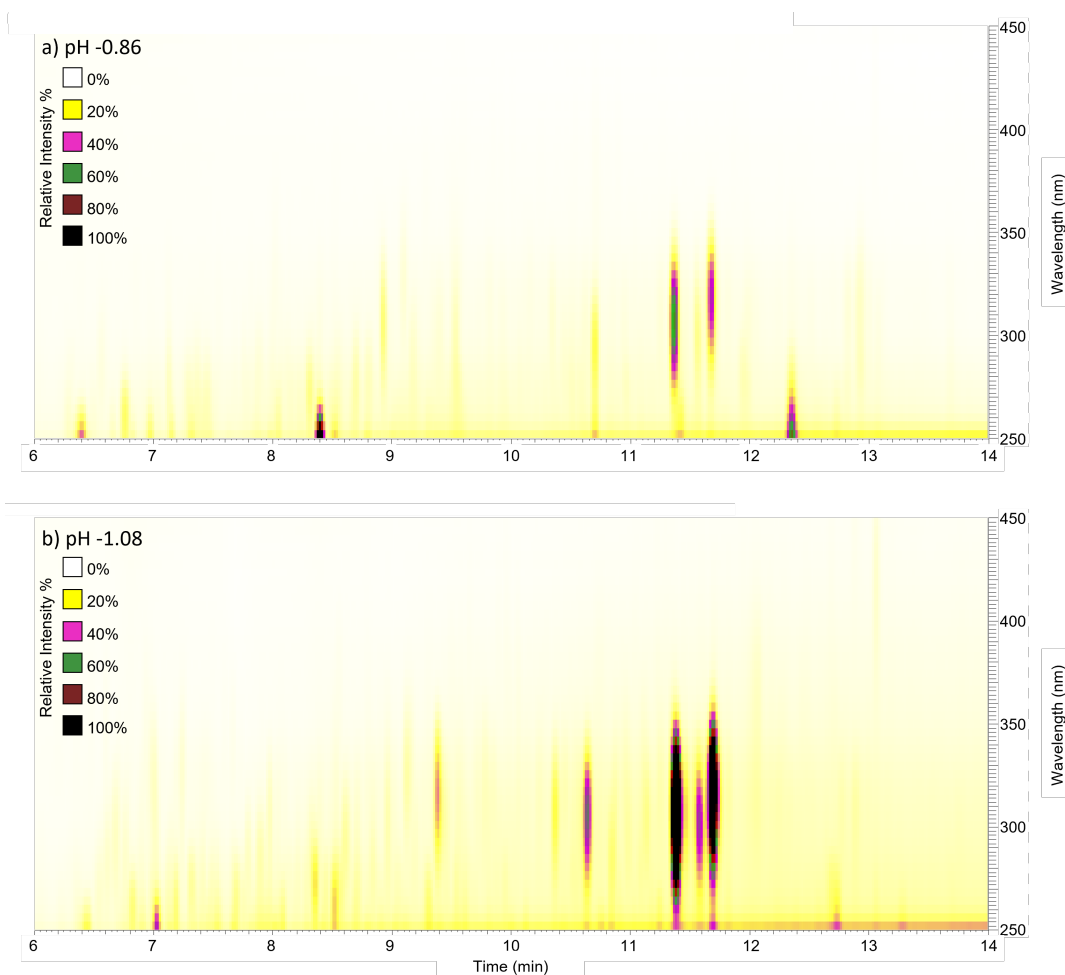


Figure 3.9: UPLC-PDA chromatograms of α -pinene ozonolysis SOA samples aged in (a) 5.6 M (pH -0.86) and (b) 10 M (pH -1.08) of H_2SO_4 .

3.4.5 Comparison of PDA and UV-Vis Absorption Spectra

Figure 3.9a showing the PDA chromatograms indicates that there are four major chromophores that absorb radiation in the near-UV region, with the longest wavelength peaks appearing at 300-350 nm when SOA is aging in 5.6 M H_2SO_4 . As the concentration of the acid increases to 10 M H_2SO_4 , a few additional peaks appear, however, all of them are still

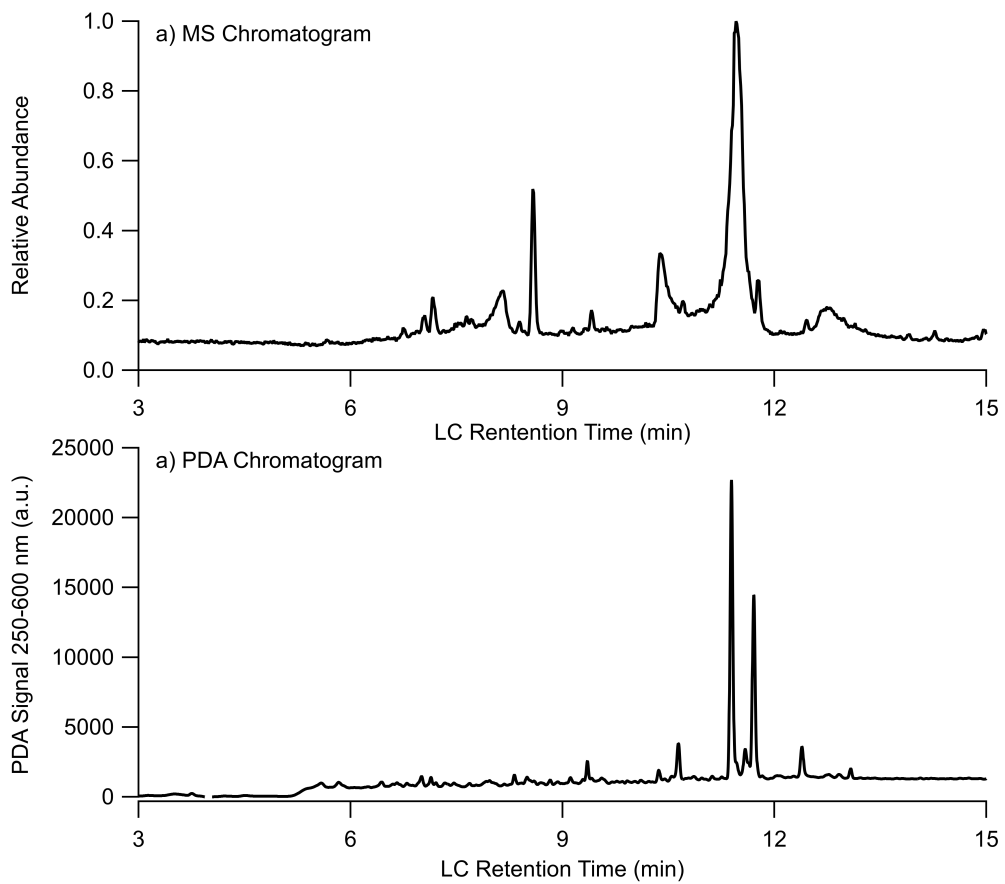


Figure 3.10: Positive ion mode HRMS and PDA chromatogram between 3-15 min for α -pinene ozonolysis SOA aged in pH -1.08 conditions for 2 days.

confined to wavelengths below 350 nm, in stark contrast with the results of Fig. 3.6, which shows measurable absorbance extending beyond 600 nm.

Initially, we could not reconcile the peak wavelengths observed in the PDA absorption spectra (Figure 3.9) and UV-Vis absorption spectra (Figure 3.6). For example, no absorption was detected by the PDA above 400 nm, even though MAC of the pH -1.08 sample extended all the way to 700 nm in Figure 3.6. After verifying the wavelength calibration of the PDA detector, a series of additional experiments was conducted to understand whether this shift was due to the lower acidity of the water-acetonitrile eluent used in UPLC. A sample of SOA aged in acid for 2 days was diluted with the solvents used in the liquid chromatography method, which is outlined in Table 3.4. The absorption spectra were collected for each sample to monitor a shift in peak absorbance, which are shown in Figure 3.11.

Table 3.4: Solution Acidity in Peak Shift Experiments. SOA samples aged at pH -1 were diluted with 1:1 ACN:H₂O and H₂O. Estimated pH was calculated using Extended Aerosol Inorganics Model (E-AIM (<http://www.aim.env.uea.ac.uk/aim/aim.php>)).

Sample	Dilution Factor	Estimated pH(E-AIM)
Control	1	-1.08
3:4 Dilution Factor	1.3	-0.97
2:3 Dilution Factor	1.5	-0.93
1:2 Dilution Factor	2	-0.817
1:3 Dilution Factor	3	-0.646
1:4 Dilution Factor	4	-0.517
1:5 Dilution Factor	5	-0.415
1:8 Dilution Factor	5	-0.2

The sample was first diluted with 1:1 ACN:H₂O, shown in Figure 3.11a, because the majority of the mobile phase constitutes of a mixture of ACN and H₂O. At a certain level of dilution, the original dominant peak at 354 nm in the spectrum shifts to 310 nm, which corresponds well to the peak seen in the PDA data. The peaks at 418 and 500 nm are also reduced. This explains why we could not detect peaks at longer wavelengths in the PDA data. Using water

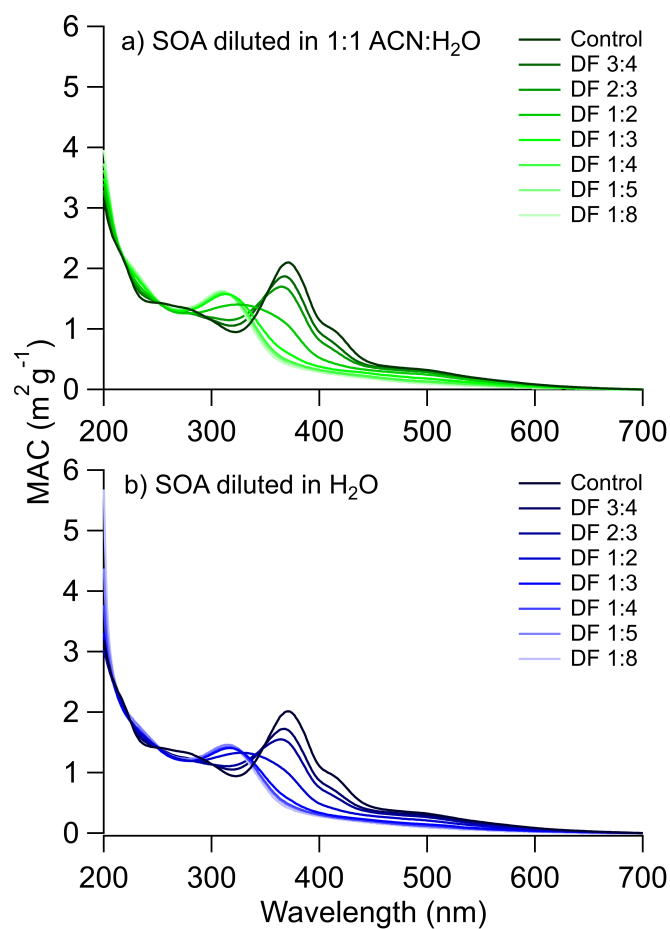


Figure 3.11: MAC absorption spectra of α -pinene ozonolysis SOA samples aged in 10 M (pH -1.08) of H_2SO_4 diluted with 1:1 ACN/ H_2O and H_2O at various dilution factors. DF, dilution factor.

instead of water-acetonitrile mixture led to similar observations (Fig. 3.11b). This type of spectral shift is most likely promoted by changing acid-base equilibria resulting from the sample dilution. There are known precedents for the absorption spectra of atmospherically-relevant compounds to be pH dependent, for example, spectra of nitrophenols shift to longer wavelengths at basic pH due to formation of phenolates.^{167–169} There have been other studies that shown that the absorption properties of imidazole-2-carboxaldehyde and pyruvic acid can be altered depending on the pH on its environment, which is prompted by acid base equilibria.^{48,170} Additionally, the pH dependence of the aerosol absorption has also been detected in field samples collected in southeastern United States and Beijing^{171,172} It should also be recognized that a large number of acid-base indicators change their spectra at well-defined pH points. It appears that the (currently unidentified) chromophoric products produced from α -pinene SOA in presence of a concentrated sulfuric acid similar have such halochromic properties. Understanding the characteristics of such halochromic chromophores is important, as water in the atmosphere, in the form of water vapor, cloud and fog droplets, and aerosol liquid water, can influence the acidity environment over a wide range.

3.5 Conclusions

Acid-catalyzed and acid-driven reactions can have a large effect on the chemical composition and properties of organic aerosol, which can spend days to weeks in the atmosphere. The impacts of highly acidic conditions on aerosol chemical composition and optical properties were explored by generating α -pinene ozonolysis SOA and aging the resulting SOA in bulk sulfuric acid solutions with atmospherically relevant acidities. We found that aging of SOA under highly acidic conditions resulted in significant changes in the SOA chemical composition, including the formation of organosulfur compounds and chromophores.

These findings are especially important in the context of the upper troposphere and the lower stratosphere (UTLS). Aerosols are widespread at high altitudes, most likely formed by condensation of gas-phase precursors brought up by deep convection.¹⁷³⁻¹⁷⁵ The aerosols in this region are primarily composed of sulfuric acid (40-80 wt%), but they also contain and significant amount organic compounds.^{4,5,7,10,81} The findings from this work further our understanding of how the chemical reactions between sulfuric acid and organic compounds can proceed over the long lifetime of the UTLS aerosols. Specifically, these interactions can change the chemical composition and optical properties of the UTLS aerosols over a long-time scale and therefore have a large influence in radiative energy fluxes. However, in this work, the experiments were performed at ambient temperatures, and it is expected that lower temperatures, such as those in the UTLS, can affect the rate of the acid catalyzed browning processes.

Chapter 4

Formation of chromophores from *cis*-pinonaldehyde in highly acidic conditions

Acknowledgement of Work

This work was done in collaboration with Jessica E. Pazienza, from the Rychnovsky Group. The project was led by me, with responsibilities encompassing the direction of the research and the execution of foundational experiments. These experiments involved aging monoterpene products in different concentrations of sulfuric acid, conducting UPLC-PDA-HRMS analysis, performing kinetic analysis, as well as determining atmospheric relevance of the formed products. Jessica E. Pazienza was responsible for synthesizing *cis*-pinonaldehyde, isolating the chromophores, devising additional synthetic experiments, and conducting NMR analysis to determine the identity of the chromophores, and contributing to the development of mechanisms.

4.1 Abstract

The highly acidic environment in atmospheric aerosol particles can promote acid-catalyzed and acid-driven reactions, including those in secondary organic aerosols (SOA). Previous studies observed enhanced absorption at visible wavelengths and significant changes in the chemical composition when SOA was exposed to sulfuric acid, however the specific chromophores could not be identified. The goals of this study are to identify the chromophores and determine the mechanism of browning in highly acidified α -pinene SOA by following the behavior of select α -pinene oxidation products, namely *cis*-pinonic acid and *cis*-pinonaldehyde, when they are exposed to highly acidic conditions. Chemical analysis of the resulting reactions was performed with ultra-performance liquid chromatography coupled with photodiode array spectrophotometry and high-resolution mass spectrometry, UV-vis spectrophotometry, and nuclear magnetic resonance spectroscopy. We found that *cis*-pinonic acid forms homoterpenyl methyl ketone while *cis*-pinonaldehyde forms 1-(4-(propan-2-ylidene)cyclopent-1-en-1-yl)ethan-1-one and two regioisomers of 1-(4-isopropylcyclopenta-1,3-dien-1-yl)ethan-1-one under highly acidic conditions.

4.2 Introduction

Atmospheric aerosols are important constituents in the atmosphere because they play a pivotal role in climate, air quality, and health.^{15,20,23} Organic compounds account for a significant fraction (20-90%) of particulate mass.^{101,176} The most common class of atmospheric aerosol is secondary organic aerosol (SOA), which is formed through nucleation, condensation, and multiphase chemical processing of oxidation products of volatile organic compounds (VOCs).^{16,22} The chemical complexity of SOA translates into a wide range of physical and chemical properties. Of particular interest to this work is the absorption coefficient of SOA,

which is often controlled by a small fraction of chromophores.¹⁷⁷

Aerosols exhibit a wide range of acidities, with SOA typically ranging between pH -1 to 5.⁴⁷ Particle acidity can be driven by the presence of sulfuric acid, which is the terminal product of atmospheric oxidation of sulfur-containing compounds. In the planetary boundary layer, there is generally enough ammonia to partly neutralize sulfuric acid, but in the stratosphere, it is common to have aerosol particles containing as much as 80% of sulfuric acid by weight.^{4,143,178} Acidity can also govern different processes in the atmosphere such as deposition, gas-particle partitioning, new particle formation, and mass and chemical composition^{47,48} There are many reactions in the atmosphere that can be acid-catalyzed or acid-driven. These include hemiacetal and acetal formation, hydration of aldehydes and ketones, aldol condensation, ring-opening reactions, oxidation of acids, and esterification of carboxylic acids.⁴⁸

One of the largest contributors to SOA is α -pinene, with estimated emissions ~ 66 Tg/year.¹⁷⁹ Both (+) and (-) enantiomers of α -pinene are emitted by vegetation. Once emitted, α -pinene can react with O_3 , OH, or NO_3 which leads to the production of multifunctional organic compounds including carbonyl, hydroxyl, peroxide, and other functional groups. *Cis*-pinonic acid and *cis*-pinonaldehyde are two major products from ozonolysis and photooxidation of both (+) and (-) α -pinene and important tracers of α -pinene chemistry. *Cis*-pinonic acid is a C10 ketocarboxylic acid with a rigid, four-membered carbon ring containing an acetyl and a carboxyl group on the opposing ends of the cyclobutene core, as shown in Figure 4.1. *Cis*-pinonaldehyde (Figure 4.1) has the same structure with a formyl group in place of the carboxyl group, making it a ketoaldehyde. These compounds are both semivolatile compounds that can either exist in the gas or particle phase and have been found in forested, urban, and rural areas. The properties and fate of *cis*-pinonic acid and *cis*-pinonaldehyde has also been extensively in the lab.^{77,96,180-184} Studies have shown the reactive uptake *cis*-pinonaldehyde

on acidic sulfate aerosols resulted in the formation of organosulfates, highlighting the importance of heterogeneous reactions.^{77,96,183}

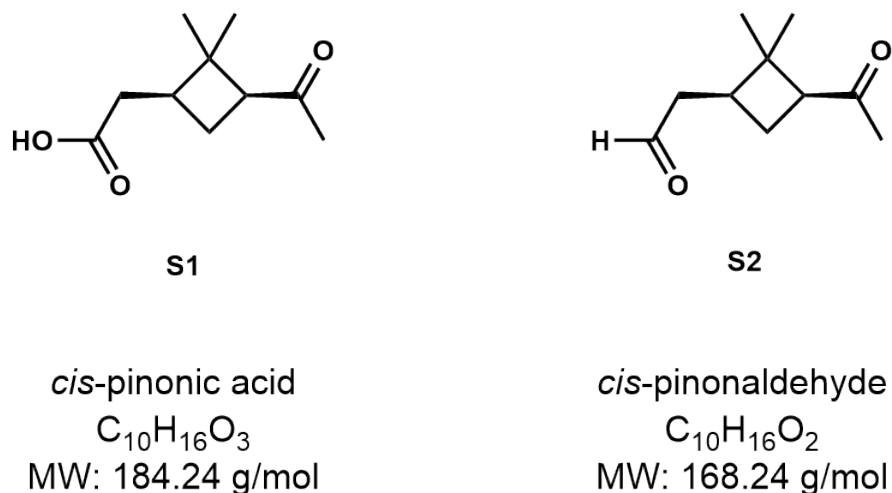


Figure 4.1: Structures of *cis*-pinonic acid and *cis*-pinonaldehyde

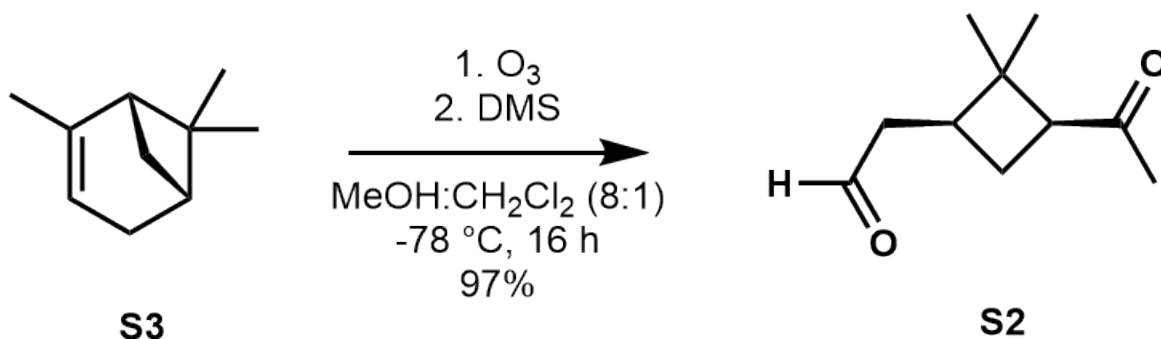
Previous work explored chemical changes that may occur upon partitioning of SOA compounds into highly acidic particles.^{141,142,185} One study found that the evaporation of bulk SOA in the presence of sulfuric acid resulted in enhanced mass-normalized absorption coefficient at visible wavelengths and significant changes in the chemical composition, including organosulfate formation.^{141,142} The following study, which offered a more careful control of pH, reported facile formation of light-absorbing compounds, also known as brown carbon, and organosulfates at highly acidic conditions (at pH \sim -1).¹⁸⁵ However, these studies could not identify specific chromophores responsible for the enhanced light absorption. The aim of this work is to determine the mechanism of browning, which refers to the formation of light-absorbing compounds, in highly acidified α -pinene SOA by following the behavior of specific common α -pinene oxidation products, namely *cis*-pinonic acid and *cis*-pinonaldehyde, when they are exposed to highly acidic conditions. Our results suggest that *cis*-pinonic acid undergoes an acid-catalyzed tautomerization when aged in highly acidic conditions, while *cis*-pinonaldehyde reacts with the acid 1-(4-(propan-2-ylidene)cyclopent-1-en-1-yl)ethan-1-one and two regioisomers of 1-(4-isopropylcyclopenta-1,3-dien-1-yl)ethan-1-one. These products

formed from *cis*-pinonaldehyde serve as building blocks for more complex compounds responsible for browning of acid-aged SOA observed in previous studies.

4.3 Experimental Methods and Materials

4.3.1 Chemicals

The following reagents were acquired from commercial sources: *cis*-pinonic acid (Sigma Aldrich, 98%), sulfuric acid (Fisher Scientific, 96%), (+)- α -pinene (Fisher Scientific, 98%), and dimethylsulfide (DMS) (Sigma Aldrich). *Cis*-pinonaldehyde was synthesized based on the following published procedures, shown in Scheme 4.1.^{186,187}



Scheme 4.1: Synthesis of *cis*-pinonaldehyde (S2)

A round bottom flask containing a stirred solution of (+)- α -pinene (0.5 mL, 3.16 mmol, 1 eq) dissolved in a solution of MeOH (28 mL) and CH₂Cl₂ (3.5 mL) was cooled to -78°C. Ozone (O₃) was bubbled through the solution via a commercial ozone generator until a blue color persisted. The ozone generator was turned off and O₂ bubbled through the solution until the blue color faded. While stirring at -78°C, DMS (4.2 mL, 56.9 mmol, 18 eq) was added dropwise. The solution was stirred overnight while gradually warming to room temperature as the dry ice/acetone bath evaporated. The reaction mixture was quenched with water,

extracted with CH_2Cl_2 (4 x 30 mL), washed with brine (1 x 60 mL), dried over Na_2SO_4 , filtered, and concentrated under reduced pressure to afford crude pinonaldehyde as a clear, colorless oil. The mixture was purified via flash chromatography (15% EtOAc/Hex isocratic) to afford S2 as a clear, colorless oil (417 mg, 97%) containing trace amounts of EtOAc. Product was too volatile to be dried under high vacuum. The following is the characterization information for S2.

^1H NMR (500 MHz, CDCl_3): δ 9.63 (s, 1H), 2.83 (dd, $J = 10.0, 7.8$ Hz, 1H), 2.57–2.20 (m, 3H), 1.94 (s, 3H), 1.85 (ddd, $J = 19.1, 9.2, 2.5$ Hz, 2H), 1.24 (s, 3H), 0.74 (s, 3H).

$^{13}\text{C}\{^1\text{H}\}$ NMR (126 MHz, CDCl_3): δ 207.3, 201.3, 54.2, 45.0, 43.2, 35.7, 30.2, 30.1, 22.7, 17.5.

ESI-TOF-MS) m/z : Calcd for $\text{C}_{10}\text{H}_{16}\text{O}_2\text{Na}^+$ $[\text{M}+\text{Na}]^+$ 191.1048; Found 191.1041.

4.3.2 Aging in Sulfuric Acid

For initial tests, *cis*-pinonic acid and *cis*-pinonaldehyde were dissolved in 10M H_2SO_4 , resulting in an effective pH of -1.08 , with dissolution in water serving as control. (The pH values cited in this work correspond to negative logarithm of molality of H^+ , which is estimated with E-AIM model.)^{143–145} Once it was confirmed that there were significant changes in the composition and optical properties of the acidified sample, additional experiments were done at varying acidities. In all cases, an aliquot of the stock *cis*-pinonic acid and *cis*-pinonaldehyde with a concentration of ~ 2000 $\mu\text{g}/\text{mL}$ was added to ~ 4 mL solution containing H_2SO_4 (Table 4.1), resulting in a mass concentration of ~ 35 – 70 $\mu\text{g}/\text{mL}$.

Table 4.1: Solution Acidity in Aging Experiments. The first column lists the molar concentration of H_2SO_4 added to the solution. The molalities of $[\text{H}^+]$ and other ions were calculated using the Extended Aerosol Inorganics Model* (E-AIM, <http://www.aim.env.uea.ac.uk/aim/aim.php>). The effective pH values listed in the last column and quoted in the paper represent the negative logarithm of molality of $[\text{H}^+]$.

Estimated Concentration of H_2SO_4	pH Meter Reading	E-AIM Output				
		$[\text{HSO}_4^-]$ (mol/kg)	$[\text{SO}_4^{2-}]$ (mol/kg)	$[\text{H}^+]$ (mol/kg)	Activity Coefficient of H^+	Effective pH = $-\log[\text{H}^+]$
0 M	5-6	-	-	-	-	Control
0.52 mM	2.7	0.0000386	0.000481	0.00100	0.96	3.00
5.6 M	-	3.96	1.67	7.30	3.7	-0.86
10 M	-	8.10	1.93	12.0	20	-1.08

*The extended aerosol inorganic model I (E-AIM) was utilized to estimate the molalities and activities of ions present in the sulfuric acid solutions.^{143–145} For consistency, we will use the effective pH in the last column to refer to experimental conditions used in this work.

4.3.3 Mass Spectrometry Analysis

Analysis of the aged monoterpene oxidation samples was conducted using a Thermo Scientific Vanquish Horizon ultra-performance liquid chromatography (UPLC) coupled with a Vanquish Horizon photodiode array (PDA) spectrophotometer and a Thermo Scientific Q Exactive Plus Orbitrap high resolution mass spectrometer to examine the chemical composition of the solution before and after aging. UPLC separation was carried out on a Waters HSS T3 column, 150×2.1 mm, with $1.8 \mu\text{m}$ particles, with the column temperature set to 30°C and a flow rate of $0.3 \text{ mL}/\text{min}$. The mobile phase consisted of water (eluent A) and acetonitrile (eluent B), each containing 0.1% formic acid. The gradient elution was programmed as follows: 0-3 min 95% eluent A; 3-14 min linear ramp to 95% eluent B; 14-16 min hold at 95% eluent B, 16-22 min return to 95% eluent A. The mass spectrometer was operated in both positive and negative ion mode with a spray voltage of 2.5 kV and a resolving power of $m/\Delta m = 1.4 \times 10^5$.

4.3.4 Spectroscopic Measurements

UV-Vis spectrophotometer (Shimadzu UV-2450) was used to monitor the formation of light-absorbing compounds over time. Aliquot of the samples were added to a 1 cm quartz cuvette and then capped to prevent evaporation. The spectrophotometer was programmed to collect a spectrum every 15 min for 24 h.

4.3.5 NMR Spectroscopy Measurements

Chemical shifts (δ) were referenced to the residual solvent peak. The ^1H NMR spectra were recorded at 500 MHz or 600 MHz using either a Bruker DRX500 (cryoprobe) or a Bruker AVANCE600 (cryoprobe) NMR, respectively. The ^{13}C NMR spectra were recorded at 126 MHz or 151 MHz on the Bruker DRX500 or Bruker AVANCE600 NMR, respectively. All NMR spectra were taken at 25°C. Chemical shifts (δ) are reported in parts per million (ppm) and referenced to residual solvent peak at 7.26 ppm (^1H) or 77.16 ppm (^{13}C) for deuterated chloroform (CDCl_3). The ^1H NMR spectral data are presented as follows: chemical shift, multiplicity (s = singlet, d = doublet, t = triplet, q = quartet, m = multiplet, dd = doublet of doublets, ddd = doublet of doublet of doublets, dddd = doublet of doublet of doublet of doublets, coupling constant(s) in hertz (Hz), and integration.

4.4 Results and Discussion

4.4.1 Ultra-Performance Liquid Chromatography

The total ion chromatograms (TIC) and PDA (190-690 nm) chromatograms of *cis*-pinonic acid aged in water for 2 days, 0.52 mM H_2SO_4 (pH 3.00), 5.6 M H_2SO_4 (pH -0.86), and 10

M H₂SO₄ (pH -1.08) are shown in Figure 4.2. The PDA (Fig. 4.2a,d), negative ion mode TIC (Fig. 4.2b,e), and positive ion mode TIC (Fig. 4.2c,f) chromatograms in pinonic acid aged in H₂O and 0.52 mM H₂SO₄ (pH 3.00) show a single major peak at 8.96 min. The PDA signal corresponds to weak absorbance of *cis*-pinonic acid due to the $n \rightarrow \pi^*$ and $\pi \rightarrow \pi^*$ transitions in the carbonyl group. The TIC signal is dominated by protonated (positive ion mode) or deprotonated (negative ion mode) *cis*-pinonic acid. The similarities between the chromatograms of *cis*-pinonic acid aged in H₂O and 0.52 mM H₂SO₄ (pH 3.00) indicate that it does not undergo acid catalyzed reactions under moderately acidic conditions.

However, when *cis*-pinonic acid was aged in highly acidic conditions, the chromatograms reveal chemical changes driven by acid-catalysis, in agreement with previous reports by Arcus and Bennett (1955).¹⁸⁸ In Figure 4.2g, which shows the PDA chromatograms of *cis*-pinonic acid aged in 5.6 M H₂SO₄ (pH -0.86), there are two peaks at 8.95 and 9.06 min. The negative ion mode TIC and SIC for m/z 183.1028 in Fig. 4.2h also has two peaks at these elution times. These peaks can be assigned to *cis*-pinonic acid and its enol tautomer, respectively. The peak at 9.06 was identified to be enol rather than the *trans*-pinonic acid because the $\pi \rightarrow \pi^*$ transition in the correspond PDA spectra is absent, as shown in Figure 4.2g. Additionally, the peak elutes later than *cis*-pinonic acid, indicating a less polar compound, consistent with the lower polarity of enol tautomers in keto-enol tautomerization. *Cis*-pinonic acid and the enol tautomer also appear the positive ion mode TIC and SIC for m/z 185.1177.

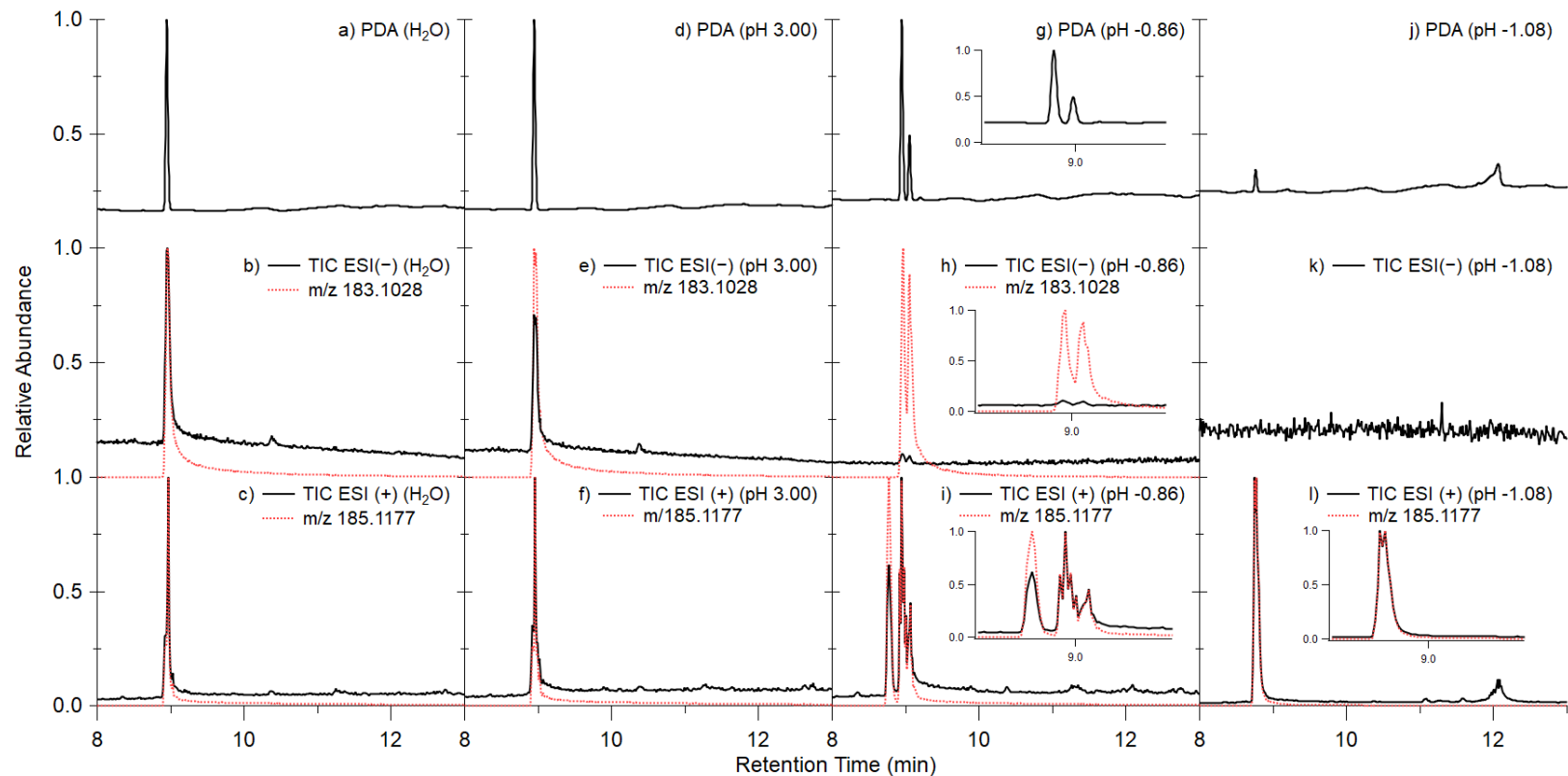
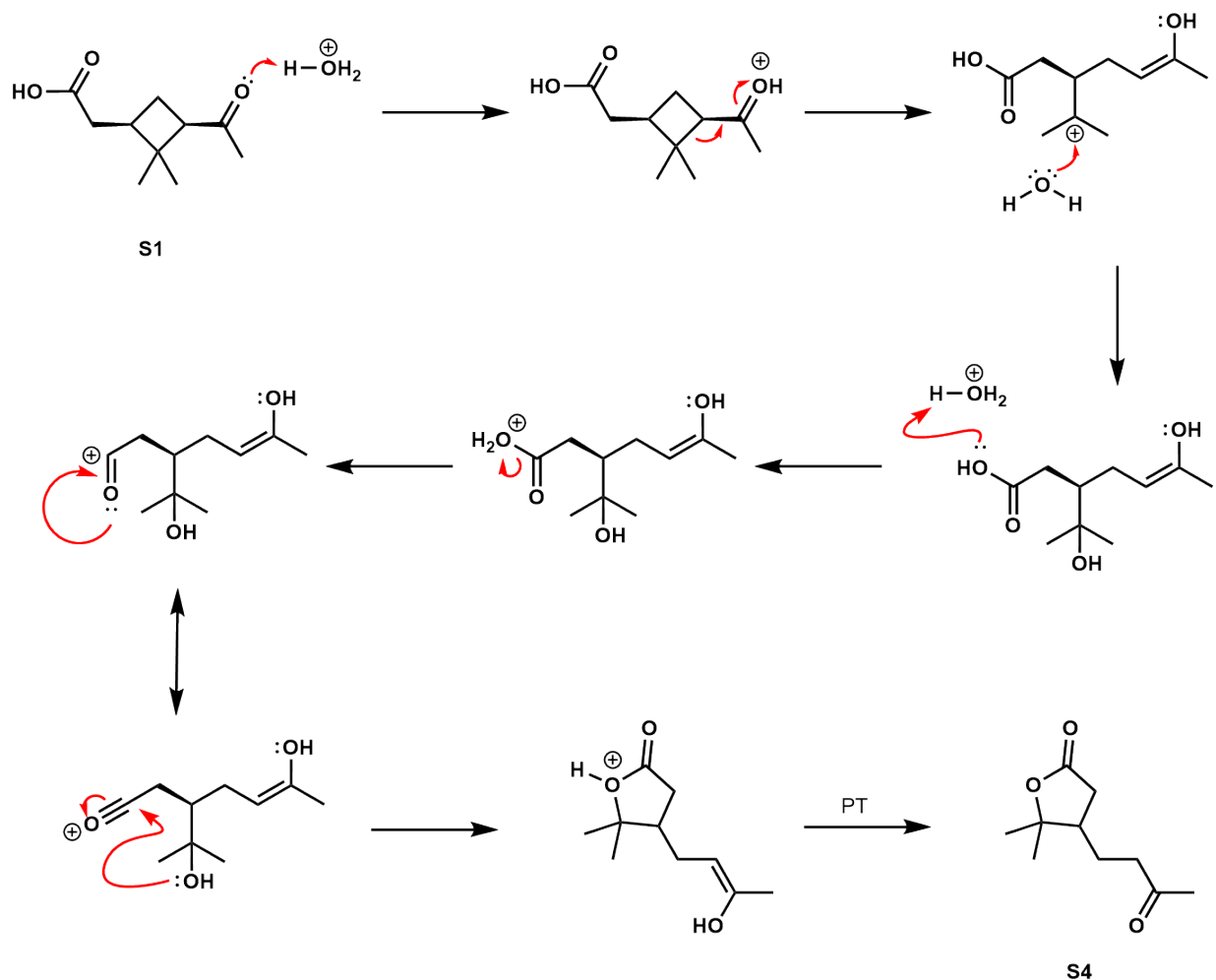


Figure 4.2: UPLC chromatograms of cis-pinonic acid aged in water for 2 days, 0.52 mM H₂SO₄ (pH 3.00), 5.6 M H₂SO₄ (pH -0.86), and 10 M H₂SO₄ (pH -1.08) in negative ion mode (b, e, h, k), position ion mode (c, f, i, l), and the corresponding PDA (a, d, g, j). Overlaid on the negative ion mode and positive ion mode TIC in red is the SIC for *m/z* 183.1028 and *m/z* 185.1177, respectively, except for TIC ESI (-) (pH -1.08). The PDA chromatograms were shifted 0.06 minutes to account for the time delay between the two detectors. All chromatograms were normalized based on the maximum peak intensity of their respective dataset.

However, the positive ion mode chromatograms also show an additional peak that eludes out at 8.78 min. This was assigned to the homoterpenyl methyl ketone as well as the corresponding enol tautomer, as shown in Scheme 4.2.¹⁸⁸ For the most acidic condition the homoterpenyl methyl ketone is the only product remaining (Figure 4.2 k,l), with no original *cis*-pinonic acid left.



Scheme 4.2: Formation of homoterpenyl methyl ketone (S4) from *cis*-pinonic acid (S1) aged in H_2SO_4 , adapted from Arcus and Bennett (1955)¹⁸⁸PT indicates proton transfer

Experiments were then repeated for *cis*-pinonaldehyde, however, positive ion mode proved to be more useful at detecting changes in chemical composition as opposed to negative ion

mode. The data described in the subsequent text pertains to the positive ion mode.

Samples in which *cis*-pinonaldehyde was aged in water (control), 0.52 mM H₂SO₄ (pH 3.00), and 1.0 M H₂SO₄ (pH -0.01) have two dominant peaks, as shown in Figure 4.3. The smaller peak at 8.94 min corresponds to *cis*-pinonic acid, an impurity that stems from the synthesis of *cis*-pinonaldehyde, while the broad peak at 9.77 min corresponds to *cis*-pinonaldehyde (the width of the peak is due to the slow hydration-dehydration equilibrium of the aldehyde group during the separation). The same peaks occur in the 0.52 mM H₂SO₄ (pH 3.00), and 1.0 M H₂SO₄ (pH -0.01) samples compared to the control study and there are no additional peaks, which indicate that these conditions do not promote acid catalyzed reactions. However, the TIC (Figure 4.4) of the sample in which *cis*-pinonaldehyde was aged in highly acidic conditions (10 M H₂SO₄) implies alternate chemical pathways. There are four significant peaks in these aging conditions at RTs of 8.77, 11.85, 12.07, and 12.22 min. Additionally, in this chromatogram, the peak corresponding to *cis*-pinonaldehyde is absent, which means that all *cis*-pinonaldehyde was consumed. The peak at 8.77 min corresponds to acid catalyzed isomerization product of the *cis*-pinonic acid impurity, homoterpenyl methyl ketone (S4). The remaining three peaks correspond to the same dominant ion in the mass spectrum (m/z 151.1117, C₁₀H₁₅O⁺), suggesting that these compounds are isomers (Figure 4.4c). The same peaks are the dominant features in the PDA chromatogram of the sample, shown in Figure 4.4b, which shows that these compounds are the chromophores of interest.

4.4.2 Kinetic Analysis

Figure 4.5 shows the absorption spectra of *cis*-pinonic acid aged in (a) 5.2 x 10⁻⁴ M (pH 3.00), and (b) 10 M (pH -1.08) solutions of H₂SO₄ as a function of time. The spectra of *cis*-pinonic acid in moderately acidic solutions (pH 3.00) are consistent with the presence of non-interacting carboxyl and carbonyl groups. The small peak at 285 nm corresponds to

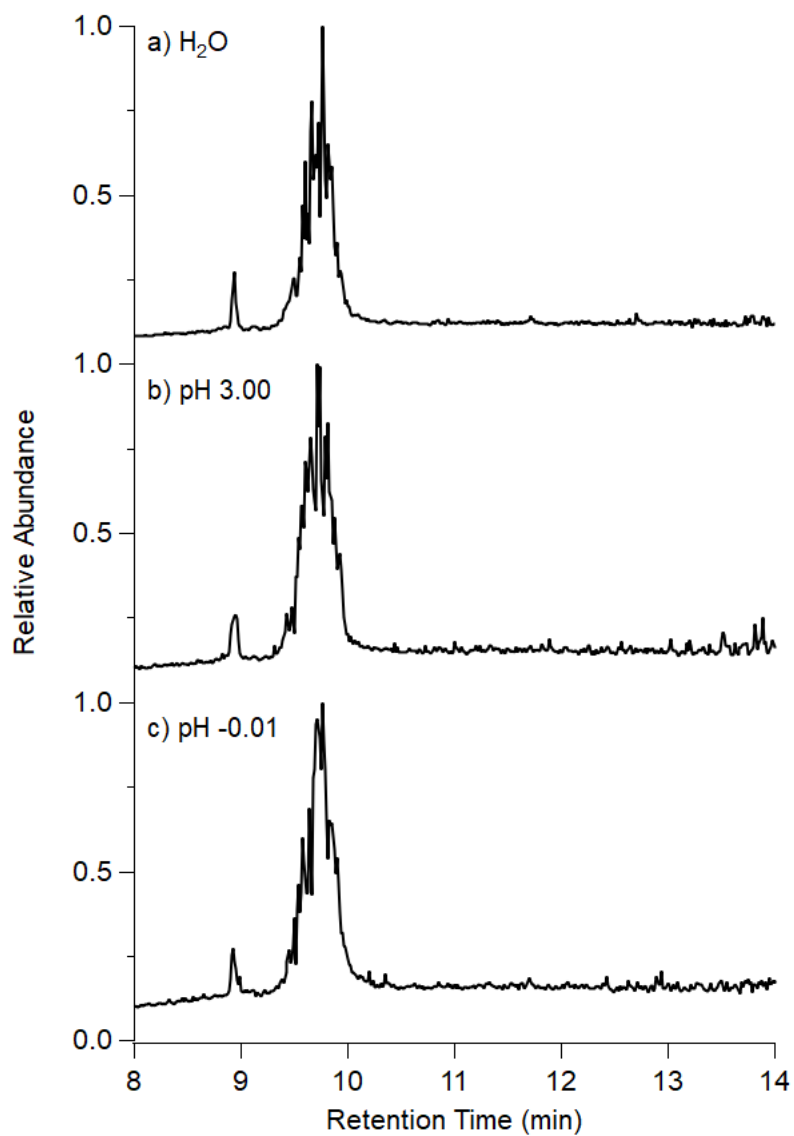


Figure 4.3: Positive ion mode TIC for cis-pinonaldehyde aged in (a) H_2O , (b) 0.52 mM H_2SO_4 (pH 3.00), and (c) 1.0 M H_2SO_4 (pH -0.01).

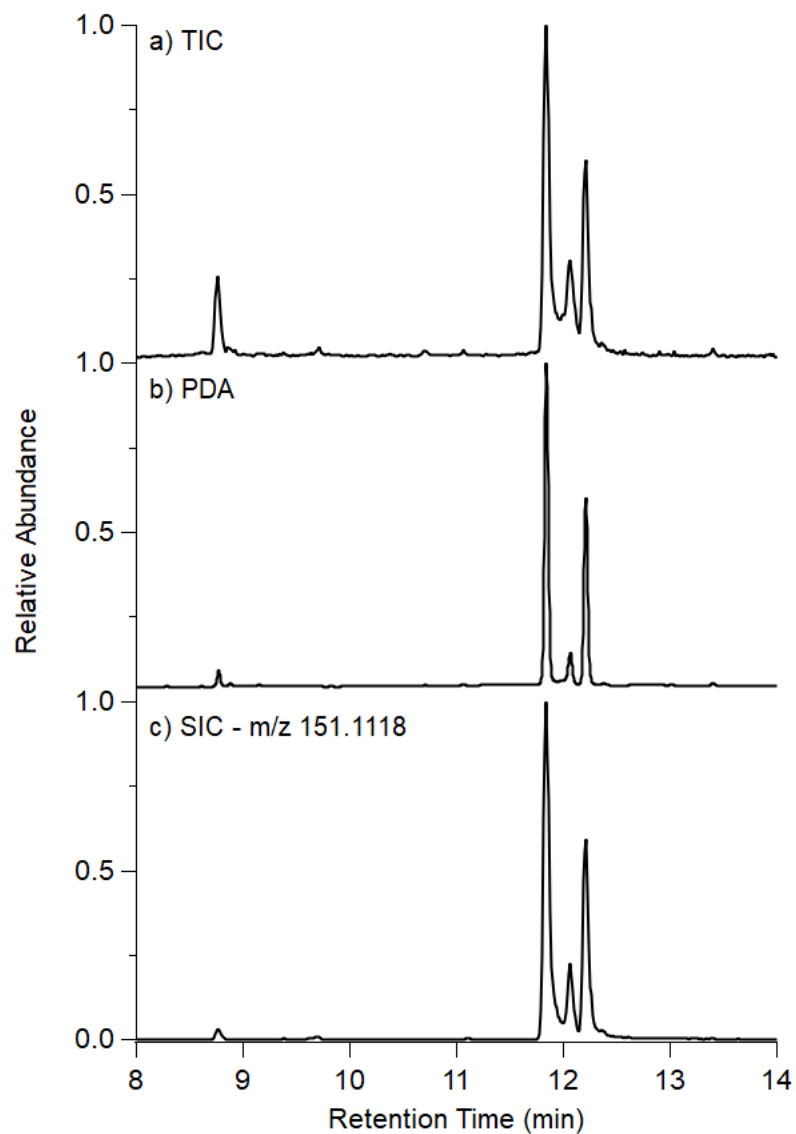


Figure 4.4: UPLC chromatograms of *cis*-pinonaldehyde aged in 10 M H₂SO₄ (c,d) in positive ion mode for TIC (a), PDA (b), and SIC (*m/z* 151.1117) (c). The PDA chromatogram was shifted 0.06 minutes to account for the time delay between the two detectors.

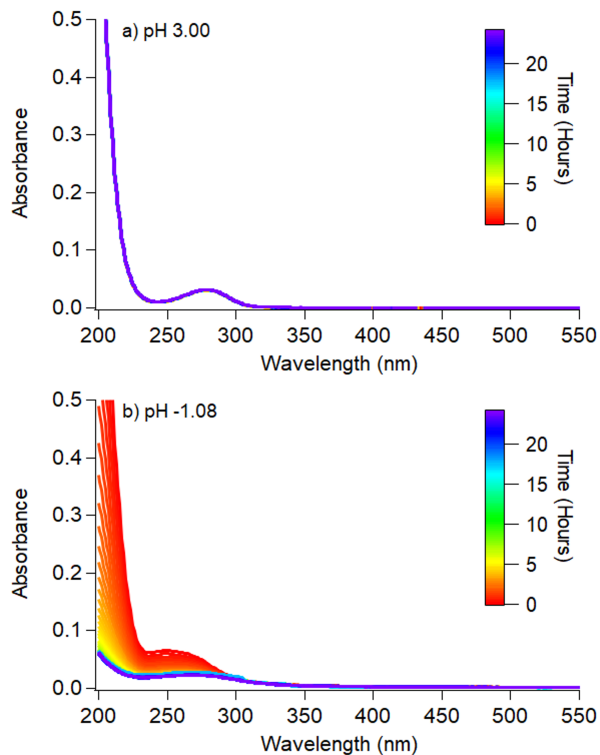


Figure 4.5: Absorption spectra of *cis*-pinonic acid aged in (a) 5.2×10^{-1} M (pH 3.00), and (b) 10 M (pH -1.08) solutions of H_2SO_4 recorded every 15 min for 24 h.

the weak $n \rightarrow \pi^*$ transition in the carbonyl group of *cis*-pinonic acid, and the larger peak below 200 nm corresponds to $\pi \rightarrow \pi^*$ transitions. As seen in Figure 4.5a, there is no change in either the $n \rightarrow \pi^*$ or $\pi \rightarrow \pi^*$ transition as function of time *cis*-pinonic acid confirming that *cis*-pinonic acid is stable under these conditions. In the *cis*-pinonic acid sample aged in 10 M (pH -1.08) H_2SO_4 (4.5b), the weak $n \rightarrow \pi^*$ transition (262 nm) and $\pi \rightarrow \pi^*$ transition (<200 nm) are still present. However, the peaks that correspond to those transitions decrease over time, indicating a structural change (e.g., tautomerization). Previous studies have shown that ketones can undergo acid catalyzed aldol condensation, however, the aldol condensation product resulting from *cis*-pinonic acid, $\text{C}_{20}\text{H}_{30}\text{O}_5$, is absent from the mass spectra.^{79,189} The evidence presented in the TIC (Figure 4.5hi) and UV-Vis spectra (Figure 4.5b) suggest that there is a structural change (e.g., tautomerization) in *cis*-pinonic acid rather than condensation reaction. In the first three hours, the reaction behaves as a first order reaction with respect to the decay of *cis*-pinonic acid, resulting in a rate constant

of $6.33 \times 10^{-5} \text{ h}^{-1}$. Arcus and Bennett (1955), reported a rate constant of $9.9 \times 10^{-2} \text{ h}^{-1}$,¹⁸⁸ however, their conversion of *cis*-pinonic acid to homoterpenyl methyl ketone was done in monochloroacetic acid at 100°C, while the reaction in this paper was done with sulfuric acid at room temperature and a lower concentration of starting material.¹⁸⁸ This suggests that the isomerization rate constant strongly depends on temperature, which is an important consideration given the wide range of ambient temperatures in the atmosphere.

The absorption spectra of *cis*-pinonaldehyde aged in 5.6 M (pH -0.86) and 10 M (pH -1.08) H_2SO_4 are shown in Figure 4.6. In Figure 4.6a, there are two dominant peaks that increase as a function of time: at 246 nm and 355 nm. Additionally, absorbance of *cis*-pinonaldehyde aged in 10 M (pH -1.08) H_2SO_4 shows 5 main peaks (Figure 4.6b) at 215 nm, 251 nm, 370 nm, 415 nm, and 500 nm. The general shape of the spectrum is very similar to that observed during aging of α -pinene SOA under the same highly acidic conditions, reproduced in Figure 4.7.¹⁸⁵ The lifetime of browning for each peak within these samples are outlined in Table 1—they are on the order of an hour at pH -1.08 .^{4.7.185} Note that there are subtle differences in the spectra of aged *cis*-pinonaldehyde and α -pinene SOA. For example, there are more distinct peaks between 200-300 nm in the *cis*-pinonaldehyde aged in 10 M H_2SO_4 , as shown in Figure 4.7b. This can be expected because there are many other compounds in the α -pinene SOA (including substituted *cis*-pinonaldehyde and *cis*-pinonic acid) that may also produce light-absorbing products under acidic conditions. However, the general shape of the spectra is the same, indicating that *cis*-pinonaldehyde is largely responsible for the chromophoric properties of the aged α -pinene SOA. Additionally, in comparison to the α -pinene SOA sample, the rate of browning for the absorption peaks is slower for the sample aged in 5.6 M H_2SO_4 (pH -0.86) and faster for the sample aged 10 M (pH -1.08) H_2SO_4 .¹⁸⁵ This is likely due to the difference in the conditions the samples were aged in (e.g., the α -pinene SOA sample had a smaller concentration of *cis*-pinonaldehyde and there are competing reactions from other compounds). It is also noted that the absorption of the products of *cis*-pinonaldehyde

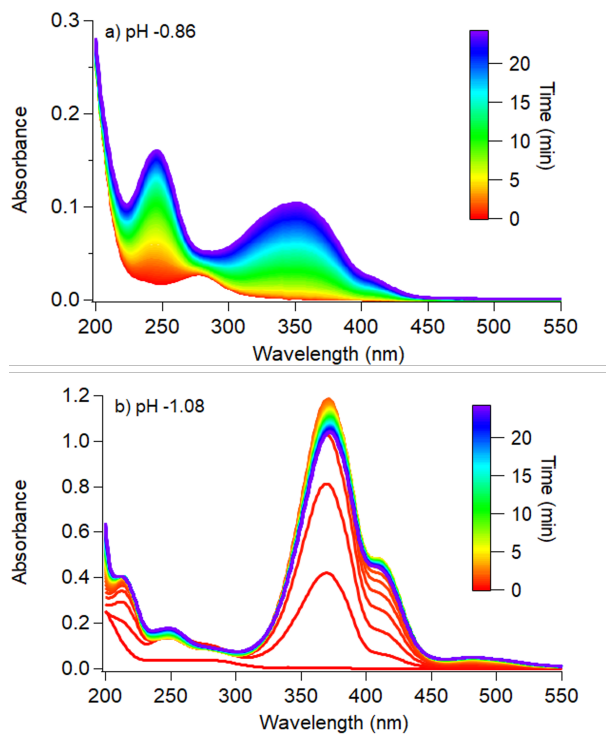


Figure 4.6: Absorption spectra of *cis*-pinonaldehyde aged in (a) 5.6 M (pH -0.86) and (b) 10 M (pH -1.08) H_2SO_4 . Each spectrum was collected every 15 min over 24 h.

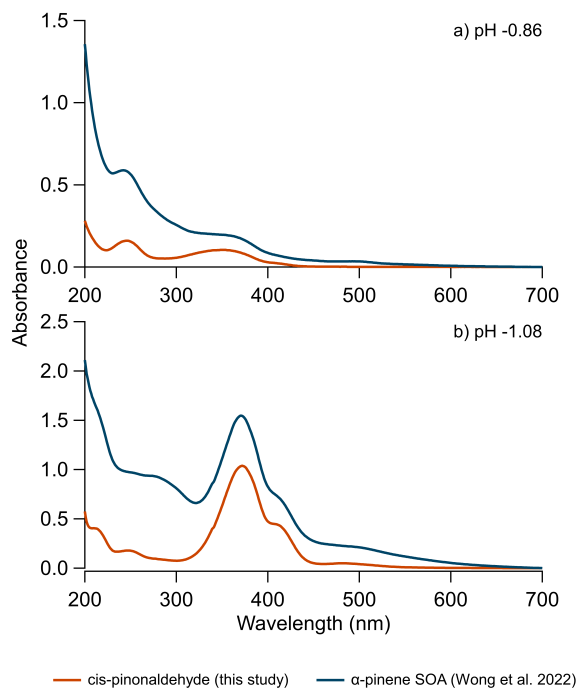


Figure 4.7: Absorption spectra of *cis*-pinonaldehyde aged in (a) 5.6 M (pH -0.86) and (b) 10 M (pH -1.08) H_2SO_4 for two days, compared to identical experiments with α -pinene SOA by Wong et al 2022.¹⁸⁵

aged in 10 M H₂SO₄ (pH -1.08) reaches a maximum and then starts to decay the longer it ages, indicating that there are other secondary reactions taking place consuming the initial chromophore. Such a decay was not observed in the acidified α -pinene SOA in the previous study,¹⁸⁵ again likely because of lower concentrations of individual reactants in the SOA.

Table 4.2: Effective lifetimes of browning for of *cis*-pinonaldehyde aged in 5.6 M (pH -0.86) and 10 M (pH -1.08) H₂SO₄, calculated by assuming pseudo-first-order reactions in the time series fits for each peak.

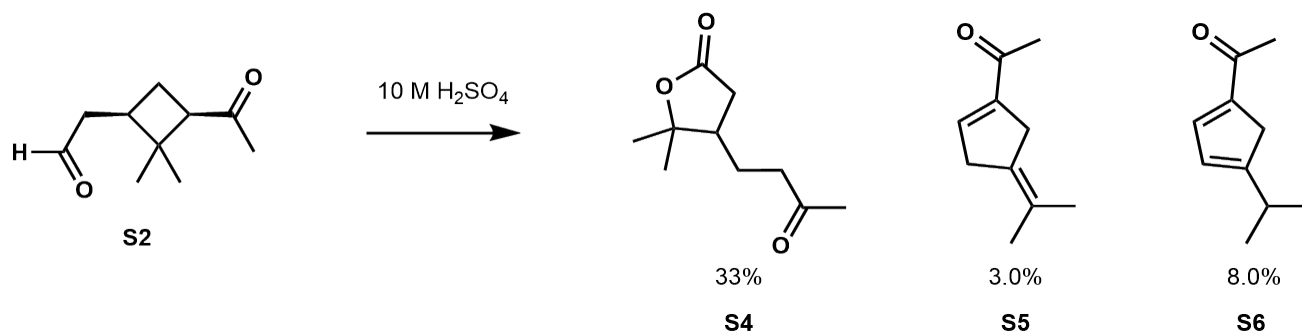
Sample	Peaks of Interest (nm)	Lifetime of Browning (h)
pH -0.86	246	18 \pm 3
pH -0.86	355	69 \pm 1
pH -1.08	215	0.47 \pm 0.03
pH -1.08	251	0.04 \pm 0.03
pH -1.08	370	0.31 \pm 0.03
pH -1.08	415	0.69 \pm 0.03
pH -1.08	500	2.4 \pm 0.2

4.4.3 Product Identification

4.4.3.1 Purification and Separation of Chromophores

The reaction of *cis*-pinonaldehyde aged in 10 M (pH -1.08) H₂SO₄ was then scaled up to generate enough material for purification and NMR analysis. The scaled-up reaction consisted of 8.5 g of *cis*-pinonaldehyde and ~500 mL of 10 H₂SO₄ (pH -1.08), resulting in a mass concentration of ~17 mg/mL. Although the concentration between these reactions differed from the experiments described previously, both reactions had H₂SO₄ in excess and turned a dark amber color suggesting their similarities. The crude solution was poured over ice and diluted with H₂O. Solid NaHCO₃ was added portion-wise while stirring vigorously and monitoring pH. Note that during the purification and separation process, NaHCO₃ was added to neutralize the acid and allow for isolation of the chromophores. However, during

this step it is possible that relative abundance of the products can change, as the reactions to form the products can be reversible. When the pH was approximately 2, the solution was partitioned with CH_2Cl_2 , extracted with CH_2Cl_2 , and washed with a saturated aqueous solution of NaHCO_3 and a saturated solution of NaCl . The organic layers were dried over Na_2SO_4 and concentrated in vacuo to afford a crude black oil. The residue was purified via flash chromatography (0-100% EtOAc/Hex) to afford S4 (3.14 g, 33%), S5 (233 mg, 3.0%), and S6 (622 mg, 8.0%) as an inseparable mixture with another constitutional isomer. Additional hydrogenation experiments were also conducted to better determine connectivity of these compounds. The following is the summary of predication structural information following the analysis described below. It is worth noting that trace amounts of *cis*-pinonic



Scheme 4.3: Summary of products formed aging of *cis*-pinonaldehyde (S2)

acid were detected in the sample of S2, which provides an explanation for the observed formation of homoterpenyl methyl ketone (S4). Furthermore, it is plausible that a reaction takes place during the aging process of *cis*-pinonaldehyde, resulting in the generation of *cis*-pinonic acid, which can contribute to the increased abundance of homoterpenyl methyl ketone.

4.4.3.2 Confirmation of Chromophores

To confirm that purified samples were the chromophores of interest, these extracts were analyzed using UPLC-PDA-HRMS and then compared to the peaks and elution times of Figure

4.4. Figure 4.8 shows the UPLC chromatograms of the separated samples, S5 (blue trace) and S6 (orange trace).

In the S5 isolated sample, the TIC (Figure 4.8a) contains 2 peaks, one at 11.03 min and another at 12.17 min. Both peaks absorb as seen in Figure 4.8b, however, only the peak that eluted out at 12.17 min has the matches the TIC retention time in *cis*-pinonaldehyde solution Figure 4.4 and the has m/z 151.1117 ($C_{10}H_{15}O^+$). This peak at 11.03 min is likely an impurity due to the purification process as this peak is not evident in Figure 4.4 and has a mass of m/z 149.0961 ($C_{10}H_{13}O^+$). In the S6 sample, the TIC (Figure 4.8a) also contains 2 peaks, one at 11.79 min and another at 12.00 min. Both peaks absorb and have m/z 151.1118 as noted by Figure 4.8b and Figure 4.8c.

In comparison to the elution time in Figure 4.8, it appears that S5 corresponds to peak at 12.21 min while S6 corresponds to the peak at 11.85 and 12.07 min. Note that there is a ~ 0.05 min delay time between the purified samples (Figure 4.8) and the unpurified sample (Figure 4.4), which is likely due to instrument fluctuations as these samples were taken a couple of weeks apart. Additionally, the constitutional isomer that corresponds to the peak at 12.07 min could not be further purified and the structure determination is limited as there were only trace amounts in the scaled-up reaction.

The PDA absorption spectra of the purified and unpurified samples are compared in Figure 4.9. The spectra for S5 and peak at 12.21 min in Figure 4.4 absorb at the same peak wavelength of 318 nm, while the S6 sample likely corresponds to the peak at 11.84 min in Figure 4.4 because they both have an absorption peak at 306 nm. Note that peak max absorption wavelength differs from Figure 4.6b, which is likely caused by a shift in the acid-base equilibria as the samples were diluted with water-acetonitrile eluent used in UPLC.¹⁸⁵ This suggests that absorption spectra of these compounds are pH dependent, which is charac-

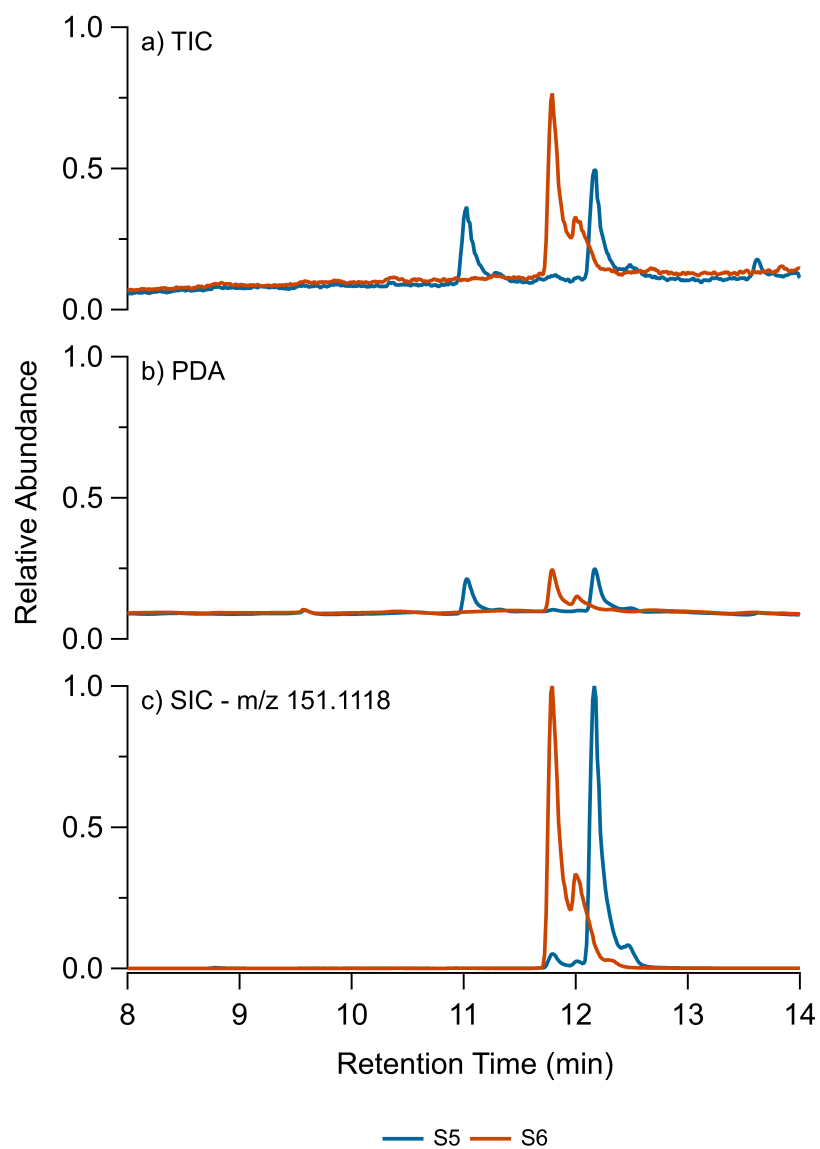


Figure 4.8: UPLC chromatograms of S5 and S6 isolated extracts in positive ion mode for TIC (a), PDA (b), and SIC (m/z 151.1117) (c). The PDA chromatogram was shifted 0.06 minutes to account for the time delay between the two detectors.

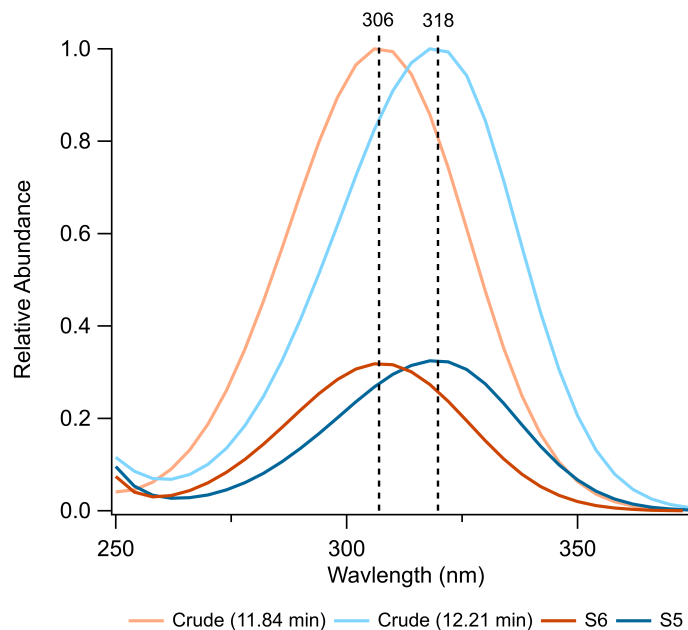


Figure 4.9: Absorption spectra from UV-Vis (red trace) and PDA (blue and green trace) from the purified sample

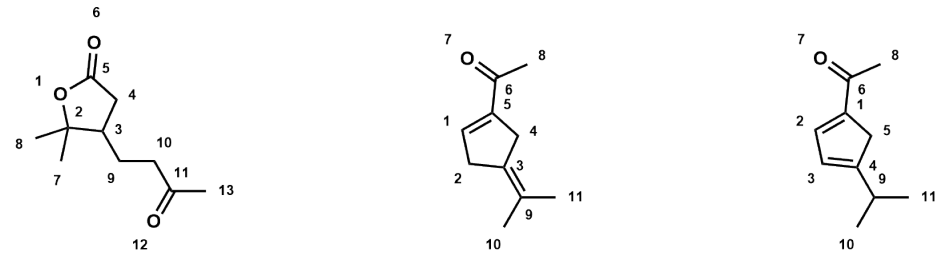
teristic of other atmospheric compounds like nitrophenols, imidazole-2-carboxaldehyde, and pyruvic acid.^{48,167–170}

4.4.3.3 NMR Analysis and Possible Mechanisms

A ^1H and ^{13}C -NMR analysis was performed to determine the structures of S4, S5 and S6 (Table 4.3).

Compound S5 was isolated as a light-yellow oil. Its high-resolution mass spectrometry gave the molecular formula of $\text{C}_{10}\text{H}_{14}\text{O}$, indicating four degrees of unsaturation. The NMR spectra indicated the presence of 2 double bonds, one tetrasubstituted (δ_{C} 133.1 (C_3 and 140.5 (C_9)) and one monosubstituted (δ_{H} 7.16 (H_1); δ_{C} 140.9 (C_1) and 146.3 (C_5)). The ^1H NMR spectrum of S5 also showed the resonances of three methyl singlets (δ_{H} 2.33 (H_8), 1.87 (H_{10} or H_{11}), 1.74 (H_{10} or H_{11})), one of which corresponds to a methyl ketone (H_8), and two methylene groups (δ_{H} 2.63 (H_2), 2.53 (H_4)). ^{13}C -NMR spectra also indicated the presence

Table 4.3: Summary of the ^1H and ^{13}C - NMR data from compounds S4, S5 and S6



Pos.	S4		S5		S6	
	δ_{H} , mult	δ_{C}	δ_{H} , mult	δ_{C}	δ_{H} , mult	δ_{C}
1			7.16 (s, 1H)	140.9		145.0
2		86.7	2.63 (d, 6.5, 2H)	29.3	7.24 (s, 1H)	143.9
3	2.17 (tdd, 11.1, 7.8, 3.8, 1H)	45.2		133.1	6.26 - 6.16 (m, 1H)	125.0
4	2.55 (dd, 17.0, 7.9, 1H) 2.24 (dd, 17.0, 11.7, 1H)	34.8	2.53 (d, 4.4, 2H)	27.8		166.1
5		175.3		146.3	3.22 (d, 1.5, 2H)	40.2
6				197.1		193.7
7	1.24 (s, 3H)	21.9				
8	1.42 (s, 3H)	27.4	2.33 (s, 3H)	26.7	2.33 - 2.30 (m, 3H)	26.0
9	1.77 (dddd, 13.5, 9.2, 6.6, 4.0, 1H) 1.51 (dddd, 13.9, 10.7, 8.7, 5.7, 1H)	23.3		140.5	2.72 (dtd, 13.7, 6.9, 1.2, 1H)	30.3
10	2.50 - 2.38 (m, 2H)	41.9			1.14 (ddd, 6.9, 2.0, 0.9, 8H).	22.8
11		207.3			1.14 (ddd, 6.9, 2.0, 0.9, 8H).	22.8
12						
13	2.14 (s, 3H)	30.1				

of five carbons: three CH₃ groups (δ_C 26.7 (C₈), 22.0 (C₁₀ or C₁₁), 21.5(C₁₀ or C₁₁)) and two CH₂ groups (δ_C 29.3 (C₂), 27.8 (C₄)). The alkenes and ketone accounted for three of the four degrees of unsaturation. Consequently, the presence of a ring as the compound's backbone is indicated to account for the fourth degree of unsaturation.

Based on the analysis presented above, it is likely that the ketone is in its protonated form, under highly acidic conditions, shown in Scheme 4.4. This facilitates an acid-catalyzed ring opening of the strained cyclobutane ring to the more favorable tertiary carbocation and then results in an elimination of the neighboring methine. Afterward, another equivalent of acid would serve to protonate the carbonyl group of the aldehyde, initiating an aldol condensation reaction, which would lead to the elimination of the secondary alcohol, giving to the proposed structure S5, 1-(4-(propan-2-ylidene)cyclopent-1-en-1-yl)ethan-1-one, a common terpene oxidation product.^{190,191} Having tentatively settled on a structural assignment of S5 as depicted in Scheme 4.3, the mechanism for its formation is illustrated below in Scheme 4.4.

Compound S6, obtained as an orange oil, had an identical molecular formula to that of S5 according to its HRMS data. The NMR data also was very similar to S5, indicating that these two compounds are structurally similar constitutional isomers. Basing our NMR analysis of this compound off the previously discussed, assuming similar functionality and structural patterns, the following associations were made. The same unsaturated methyl ketone was observed in both the ¹H and ¹³C NMR (δ_C 193.7 (C₆), 26.0 (C₈); δ_H 2.33-2.30 (H₈). However, rather than an exocyclic isopropene unit substituting the five-membered ring, there was an isopropyl group (δ_C 30.3 (C₉) 22.8 (C₁₀, C₁₁); δ_H 2.72 (H₉), 1.14 (H₁₀, H₁₁). In the ¹³C spectra also suggested the the presence of two alkenes (δ_C 145.0 (C₁), 143.9 (C₂), 125.0 (C₃), 166.1 (C₄)), with one of them existing as the unsaturated ketone. However, the substitution pattern differed for this compound' s alkenes however, given the presence of two alkene protons (δ_H 7.24 (H₂), 6.26-6.16 (H₃). Thus, it was concluded that there was

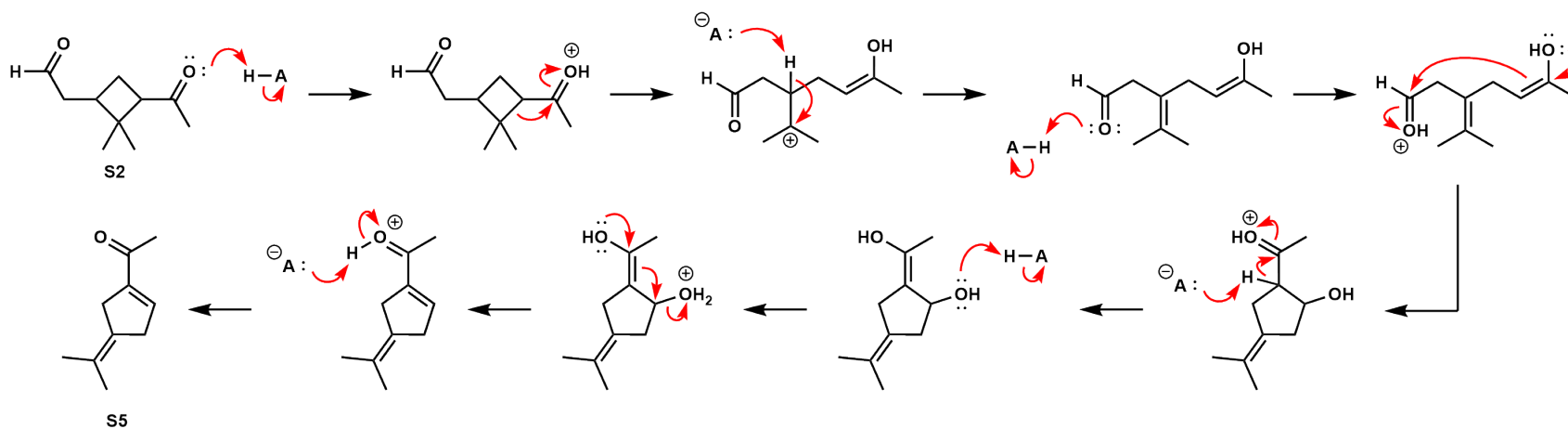
either a disubstituted alkene and a tetrasubstituted alkene or two trisubstituted alkenes.

Comprehensive study of the 2D NMR spectra of S6 led us to propose three potential structures that were indistinguishable by spectroscopic or mass spectrometric means. To gain a better understanding of the structures of these chromophores, additional hydrogenation experiments were also conducted to better determine connectivity. The identical product of the hydrogenation reaction of S6 is a known, characterized compound.¹⁹² According to the NMR analysis of hydrogenated compounds, the product(s) that were isolated was different from that reported by Degrado et al, (2002).¹⁹² Therefore, it was concluded that the third chromophore with a molecular formula of C₁₀H₁₄O was the 1,3-disubstituted cyclopentadiene (S7). Compounds S6 and S7 are regioisomers of each other and formed through nearly identical mechanisms, which are shown in Scheme 4.5. This mechanism is also similar to the one for S5 (Scheme 4.4), however, the mechanism for S6 and S7 (Scheme 4.5) includes an additional step of a hydride shift.

4.5 Conclusions

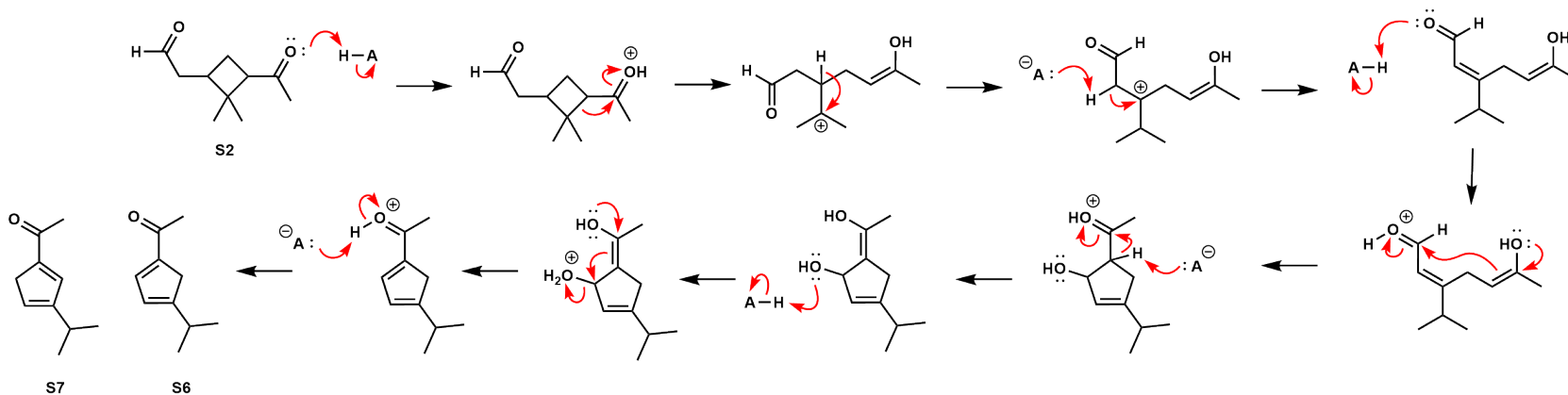
The composition and optical properties of organic aerosol can undergo significant changes due to acid-catalyzed and acid-driven reactions. The impacts of highly acidic conditions on *cis*-pinonic acid and *cis*-pinonaldehyde were explored by aging these compounds in bulk sulfuric acid solutions with atmospherically relevant acidities. It was found that *cis*-pinonic acid forms homoterpenyl methyl ketone while *cis*-pinonaldehyde forms 1-(4-(propan-2-ylidene)cyclopent-1-en-1-yl)ethan-1-one and two regioisomers of 1-(4-isopropylcyclopenta-1,3-dien-1-yl)ethan-1-one under highly acidic conditions. These conclusions hold particular significance for the upper troposphere and lower stratosphere (UTLS) regions, as well as areas characterized by substantial SO₂ pollution, as these areas have been documented highly acidic aerosols with

negative pH.^{4,5,7,10,49,50,58,61} Further work should be done with other biogenic and anthropogenic SOA to identify if acidic aging is a large driver in these systems.



Scheme 4.4: Formation of 1-(4-(propan-2-ylidene)cyclopent-1-en-1-yl)ethan-1-one (S5), from the acid-catalyzed reaction of *cis*-pinonaldehyde (S2)

94



Scheme 4.5: Formation of 1-(4-isopropylcyclopenta-1,3-dien-1-yl)ethan-1-one (S6, S7) from the acid catalyzed reaction of *cis*-pinonaldehyde (S2)

Chapter 5

Biogenic and anthropogenic secondary organic aerosols become fluorescent after highly acidic aging

5.1 Abstract

Primary biological aerosol particles (PBAP) and secondary organic aerosols (SOA) both contain organic compounds that share similar chemical and optical properties. Fluorescence is often used to characterize PBAP; however, the accuracy of such measurements may be hindered due to interferences from fluorophores in SOA. Despite extensive efforts to understand the aging of SOA under acidic conditions, little is known about how these processes affect fluorescence of SOA and thereby their interference with the fluorescence measurements of PBAP. The objective of this study is to investigate the fluorescence of SOA and understand the influence of acidity on the optical properties of organic aerosols and potential interference for the analysis of bioaerosols. SOA was generated from by O_3 or OH-initiated oxidation of

d-limonene or α -pinene, as well as by OH-initiated oxidation of toluene or xylene. The SOA compounds were then aged by exposure to varying concentrations of aqueous H_2SO_4 for two days. Absorption and fluorescence spectrophotometry were used to examine the changes in optical properties before and after aging. The key observation was the appearance of strongly light-absorbing and fluorescent compounds at $\text{pH} = \sim -1$ suggesting that acidity is a major driver of SOA aging. The aged SOA from biogenic precursors (d-limonene and α -pinene) resulted in stronger fluorescence than aged SOA from toluene and xylene. The absorption spectra of aged SOA changed drastically in shape upon dilution, whereas the shapes of the fluorescence spectra remained the same, suggesting that fluorophores and chromophores in SOA are separate sets of species. The fluorescence spectra of aged SOA overlapped with fluorescence spectra of PBAP, suggesting that SOA exposed to highly acidic conditions can be confused with PBAP detected by fluorescence-based methods. These processes are likely to play a role in the atmospheric regions where high concentrations of H_2SO_4 persist, such as upper troposphere and lower stratosphere.

5.2 Introduction

Our understanding of the extent to which aerosols contribute to global climate change is still limited. Organic aerosols, which include bioaerosols (also known as primary biological aerosol particles –PBAP) and secondary organic aerosols (SOA), account for a dominant fraction of particulate matter in the lower troposphere and can heavily influence air quality and radiative forcing.¹⁰¹ PBAP contains biological components such bacteria, viruses, fungi, biological molecules,¹⁹³ while secondary organic aerosols are formed from the oxidation of biogenic and anthropogenic volatile organic compounds (VOCs).^{16,22}

PBAP and SOA are extremely complex, and both contain organic compounds that share

similar chemical and optical properties, including the ability to fluoresce.¹⁹⁴ Many atmospheric organic species with significant conjugation of π -bonds, including amino acids with aromatic functional groups (e.g., tryptophan), vitamins, and humic-like substances, have been identified as efficient fluorophores.^{177,195,196} The ability to detect and analyze these fluorophores using fluorescence spectroscopy has proved useful for understanding the chemical composition, sources, and chemical reactions of atmospheric aerosols.^{197,198} However, the presence of weakly-fluorescent compounds in SOA complicates the applications of fluorescence spectroscopy to quantitative and qualitative analysis of PBAP, as the interferences of non-biological particles, such as SOA, can skew the data and conclusions.^{146,196,199–201} This problem is further complicated as organic aerosols undergo chemical and physical transformations during transport as they are exposed to different environmental conditions, such as acidity.

Acidity of the atmospheric aqueous phase can vary significantly. Cloud and fog droplets tend to be less acidic with a pH +2 to +7, while aerosol particles are more acidic with effective pH values from -1 to +8.⁴⁷ This property is dependent on the source of the particles, their chemical composition, and ambient relative humidity (as aerosol liquid water serves to dilute the acids in particles). Acidity plays a crucial role in many chemical reactions of organic compounds, including those found in the SOA. These acid catalyzed reactions include hemiacetal and acetal formation, hydration of aldehydes and ketones, aldol condensation of carbonyls, esterification of carboxylic acids, and ring opening of epoxides, to name a few.⁴⁸ Thus, comprehending the role of acidity in the chemical and physical transformation of these complex organic aerosols can provide valuable insights into how acidity impacts their properties, including fluorescence.

Many field studies that have reported highly acidic aerosols (with negative pHs), specifically in Southeastern Asia, the Eastern United States, China, and other locations, likely due

to the high emissions of SO_2 .^{49,50,58,61} Additionally, stratospheric aerosols have been known to be very acidic, resulting in stratospheric particles that can contain 40-80 wt% H_2SO_4 originating from the injection of SO_2 from volcanic eruptions, resulting in a pH between -0.8 and -1.^{3,4,7-10} Although there are observations of acidity levels this high and reports of organic aerosols the upper troposphere and lower stratosphere, laboratory studies on the aging of SOA under these conditions remain limited. A recent study of α -pinene ozonolysis SOA reported that acidity is a major driver of SOA aging, resulting in a large change in the chemical composition and optical properties of SOA in presence of concentrated H_2SO_4 , including the formation of unidentified fluorophores.¹⁸⁵ This prompts a question whether other types of biogenic and anthropogenic SOA can become fluorescent after being exposed to highly acidic conditions.

Despite significant efforts to understand the aging of SOA under high acidity conditions, little is known how these processes affect fluorescence and thereby their interference with the fluorescence measurements of PBAP. Additionally, studying the fluorescence properties of SOA could provide valuable insights into the acid-catalyzed reactions and chemical composition of the fluorophores. The objective of this study is to investigate the excitation-emission spectroscopy of SOA generated from various precursors to understand the influence of acidity on the optical properties of organic aerosols. We demonstrate that highly acidic conditions promote acid catalyzed reactions and thereby form fluorophores in SOA that can interfere with detection of PBAP by fluorescent methods.

Table 5.1: Aging Experiments Summary

SOA Precursor	Oxidant	Collection Time (hours)	Mass of SOA Extracted in Segment (mg)	Estimated Concentration of H ₂ SO ₄	Effective pH = -log[H ⁺]
APIN	O ₃	3.5	0.951	-	-
APIN	O ₃	3.5	0.974	0.52 mM	3.00
APIN	O ₃	3.5	1.110	10	-1.08
LIM	O ₃	3.3	1.036	-	-
LIM	O ₃	3.3	1.243	0.52 mM	3.00
LIM	O ₃	3.3	1.031	10	-1.08
APIN	OH	7.2	0.814	-	-
APIN	OH	7.2	0.841	0.52 mM	3.00
APIN	OH	7.2	0.736	10	-1.08
LIM	OH	7.3	0.755	-	-
LIM	OH	7.3	0.744	0.52 mM	3.00
LIM	OH	7.3	0.694	10	-1.08
TOL	OH	14	0.906	-	-
TOL	OH	14	0.988	0.52 mM	3.00
TOL	OH	14	0.887	10	-1.08
XYL	OH	14	0.583	-	-
XYL	OH	14	0.610	0.52 mM	3.00
XYL	OH	14	0.594	10	-1.08

5.3 Experimental Methods and Materials

5.3.1 Formation of SOA

SOA generated from six different types of precursor combinations were studied in this work: α -pinene (Arcos, 98%) ozonolysis (APIN/O₃), d-limonene (Sigma Aldrich, 99%) ozonolysis (LIM/O₃), α -pinene photooxidation (APIN/OH), d-limonene photooxidation (LIM/OH), toluene (Fisher, 99%) low-NO_x photooxidation (TOL/OH), p-xylene (Sigma Aldrich, 99%) low-NO_x photooxidation (XYL/OH). A summary of all samples made in this study can be found in Table 5.1. Two types of techniques were used to generate SOA as previously described.^{148,185,202}

In brief, SOA formed from O₃-initiated oxidation was prepared from the oxidation of d-limonene (LIM) and α -pinene (APIN) by ozone (O₃) using a 20 L continuous flow reactor. Ozone was generated using a commercial ozone generator (OzoneTech OZ2SS-SS) and introduced into the reactor in a 0.5 slm (standard liters per minute) flow of oxygen. Liquid VOC precursor was injected at 25 μ L/hr into a 5 slm flow of air. The initial mixing ratios concentrations of VOC and O₃ were \sim 14 ppm and \sim 10 ppm, respectively. A charcoal denuder was used to scrub excess O₃ from the flow before SOA collection. SOA was collected for about 2 h to achieve a mass of \sim 2-4 mg, enough for the analysis described below.

For photooxidation (OH) initiated SOA, a different flow reactor was used as described in previous studies.^{202,203} This oxidation flow reactor consisted of 8 L quartz reaction vessel surrounded by two 254 nm UV lamps inside a Rayonet RPR100 photochemical reactor. To initiate the reaction, pure VOC was injected into dry air flowing at 0.3 slm through the vessel using a syringe pump, where it mixed with 0.7 slm flow of humidified air and 0.3 slm flow containing O₃. The UV lamps in the reactor photolyzed O₃, thereby producing OH by reacting O(1D) with H₂O. OH (along with trace amounts of O₃), subsequently reacted with VOC precursors, and the resulting SOA was collected from the exit tube for up to 14 h to obtain about \sim 2-3 mg in mass.

In both cases, the SOA was collected onto stage 7 (0.32–0.56 μ m) of a micro-orifice uniform deposit impactor (MOUDI; MSP Corp. (TSI) model 110-R) for 2-14 h on a foil substrate at a flow of 30 slm. Since the flow from the reactors was lower, the make-up air came from HEPA-filtered laboratory air.

Table 5.2: Solution Acidity in Dilution Experiments. SOA samples aged at 10M H₂SO₄ were diluted in water. pH was estimated using Extended Aerosol Inorganics Model (E-AIM (<http://www.aim.env.uea.ac.uk/aim/aim.php>)).

Sample	Dilution Factor	Estimated pH (E-AIM)
Control (undiluted)	1	-1.08
1:2 Dilution Factor	2	-0.817
1:3 Dilution Factor	3	-0.646
1:4 Dilution Factor	4	-0.517

5.3.2 Aging in Sulfuric Acid

The protocol used to age SOA in various acidic conditions followed the previously described procedure.¹⁸⁵ Each SOA substrate was cut into three approximately equal segments, and each segment was then extracted in 4 mL acetonitrile using a shaker. The acetonitrile was removed with a rotary evaporator at $\sim 25^{\circ}\text{C}$ (low temperature was used to prevent evaporation of SOA compounds). Water or a solution containing sulfuric acid was added to the vial to dissolve the SOA residue, resulting in a mass concentration of $\sim 200\ \mu\text{g}/\text{mL}$. This concentration was chosen to generate sufficient signal to noise for the analysis described below. The SOA extracts were then left to age for two days in the dark prior to analysis.

Additional experiments were conducted with SOA aged in 10 M H₂SO₄ (pH -1.08) and then diluted with an acid-free solvent to examine the changes in the fluorescence molecules due to acid–base equilibria. These samples were similarly aged in acid for two days before the dilution experiments. Further information on these samples can also be found in Table 5.2.

5.3.3 Spectroscopic Measurements

The aged solutions of SOA were analyzed using Cary Eclipse fluorescence spectrometer. The parameters used for these experiments mimic past studies of SOA fluorescence in

our group.^{146,185,200,204,205} The background for the fluorescence spectrum was obtained using deionized water and the samples analyzed were the SOA aged in H₂SO₄ after 2 days (we verified that sulfuric acid solutions without SOA did not fluoresce). The excitation wavelength varied over the 200–500 nm range in 5 nm steps, and the emitted fluorescence was recorded over the 300–600 nm range in 2 nm steps for the excitation–emission spectra at a scan rate of 1200 nm/min, resulting in excitation-emission matrices (EEM). The fluorescence intensities were corrected for Rayleigh and Raman scattering and inner filter effects using previously described methods and then converted into Quinine Sulfate Units (QSU).^{200,204,205} In brief, the absorption spectrum of the sample of interest was taken into account and the inner filter effect was corrected by using the following equation, where F_{corr} is the corrected fluorescence intensity, F_{obs} is the observed fluorescence intensity, A_{ex} and A_{em} are the raw absorbance values of the excitation/emission wavelength pair at which the intensity was measured, and the factor of 0.5 assumes that most of the fluorescence is collected from the middle of a 1.0 cm cuvette.

$$F_{\text{corr}} = F_{\text{obs}} \times 10^{0.5(A_{\text{ex}} + A_{\text{em}})} \quad (5.1)$$

Rayleigh and Raman scattering were addressed by subtracting the appropriate blank EEM from the sample EEM (despite this correction, the EEM plots still contain residual contribution from the first and second order Rayleigh scattering). Finally, intensities of the SOA samples were converted to QSU by dividing the intensities by the corrected fluorescence intensity of QS at the excitation/emission peak of 350/450 nm, in which 1 QSU = 0.1 ppm quinine sulfate in 0.05 M H₂SO₄ solution.

Absorption spectra of the SOA samples were taken with spectrophotometer (Shimadzu UV-2450). Raw absorbance values were converted to mass absorption coefficient (MAC) values cm² g⁻¹, using the following equation, where A_{10} is the measured base-10 absorbance, C_{mass}

(g cm⁻³) is the concentration of the SOA in solution, and b (cm) is the path length (standard quartz 10 mm cuvettes were used in these experiments):

$$MAC(\lambda) = \frac{A_{10}(\lambda) \times \ln(10)}{b \times C_{mass}} \quad (5.2)$$

The mass concentration only included the starting mass of SOA in solution, it did not include the masses of any of the products that may have formed during aging.

5.4 Results and Discussion

5.4.1 Fluorescence at Varying Acidities

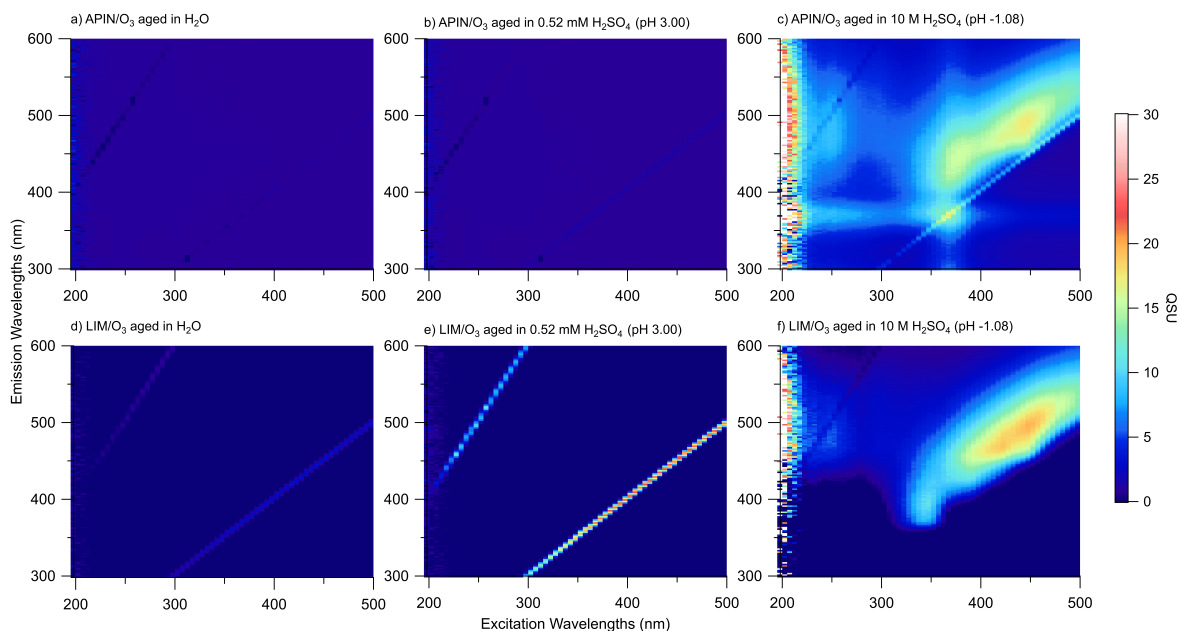


Figure 5.1: EEM plots for APIN/O₃ and LIM/O₃ SOA aged in H₂O, 0.52 H₂SO₄ (pH 3.00), and 10M H₂SO₄ (pH -1.08) for 2 days

Excitation-emission spectra of organic compounds in environmental samples are often presented as a 3-D excitation-emission matrix (EEM), which displays the intensity as a contour plot as function of the excitation and emission wavelengths.^{205,206} Figure 5.1 shows the EEM

plots for APIN/O₃ and LIM/O₃ SOA aged in H₂O, 0.52 H₂SO₄ (pH 3.00), and 10M H₂SO₄ (pH -1.08) for 2 days. In the control studies for APIN/O₃ (Figure 5.1a) and LIM/O₃ (Figure 5.1d) there is no evidence of fluorescence in the SOA mixture, as the intensities are low throughout the entire excitation wavelength range. This finding is consistent with previous work by Bones et al. (2010) and Lee et al. (2013), who reported no fluorescence in their respective controls for LIM/O₃ and APIN/O₃, and further supported by previous study by Wong et al. (2022), who showed that water does not have a significant influence on the chemical aging in SOA.^{146,185,199} Aging of SOA in 0.52 H₂SO₄ (pH 3.00) results in a plots (Figure 5.1b,e) that look very similar to the nonacidified controls, with no evidence of fluorophores appearing in the SOA. This indicates that moderately acidic conditions do not promote chemical reactions that lead to fluorescent compounds, which is consistent with no change in chemical composition of SOA at pH 3 reported in a previous study.¹⁸⁵ However, when the SOA is aged in 10M H₂SO₄ (pH -1.08), the plots look notably different (Figure 5.1c,f). For APIN SOA, there are four main regions: a strong peak with at Ex/Em at 350-500/450-575 nm, a moderately strong peak at Ex/Em = 350-375/350-400 nm, and two weaker peaks at Ex/Em = < 275/450-550 nm and Ex/Em = < 300/350-400 nm. For the LIM/O₃, there are only 3 regions that exhibit fluorescence: a strong peak at Ex/Em = 350-500/400-575 nm, a moderately strong peak (tail) at Ex/Em = 330-360/375-425 nm, and finally a weak peak at Ex/Em = 200-275/425-550 nm. The appearance of these peaks indicates that aging these SOA samples in acid promotes reactions leading to the formation of fluorophores.

The same experiments were repeated for APIN/OH and LIM/OH to examine the role of the oxidant in the formation of fluorophores. Similar to the case with the ozonolysis SOA, the unacidified control (Figure 5.2a,d) and samples aged in moderately acidic conditions (pH 3) do not produce any fluorophores, whereas the highly acidic conditions result in fluorescent solutions. For APIN/OH samples, there are two regions where the sample fluorescence is observed: a strong peak at Ex/Em = 350-500/450-575 nm and a weak peak at Ex/Em =

250/450-500 nm. On the other hand, LIM/OH has three regions in the EEM: a strong peak at $E_x/E_m = 350-500/400-575$ nm, a moderate peak (tail) at $E_x/E_m = 325-360/350-400$ nm and a weaker peak at $E_x/E_m = 200-300/450-550$ nm. In all systems, fluorophores do not

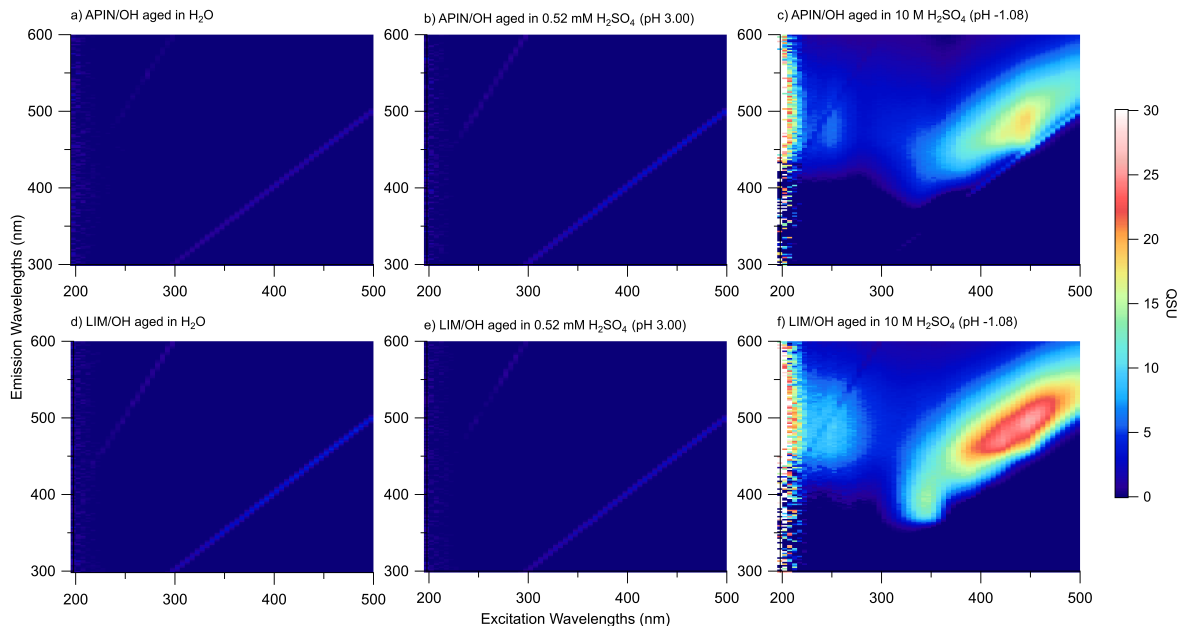


Figure 5.2: EEM plots for APIN/OH and LIM/OH SOA aged in H_2O , $0.52 H_2SO_4$ (pH 3.00), and $10M H_2SO_4$ (pH -1.08) for 2 days

form until the SOA samples are exposed to highly acidic conditions. However, the resulting fluorescence spectra are different for the APIN and LIM SOA, except for the shared strong peak at $E_x/E_m = 350-500/400-575$ nm. Although both APIN and LIM are both monoterpenes ($C_{10}H_{16}$), they have different structures, resulting in oxidation products of APIN being more sterically constrained. This subtle difference in molecular rigidity accounted for vastly different reactivity of APIN and LIM SOA with ammonia and amines,²⁰⁷ and it is may also be responsible for the difference in fluorescent properties of acid-aged SOA.

In the LIM/OH and LIM/ O_3 systems, both samples showed the same fluorescence peaks, but at different intensities. The photooxidation SOA (Figure 5.2f) has a higher fluorescence intensity than the ozonolysis SOA (Figure 5.1f), despite both samples having the same mass concentration, suggesting that the concentration of fluorophores in the LIM/OH SOA was

higher than in the LIM/O₃ SOA. Additionally, the relative intensities of the fluorescence regions within the EEM could give us insight into the composition of these fluorophores. The peaks at Ex/Em = 350-500/400-575 nm and Ex/Em = 200-300/450-550 nm are indicative of highly oxygenated compounds, while the peak at Ex/Em = 325-360/350-400 nm corresponds to less oxygenated molecules.²⁰⁸ Based on this classification, it seems that both LIM/OH and LIM/O₃ samples contain highly oxygenated and less oxygenated molecules, but LIM/O₃ SOA tends to have more fluorophores on the whole, as indicated by the higher intensity of the EEM peaks.

The APIN/OH and APIN/O₃ SOA had similar features in the EEM, but also notable differences. Common to both systems are the strong peak at Ex/Em = 350-500/450-575 nm and a weaker peak at Ex/Em = 250/450-500 nm, which correlate to highly oxygenated species.²⁰⁸ However, APIN/O₃ SOA has two additional regions where it fluoresces: a moderate peak at Ex/Em = 350-375/350-400 nm and a weak peak at Ex/Em = < 300/350-400 nm. These two peaks indicate the formation of less oxygenated fluorophores from acid catalysis.²⁰⁸ The APIN/OH and APIN/O₃ SOA have largely similar compounds, but in the APIN/OH system, RO₂ + HO₂ pathway is more important resulting in more products with hydroperoxide functionalities.¹²⁹ This could give us insight into what compounds have the ability to form fluorophores upon acid catalysis. Finally, Figure 5.3 shows the EEM spectra for anthropogenic SOA aged in varying acidic conditions. Similar to the behavior of biogenic SOA, fluorescence does not occur until the SOA is aged in highly acidic conditions. For TOL/OH and XYL/OH samples aged in 10M H₂SO₄ (pH -1.08), there are two regions of fluorescence: a moderate peak at Ex/Em = 325-375/375-425 nm and a weaker peak at Ex/Em = 300-500/425-550 nm. Compared to the biogenic photooxidation SOA, the fluorescence intensity of anthropogenic photooxidation SOA is significantly lower, with regions with the highest intensity having a difference of ~ 15 QSU. The presence of these two regions implies that the fluorophores include both less and highly oxygenated compounds, with less oxygenated

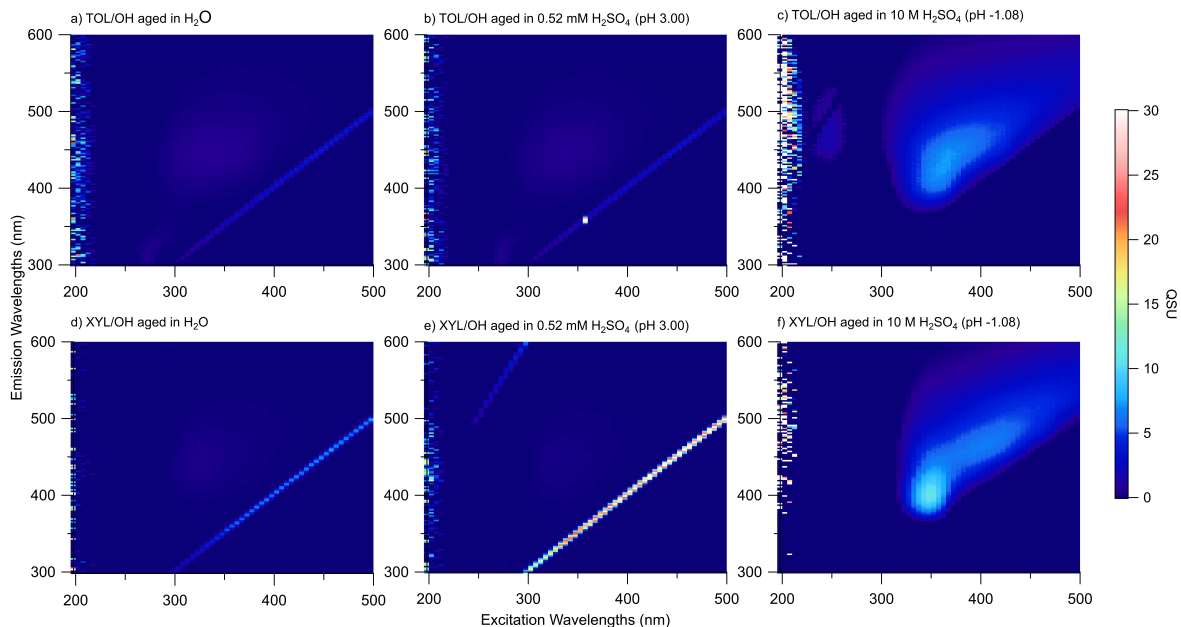


Figure 5.3: EEM plots for TOL/OH and XYL/OH SOA aged in H_2O , $0.52 \text{ H}_2\text{SO}_4$ (pH 3.00), and $10 \text{ M H}_2\text{SO}_4$ (pH -1.08) for 2 days

fluorophores being more prevalent.²⁰⁸ Based on this comparison, anthropogenic SOA do produce fluorophores upon acidic aging, but less effectively compared to biogenic SOA. Further

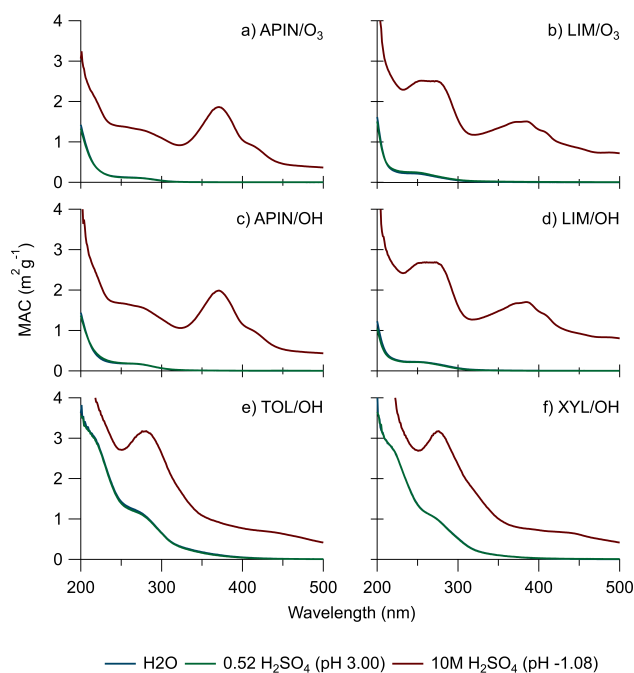


Figure 5.4: MAC spectra of biogenic and anthropogenic SOA aged in H_2O , $0.52 \text{ H}_2\text{SO}_4$ (pH 3.00), and $10 \text{ M H}_2\text{SO}_4$ (pH -1.08) for 2 days

evidence that acidity is a major driver of SOA aging is shown in Figure 5.4, which compares the MAC spectra of biogenic and anthropogenic SOA aged 10M H₂SO₄ (pH -1.08) for 2 days. For each of the samples, MAC of SOA aged in H₂O and 0.52 H₂SO₄ (pH 3.00) are essentially identical. However, SOA aged in 10M H₂SO₄ (pH -1.08) shows a different spectrum, with prominent absorbance between 200-400 nm, and extending far in the visible range, indicating the formation of highly conjugated compounds. The overlap with the visible part of the solar spectrum is especially important: the acid-aged SOA will have a much strong direct forcing on climate compared to the unaged ones.

5.4.2 Fluorescence and Acid–Base Equilibria

A series of additional experiments was conducted to test the sensitivity of MAC and fluorescence spectra to acid-base equilibria. A sample of SOA aged in acid for two days was diluted with 1:1 ACN/H₂O and the absorption spectra were collected for each sample to monitor a shift in peak absorbance (Figure 5.5). The APIN systems (Figure 5.5a,c) exhibited a dramatic peak shift in the strong near-UV band from 370 nm to 310 nm. The LIM systems (Figure 5.5b,d) had a similar dramatic change in the shape of the MAC spectra. Specifically, the peaks at 264 nm and 378 nm disappeared, and a new peak grew at 239 nm upon dilution. SOA generated from anthropogenic precursors (Figure 5.5e,f) has a considerably smaller shift in the spectrum of the order of 6 nm. Due to the solvent used the dilution process, it is likely that the polarity of the system changed which would result in a small shift in the MAC spectra for the anthropogenic SOA. It is clear that the MAC spectra are strongly pH dependent at high acidity, especially for biogenic SOA. We note that these shifts arise only from dilution by a factor of 4, which changes the effective pH by less than 0.5 units. This is sufficient to deprotonate the chromophore causing a change in the absorption spectrum.

Studies have shown that atmospheric compounds have absorption spectra that are pH dependent.

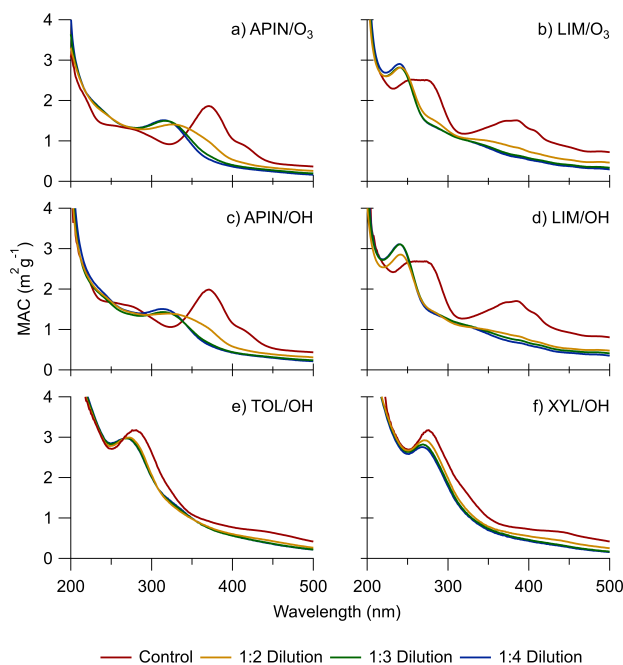


Figure 5.5: MAC spectra of biogenic and anthropogenic SOA aged in 10 M (pH -1.08) of H_2SO_4 and then diluted with 1:1 ACN/ H_2O at various dilution factors

dent. For example, the spectra of nitrophenols shift to longer wavelengths at basic pH due to formation of phenolates.^{167,168,209} Absorption spectra of imidazole-2-carboxaldehyde and pyruvic acid solutions can be altered depending on the pH, which is prompted by complex acid base equilibria in these systems.^{48,170} Additionally, the pH dependence of the aerosol absorption has also been detected in field samples collected in southeastern United States and Beijing.^{171,172} The results presented here conform that absorption spectra of acid-aged SOA become very sensitive to pH in acidic particles.

The diluted samples were also analyzed using fluorescence spectrophotometry to see if there were corresponding shifts in the EEM peaks. The resulting EEM graphs for biogenic O_3 SOA, biogenic OH SOA, and anthropogenic SOA are shown in Figures 5.6, 5.7, and 5.8. Note that the scales differ from that in Figures 5.1, 5.2, and 5.3 to account for the dilution in fluorophores in the sample.

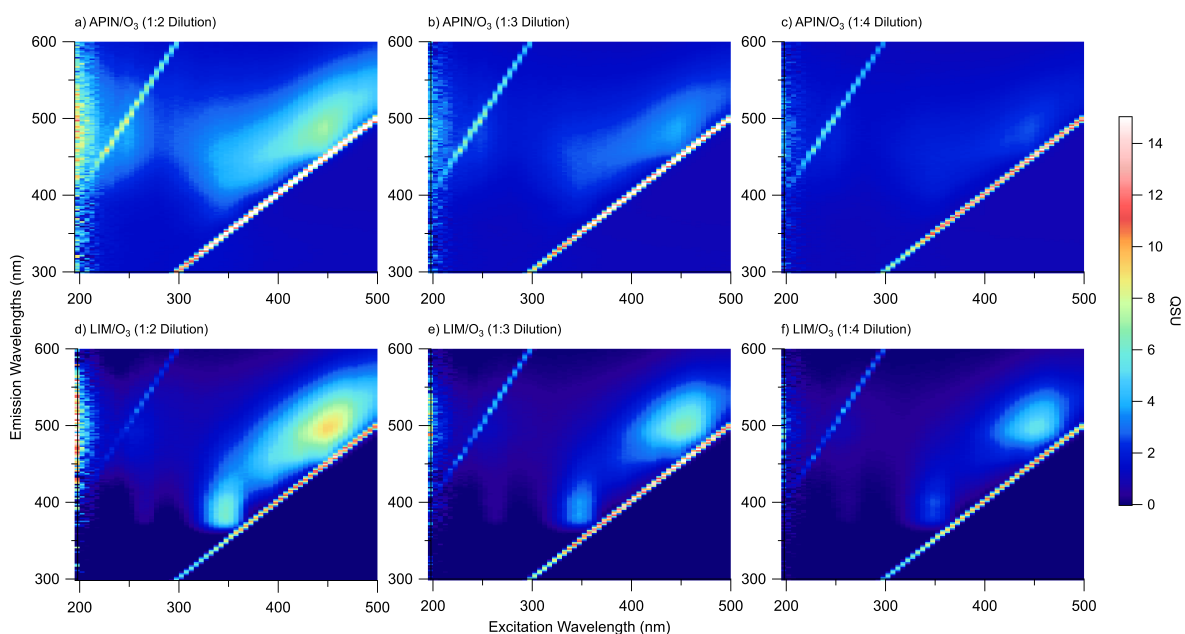


Figure 5.6: EEM plots for APIN/O₃ and LIM/O₃ SOA aged in 10M H₂SO₄ (pH -1.08) for 2 days and then diluted with 1:1 ACN/H₂O at 1:2 (a,d), 1:3 (b,e), and 1:4 (c,f) dilution factors

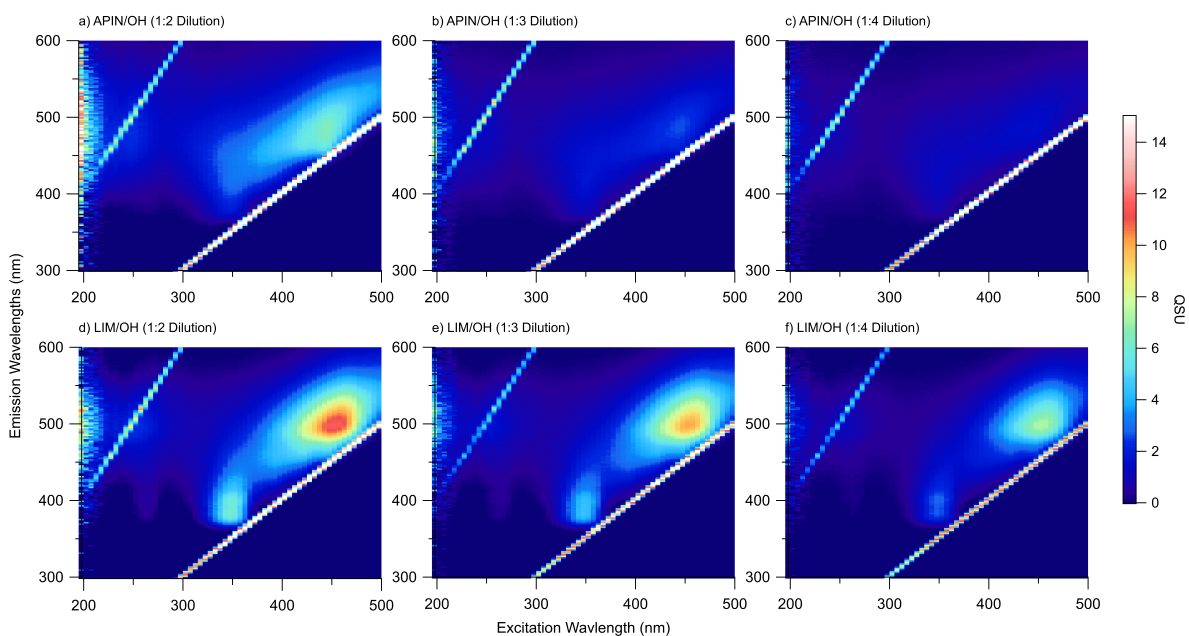


Figure 5.7: EEM plots for APIN/OH and LIM/OH SOA aged in 10M H₂SO₄ (pH -1.08) for 2 days and then diluted with 1:1 ACN/H₂O at 1:2 (a,d), 1:3 (b,e), and 1:4 (c,f) dilution factors

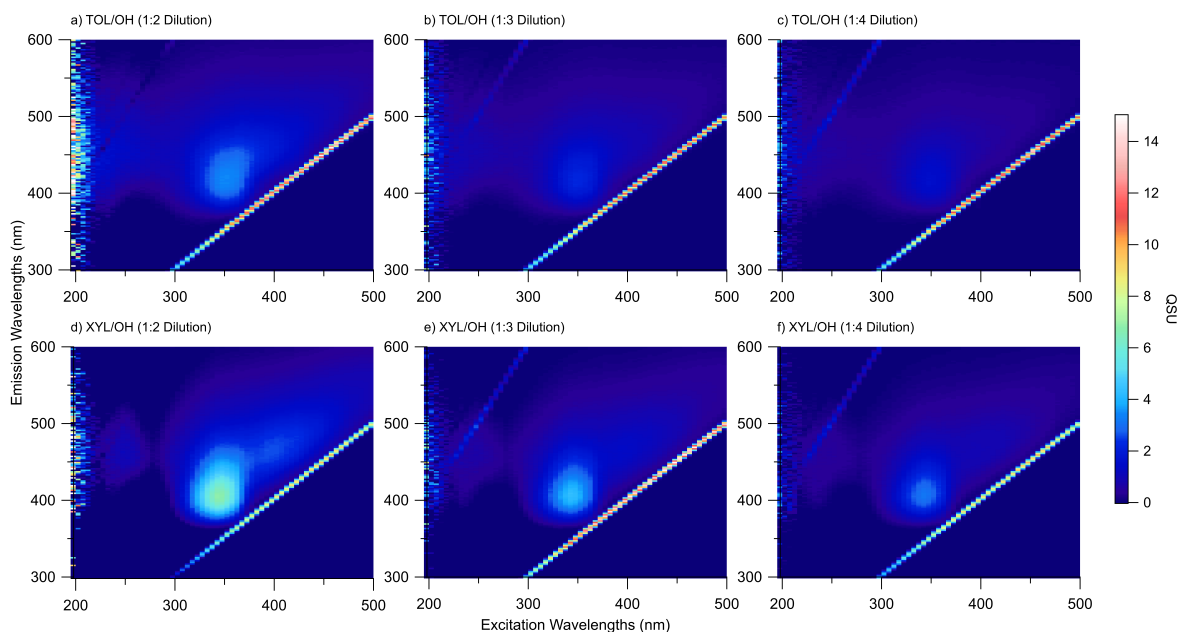


Figure 5.8: EEM plots for TOL/OH and XYL/OH SOA aged in 10M H_2SO_4 (pH -1.08) for 2 days and then diluted with 1:1 ACN/ H_2O at 1:2 (a,d), 1:3 (b,e), and 1:4 (c,f) dilution factors

The peaks in the diluted sample appeared at the same excitation and emission wavelength as in the undiluted sample (Figure 5.1cf, 5.2cf, 5.3cf), although with reduced intensity due to sample dilution. No evidence of spectral shifts was observed, indicating that the fluorescence was not strongly affected by acid-base equilibria after the SOA samples underwent highly acidic aging followed by dilution. To verify whether the reduced intensity in the EEM scaled with the sample dilution, the maximum fluorescence intensity of each sample was plotted against the mass concentration (Figure 5.9). In all cases, the maximum fluorescence intensity decreases in proportion to the SOA mass concentration in the solution. This suggests that the reduced intensity is due to sample dilution rather than acid-base equilibria affecting their fluorescence. Overall, the lack of spectral shifts in the EEM data, as compared to the strong changes in the MAC spectra, suggests that the fluorophores and chromophores in these SOA systems are distinct sets of compounds, that respond differently to acid-base equilibria.

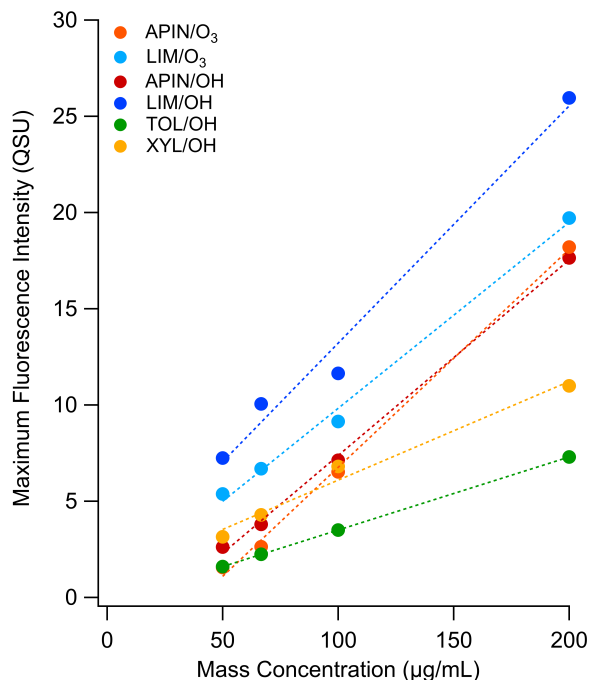


Figure 5.9: Maximum fluorescence intensity as a function of mass concentration for each SOA sample aged in 10M H₂SO₄ (pH -1.08) for 2 days and then diluted with 1:1 ACN/H₂O at various dilutions factors

5.4.3 Interferences with Bioaerosol Fluorescence

The use of fluorescence spectroscopy to carry out quantitative and qualitative analysis of aerosol particles, especially PBAP, is common.²¹⁰ However, now that this study has identified the formation fluorophores from aging SOA in highly acidic conditions, it is important to understand how these fluorophores interference with the analysis of PBAP. Based on the previous literature,¹⁹⁶ the two main classes of biological components that have similar spectral characteristics to the fluorophores formed in this study are 1) coenzymes and vitamins and 2) structural biopolymers and cell wall compounds.

Cofactors, coenzymes, and vitamins exhibit fluorescence due to heterocyclic aromatic rings within their molecular structures, such as those in pyridines, pteridines, pyridoxines, and flavins.^{211,212} For example, riboflavin is a ubiquitous coenzymatic redox carrier in most or-

ganisms and photoreceptors in plants and fungi. Riboflavin fluoresces at Ex/Em = 280-500/520-560 nm,^{211,213-216} which overlaps with the strong fluorescence peak in the biogenic SOA at Ex/Em at 350-500/450-575 nm. Other cofactors, coenzymes, and vitamins that interfere with the SOA fluorophores include NADPH, pyridoxine, pyridoxamine, neopterin and ergosterol, which are found in bioaerosols derived or contain fungi, plants, bacterial, microorganisms, and bacteria.^{213-215,217-220}

Fluorophores can also be found in structural biopolymers and cell wall compounds that are critical to many organisms and are prevalent in the atmosphere. For instance, cellulose and chitin, which are present in plants, fungi, and algae, can fluoresce at Ex/Em at 250-350/350-500 nm²²¹⁻²²³ and Ex/Em at 335/413 nm,²²⁴⁻²²⁶ respectively. However, the interference of peak in LIM/OH, LIM/O₃, TOL/OH, and XYL/OH SOA after acidic aging at Ex/Em 325-375/375-425 nm can cause complications in the analysis of these spectral regions and potentially lead to an overestimation of the biological components. Therefore, it is essential for researchers to carefully consider the presence of non-biological fluorophores in their analyses of biological components using fluorescence spectroscopy and to account for likely interference from aged SOA particles, especially if they were exposed to acidic conditions.

5.5 Conclusions

The acidity of atmospheric particles can have a large effect on the chemical processing of organic compounds in these particles and thereby their optical properties. The impacts of highly acidic conditions on the optical properties of particulate organics were explored by generating SOA from various precursors and aging the resulting SOA in bulk sulfuric acid solutions with atmospherically relevant acidities. We found that highly acidic conditions

(corresponding to $\text{pH} \sim -1$) resulted in the formation of chromophores and fluorophores after two days of aging, a time comparable to residence time for aerosol particles in the atmosphere.

The ability to detect and analyze fluorophores in PBAP using fluorescence spectroscopy has proven useful for understanding the sources and types of PBAP in the atmosphere.^{197,198} However, this study has shown that acidity is a major driver of the formation of fluorophores in particles of nonbiological origin, which presents challenges for quantitative and qualitative analysis of PBAP due to interferences from SOA.^{146,196,199–201}

These findings may be especially important in the context of aerosol processing in the upper troposphere and the lower stratosphere (UTLS). Organic compounds in UTLS particles are formed by the condensation of gas-phase precursors brought up by deep convection onto preexisting particles.^{173–175} The aerosols in this region are primarily composed of sulfuric acid (40–80 wt%), but they are also known to contain significant amounts of organic compounds.^{4,7,10} These results suggest that organic material in these particles should become fluorescent making it hard to distinguish these particles from PBAP by fluorescence methods. The findings from this work provide a first glimpse of how the chemical reactions between sulfuric acid and organic compounds can proceed over the long lifetime of the UTLS aerosols. Further studies should include identifying the structures for chromophores and fluorophores and doing these experiments at lower temperatures representative of UTLS.

Chapter 6

Conclusions and Future Directions

Atmospheric particles, droplets and environmental films are characterized by a range of acidities that affect both chemical and physical processes occurring in these environments. The work presented in this thesis demonstrated that sulfuric acid plays a significant role in the aging processes of secondary organic aerosol (SOA). This was done through a series of laboratory experiments that offered a detailed molecular-level understanding of the chemical interactions between monoterpene oxidation products and inorganic compounds like sulfuric acid.

Chapter 2 presented evidence that the presence of water leads to subtle changes in the chemical composition of α -pinene ozonolysis SOA. The observed extent of these changes, as judged from mass spectrometric analysis of SOA before and after aging, was relatively small, suggesting that hydrolysis and hydration are not major aging mechanisms for this type of SOA in the atmosphere. This observation can likely be generalized to SOA derived from low- NO_x oxidation of other biogenic volatile organic compounds (VOCs), however, it should not be generalized to all types SOA. Future studies should examine long-term aging of SOA from high- NO_x oxidation because such SOA contains organonitrates, an important atmospheric

constituent that is well known to hydrolyze. It will also be important to examine long-term stability of SOA derived from oxidation of aromatic VOCs, which have very different types of compounds compared to biogenic SOA.

Chapter 3 presented evidence that elevated concentrations sulfuric acid of aerosol particles plays vital role in changing the chemical composition and optical properties in α -pinene SOA. Specifically, under extremely concentrated sulfuric acid conditions corresponding to negative pH, SOA compounds undergo chemical reactions producing light-absorbing compounds as well as compounds containing sulfur. These conclusions are important for the upper troposphere and lower stratosphere (UTLS), as sulfuric acid is ubiquitous in this region, and organic compounds have been observed at these altitudes as well. The experiments described here were performed at ambient temperatures, and it is expected that lower temperatures, such as those in the UTLS, can affect the rate of the acid-catalyzed browning processes. Investigating the kinetic limitations of these reactions and the effect of temperature will provide a better understanding of the chemical reactions and their temperature dependence in the upper troposphere and lower stratosphere. In addition, it would be of interest to collect enough aerosol at these altitudes to perform mass spectrometric analysis that would compare the compounds observed in this study and in the field.

Chapter 4 identified the key mechanistic steps in the formation of the chromophores from acid-catalyzed reactions of α -pinene oxidation products, in support of measurements presented in Chapter 3. To broaden the scope of this research, it would be desirable to study how other major classes of organic compounds found in atmospheric aerosols behave in presence of concentrated sulfuric acid. It can be expected that in addition to carbonyl compounds studied in this work, sulfuric acid can react with carbohydrates (found in biomass burning smoke), polyols (found in isoprene SOA), nitrophenols (common in combustion aerosols) and organonitrates (found in high-NO_x SOA). Such targeted laboratory studies will improve our

understanding of chemical transformations in atmospheric particulate matter.

Chapter 5 offered evidence that biogenic and anthropogenic SOA form light-absorbing and fluorescent compounds upon exposure to strong acids. The next step would be to look for evidence of this chemistry by examining fluorescent properties of atmospheric particles such as those found in UTLS or downwind from strong sulfur dioxide emission sources.

In conclusion, this work provides compelling evidence that sulfuric acid plays a significant role in driving the aging processes in secondary organic aerosols. However, the discussed topics and methods only scratch the surface of the diverse reactions and properties exhibited by organic aerosols when they interact with acids, under conditions typical of the upper troposphere and lower stratosphere. Consequently, further research is necessary to fully comprehend the chemical fate of organic aerosols throughout their lifespan aloft.

References

- (1) Seinfeld, J. H.; Pandis, S. N., *Atmospheric Chemistry and Physics: From Air Pollution to Climate Change*, 3rd ed.; Wiley: 2016.
- (2) Finlayson-Pitts, B. J.; Pitts, J. N., *Chemistry of the upper and lower atmosphere : theory, experiments, and applications*; Academic Press: 2000, p 969.
- (3) Clegg, S. L.; Brimblecombe, P.; Wexler, A. S. Thermodynamic Model of the System $\text{H}^+ - \text{NH}_4^+ - \text{SO}_4^{2-} - \text{NO}_3^- - \text{H}_2\text{O}$ at Tropospheric Temperatures. *Journal of Physical Chemistry A* **1998**, *102*, 2137–2154.
- (4) Tabazadeh, A.; Toon, O. B.; Clegg, S. L.; Hamill, P. A new parameterization of $\text{H}_2\text{SO}_4/\text{H}_2\text{O}$ aerosol composition: Atmospheric implications. *Geophysical Research Letters* **1997**, *24*, 1931–1934.
- (5) Van Wyngarden, A. L.; Pérez-Montaña, S.; Bui, J. V. H.; Li, E. S. W.; Nelson, T. E.; Ha, K. T.; Leong, L.; Iraci, L. T. Complex chemical composition of colored surface films formed from reactions of propanal in sulfuric acid at upper troposphere/lower stratosphere aerosol acidities. *Atmospheric Chemistry and Physics* **2015**, *15*, 4225–4239.
- (6) Muralikrishna, I. V.; Manickam, V. Air Pollution Control Technologies. *Environmental Management* **2017**, 337–397.
- (7) Froyd, K. D.; Murphy, D. M.; Sanford, T. J.; Thomson, D. S.; Wilson, J. C.; Pfister, L.; Lait, L. Aerosol composition of the tropical upper troposphere. *Atmospheric Chemistry and Physics* **2009**, *9*, 4363–4385.
- (8) Murphy, D. M.; Thomson, D. S.; Mahoney, M. J. In Situ Measurements of Organics, Meteoritic Material, Mercury, and Other Elements in Aerosols at 5 to 19 Kilometers. *Science* **1998**, *282*, 1664–1669.
- (9) Murphy, D. M.; Froyd, K. D.; Schwarz, J. P.; Wilson, J. C. Observations of the chemical composition of stratospheric aerosol particles. *Quarterly Journal of the Royal Meteorological Society* **2014**, *140*, 1269–1278.
- (10) Murphy, D. M.; Cziczo, D. J.; Hudson, P. K.; Thomson, D. S. Carbonaceous material in aerosol particles in the lower stratosphere and tropopause region. *Journal of Geophysical Research: Atmospheres* **2007**, *112*, D04203/1–D04203/10.
- (11) Whitby, K. T. The physical characteristics of sulfur aerosols. *Atmospheric Environment (1967)* **1978**, *12*, 135–159.

- (12) Raes, F.; Van Dingenen, R.; Vignati, E.; Wilson, J.; Putaud, J. P.; Seinfeld, J. H.; Adams, P. Formation and cycling of aerosols in the global troposphere, 2000.
- (13) Whitby, K. T.; Cantrell, B. In *International Conference on Environmental Sensing and Assessment*, Las Vegas, Nevada, 1976.
- (14) Colbeck, I.; Lazaridis, M. Aerosols and environmental pollution. *Naturwissenschaften* **2010**, *97*, 117–131.
- (15) Shiraiwa, M. et al. Aerosol Health Effects from Molecular to Global Scales, 2017.
- (16) Ervens, B.; Turpin, B. J.; Weber, R. J. Secondary organic aerosol formation in cloud droplets and aqueous particles (aqSOA): A review of laboratory, field and model studies. *Atmospheric Chemistry and Physics* **2011**, *11*, 11069–11102.
- (17) Petzold, A.; Kärcher, B., *Aerosols in the Atmosphere*. In: Schumann, U. (eds) *Atmospheric Physics. Research Topics in Aerospace*. Springer, Berlin, Heidelberg: 2012, pp 37–53.
- (18) Toossi, R.; Novakov, T. The lifetime of aerosols in ambient air: Consideration of the effects of surfactants and chemical reactions. *Atmospheric Environment (1967)* **1985**, *19*, 127–133.
- (19) Tsigaridis, K. et al. The AeroCom evaluation and intercomparison of organic aerosol in global models. *Atmospheric Chemistry and Physics* **2014**, *14*, 10845–10895.
- (20) Hyslop, N. P. Impaired visibility: the air pollution people see. *Atmospheric Environment* **2009**, *43*, 182–195.
- (21) Hunten, D. M. Residence times of aerosols and gases in the stratosphere. *Geophysical Research Letters* **1975**, *2*, 26–28.
- (22) Kanakidou, M. et al. Organic aerosol and global climate modelling: A review, 2005.
- (23) Myhre, G.; Myhre, C. E. L.; Samset, B. H.; Storelvmo, T. Aerosols and their Relation to Global Climate and Climate Sensitivity. *Nature Education Knowledge* **2013**, *4*, 7.
- (24) Ng, N. L.; Kroll, J. H.; Chan, A. W.; Chhabra, P. S.; Flagan, R. C.; Seinfeld, J. H. Secondary organic aerosol formation from m-xylene, toluene, and benzene. *Atmospheric Chemistry and Physics* **2007**, *7*, 3909–3922.
- (25) Song, C.; Na, K.; Cocker, D. R. Impact of the hydrocarbon to NO_x ratio on secondary organic aerosol formation. *Environmental Science and Technology* **2005**, *39*, 3143–3149.
- (26) Presto, A. A.; Huff Hartz, K. E.; Donahue, N. M. Secondary organic aerosol production from terpene ozonolysis. 2. Effect of NO_x concentration. *Environmental Science and Technology* **2005**, *39*, 7046–7054.
- (27) Hatakeyama, S.; Izumi, K.; Fukuyama, T.; Akimoto, H.; Washida, N. Reactions of OH with α -pinene and β -pinene in air: Estimate of global CO production from the atmospheric oxidation of terpenes. *Journal of Geophysical Research: Atmospheres* **1991**, *96*, 947–958.

- (28) Kroll, J. H.; Ng, N. L.; Murphy, S. M.; Flagan, R. C.; Seinfeld, J. H. Secondary organic aerosol formation from isoprene photooxidation. *Environmental Science and Technology* **2006**, *40*, 1869–1877.
- (29) Ervens, B.; Carlton, A. G.; Turpin, B. J.; Altieri, K. E.; Kreidenweis, S. M.; Feingold, G. Secondary organic aerosol yields from cloud-processing of isoprene oxidation products. *Geophysical Research Letters* **2008**, *35*, 2816.
- (30) D’Ambro, E. L. et al. Molecular composition and volatility of isoprene photochemical oxidation secondary organic aerosol under low- and high-NO_x conditions. *Atmospheric Chemistry and Physics* **2017**, *17*, 159–174.
- (31) Liu, S.; Jiang, X.; Tsona, N. T.; Lv, C.; Du, L. Effects of NO_x, SO₂ and RH on the SOA formation from cyclohexene photooxidation. *Chemosphere* **2019**, *216*, 794–804.
- (32) You, Y.; Smith, M. L.; Song, M.; Martin, S. T.; Bertram, A. K. Liquid–liquid phase separation in atmospherically relevant particles consisting of organic species and inorganic salts. *International Reviews in Physical Chemistry* **2014**, *33*, 43–77.
- (33) You, Y.; Renbaum-Wolff, L.; Carreras-Sospedra, M.; Hanna, S. J.; Hiranuma, N.; Kamal, S.; Smith, M. L.; Zhang, X.; Weber, R. J.; Shilling, J. E.; Dabdub, D.; Martin, S. T.; Bertram, A. K. Images reveal that atmospheric particles can undergo liquid–liquid phase separations. *Proceedings of the National Academy of Sciences of the United States of America* **2012**, *109*, 13188–13193.
- (34) Gao, S.; Ng, N. L.; Keywood, M.; Varutbangkul, V.; Bahreini, R.; Nenes, A.; He, J.; Yoo, K. Y.; Beauchamp, J. L.; Hodyss, R. P.; Flagan, R. C.; Seinfeld, J. H. Particle phase acidity and oligomer formation in secondary organic aerosol. *Environmental Science and Technology* **2004**, *38*, 6582–6589.
- (35) Iinuma, Y. et al. Laboratory studies on secondary organic aerosol formation from terpenes. *Faraday Discussions* **2005**, *130*, 279–294.
- (36) Lambe, A. T.; Chhabra, P. S.; Onasch, T. B.; Brune, W. H.; Hunter, J. F.; Kroll, J. H.; Cummings, M. J.; Brogan, J. F.; Parmar, Y.; Worsnop, D. R.; Kolb, C. E.; Davidovits, P. Effect of oxidant concentration, exposure time, and seed particles on secondary organic aerosol chemical composition and yield. *Atmospheric Chemistry and Physics* **2015**, *15*, 3063–3075.
- (37) Kristensen, K.; Jensen, L. N.; Glasius, M.; Bilde, M. The effect of sub-zero temperature on the formation and composition of secondary organic aerosol from ozonolysis of alpha-pinene. *Environmental Science: Processes & Impacts* **2017**, *19*, 1220–1234.
- (38) Li, J.; Wang, W.; Li, K.; Zhang, W.; Peng, C.; Zhou, L.; Shi, B.; Chen, Y.; Liu, M.; Li, H.; Ge, M. Temperature effects on optical properties and chemical composition of secondary organic aerosol derived from n-dodecane. *Atmospheric Chemistry and Physics* **2020**, *20*, 8123–8137.
- (39) Deng, Y.; Inomata, S.; Sato, K.; Ramasamy, S.; Morino, Y.; Enami, S.; Tanimoto, H. Temperature and acidity dependence of secondary organic aerosol formation from α -pinene ozonolysis with a compact chamber system. *Atmospheric Chemistry and Physics* **2021**, *21*, 5983–6003.

- (40) Faust, J. A.; Wong, J. P. S.; Lee, A. K. Y.; Abbatt, J. P. D. Role of Aerosol Liquid Water in Secondary Organic Aerosol Formation from Volatile Organic Compounds. *Environmental Science & Technology* **2017**, *51*, 1405–1413.
- (41) Wong, J. P. S.; Lee, A. K. Y.; Abbatt, J. P. D. Impacts of Sulfate Seed Acidity and Water Content on Isoprene Secondary Organic Aerosol Formation. *Environmental Science & Technology* **2015**, *49*, 13215–13221.
- (42) Odum, J. R.; Hoffmann, T.; Bowman, F.; Collins, D.; Flagan, R. C.; Seinfeld, J. H. Gas/Particle Partitioning and Secondary Organic Aerosol Yields. *Environ. Sci. Technol.* **1996**, *30*, 2580–2585.
- (43) Hu, K. S.; Darer, A. I.; Elrod, M. J. Thermodynamics and kinetics of the hydrolysis of atmospherically relevant organonitrates and organosulfates. *Atmospheric Chemistry and Physics* **2011**, *11*, 8307–8320.
- (44) Häkkinen, S. A.; McNeill, V. F.; Riipinen, I. Effect of inorganic salts on the volatility of organic acids. *Environmental Science and Technology* **2014**, *48*, 13718–13726.
- (45) Mikhailov, E.; Vlasenko, S.; Martin, S. T.; Koop, T.; Pöschl, U. Amorphous and crystalline aerosol particles interacting with water vapor: Conceptual framework and experimental evidence for restructuring, phase transitions and kinetic limitations. *Atmospheric Chemistry and Physics* **2009**, *9*, 9491–9522.
- (46) Carrico, C. M.; Petters, M. D.; Kreidenweis, S. M.; Sullivan, A. P.; McMeeking, G. R.; Levin, E. J.; Engling, G.; Malm, W. C.; Collett, J. L. Water uptake and chemical composition of fresh aerosols generated in open burning of biomass. *Atmospheric Chemistry and Physics* **2010**, *10*, 5165–5178.
- (47) Pye, H. O. T. et al. The acidity of atmospheric particles and clouds. *Atmos. Chem. Phys* **2020**, *20*, 4809–4888.
- (48) Tilgner, A.; Schaefer, T.; Alexander, B.; Barth, M. C.; Collett, J. L.; Fahey, K. M.; Nenes, A.; Pye, H. O.; Herrmann, H.; McNeill, V. F. Acidity and the multiphase chemistry of atmospheric aqueous particles and clouds. *Atmospheric Chemistry and Physics* **2021**, *21*, 13483–13536.
- (49) Guo, H.; Xu, L.; Bougiatioti, A.; Cerully, K. M.; Capps, S. L.; Hite, J. R.; Carlton, A. G.; Lee, S. H.; Bergin, M. H.; Ng, N. L.; Nenes, A.; Weber, R. J. Fine-particle water and pH in the southeastern United States. *Atmospheric Chemistry and Physics* **2015**, *15*, 5211–5228.
- (50) Guo, H.; Sullivan, A. P.; Campuzano-Jost, P.; Schroder, J. C.; Lopez-Hilfiker, F. D.; Dibb, J. E.; Jimenez, J. L.; Thornton, J. A.; Brown, S. S.; Nenes, A.; Weber, R. J. Fine particle pH and the partitioning of nitric acid during winter in the northeastern United States. *Journal of Geophysical Research: Atmospheres* **2016**, *121*, 355–10.
- (51) Tan, T.; Hu, M.; Li, M.; Guo, Q.; Wu, Y.; Fang, X.; Gu, F.; Wang, Y.; Wu, Z. New insight into PM_{2.5} pollution patterns in Beijing based on one-year measurement of chemical compositions. *Science of The Total Environment* **2018**, *621*, 734–743.

- (52) Wang, H.; Ding, J.; Xu, J.; Wen, J.; Han, J.; Wang, K.; Shi, G.; Feng, Y.; Ivey, C. E.; Wang, Y.; Nenes, A.; Zhao, Q.; Russell, A. G. Aerosols in an arid environment: The role of aerosol water content, particulate acidity, precursors, and relative humidity on secondary inorganic aerosols. *Science of The Total Environment* **2019**, *646*, 564–572.
- (53) Xue, J.; Lau, A. K.; Yu, J. Z. A study of acidity on PM_{2.5} in Hong Kong using online ionic chemical composition measurements. *Atmospheric Environment* **2011**, *45*, 7081–7088.
- (54) Squizzato, S.; Masiol, M.; Brunelli, A.; Pistollato, S.; Tarabotti, E.; Rampazzo, G.; Pavoni, B. Factors determining the formation of secondary inorganic aerosol: A case study in the Po Valley (Italy). *Atmospheric Chemistry and Physics* **2013**, *13*, 1927–1939.
- (55) Guo, H.; Otjes, R.; Schlag, P.; Kiendler-Scharr, A.; Nenes, A.; Weber, R. J. Effectiveness of ammonia reduction on control of fine particle nitrate. *Atmospheric Chemistry and Physics* **2018**, *18*, 12241–12256.
- (56) Tao, Y.; Murphy, J. G. The sensitivity of PM_{2.5} acidity to meteorological parameters and chemical composition changes: 10-year records from six Canadian monitoring sites. *Atmospheric Chemistry and Physics* **2019**, *19*, 9309–9320.
- (57) Usher, C. R.; Michel, A. E.; Grassian, V. H. Reactions on Mineral Dust. *Chemical Reviews* **2003**, *103*, 4883–4939.
- (58) Battaglia, M. A.; Douglas, S.; Hennigan, C. J. Effect of the Urban Heat Island on Aerosol pH. *Environmental Science and Technology* **2017**, *51*, 13095–13103.
- (59) Nah, T.; Guo, H.; Sullivan, A. P.; Chen, Y.; Tanner, D. J.; Nenes, A.; Russell, A.; Lee Ng, N.; Gregory Huey, L.; Weber, R. J. Characterization of aerosol composition, aerosol acidity, and organic acid partitioning at an agriculturally intensive rural southeastern US site. *Atmospheric Chemistry and Physics* **2018**, *18*, 11471–11491.
- (60) Murphy, J. G.; Gregoire, P. K.; Tevlin, A. G.; Wentworth, G. R.; Ellis, R. A.; Markovic, M. Z.; VandenBoer, T. C. Observational constraints on particle acidity using measurements and modelling of particles and gases. *Faraday Discussions* **2017**, *200*, 379–395.
- (61) Cheng, C.; Wang, G.; Meng, J.; Wang, Q.; Cao, J.; Li, J.; Wang, J. Size-resolved airborne particulate oxalic and related secondary organic aerosol species in the urban atmosphere of Chengdu, China. *Atmospheric Research* **2015**, *161-162*, 134–142.
- (62) Pszenny, A. A.; Moldanová, J.; Keene, W. C.; Sander, R.; Maben, J. R.; Martinez, M.; Crutzen, P. J.; Perner, D.; Prinn, R. G. Halogen cycling and aerosol pH in the Hawaiian marine boundary layer. *Atmospheric Chemistry and Physics* **2004**, *4*, 147–168.
- (63) Vieira-Filho, M.; Pedrotti, J. J.; Fornaro, A. Water-soluble ions species of size-resolved aerosols: Implications for the atmospheric acidity in São Paulo megacity, Brazil. *Atmospheric Research* **2016**, *181*, 281–287.

- (64) Bougiatioti, A.; Nikolaou, P.; Stavroulas, I.; Kouvarakis, G.; Weber, R.; Nenes, A.; Kanakidou, M.; Mihalopoulos, N. Particle water and pH in the eastern Mediterranean: Source variability and implications for nutrient availability. *Atmospheric Chemistry and Physics* **2016**, *16*, 4579–4591.
- (65) Hennigan, C. J.; Izumi, J.; Sullivan, A. P.; Weber, R. J.; Nenes, A. A critical evaluation of proxy methods used to estimate the acidity of atmospheric particles. *Atmospheric Chemistry and Physics* **2015**, *15*, 2775–2790.
- (66) Liu, M.; Song, Y.; Zhou, T.; Xu, Z.; Yan, C.; Zheng, M.; Wu, Z.; Hu, M.; Wu, Y.; Zhu, T. Fine particle pH during severe haze episodes in northern China. *Geophysical Research Letters* **2017**, *44*, 5213–5221.
- (67) Jia, L.; Xu, Y. Different roles of water in secondary organic aerosol formation from toluene and isoprene. *Atmospheric Chemistry and Physics* **2018**, *18*, 8137–8154.
- (68) Song, S.; Gao, M.; Xu, W.; Shao, J.; Shi, G.; Wang, S.; Wang, Y.; Sun, Y.; McElroy, M. B. Fine-particle pH for Beijing winter haze as inferred from different thermodynamic equilibrium models. *Atmospheric Chemistry and Physics* **2018**, *18*, 7423–7438.
- (69) Young, A. H.; Keene, W. C.; P Pszenny, A. A.; Sander, R.; Thornton, J. A.; Riedel, T. P.; Maben, J. R.; Keene, W. C.; P Pszenny, A. A.; Sander, R.; Thornton, J. A.; Riedel, T. P.; Maben, J. R. Phase partitioning of soluble trace gases with size-resolved aerosols in near-surface continental air over northern Colorado, USA, during winter. *Journal of Geophysical Research: Atmospheres* **2013**, *118*, 9414–9427.
- (70) De Haan, D. O.; Corrigan, A. L.; Tolbert, M. A.; Jimenez, J. L.; Wood, S. E.; Turley, J. J. Secondary organic aerosol formation by self-reactions of methylglyoxal and glyoxal in evaporating droplets. *Environmental Science and Technology* **2009**, *43*, 8184–8190.
- (71) Yasmeen, F.; Sauret, N.; Gal, J. F.; Maria, P. C.; Massi, L.; Maenhaut, W.; Claeys, M. Characterization of oligomers from methylglyoxal under dark conditions: A pathway to produce secondary organic aerosol through cloud processing during nighttime. *Atmospheric Chemistry and Physics* **2010**, *10*, 3803–3812.
- (72) Sareen, N.; Schwier, A. N.; Shapiro, E. L.; Mitroo, D.; McNeill, V. F. Secondary organic material formed by methylglyoxal in aqueous aerosol mimics. *Atmospheric Chemistry and Physics* **2010**, *10*, 997–1016.
- (73) Maroń, M. K.; Takahashi, K.; Shoemaker, R. K.; Vaida, V. Hydration of pyruvic acid to its geminal-diol, 2,2-dihydroxypropanoic acid, in a water-restricted environment. *Chemical Physics Letters* **2011**, *513*, 184–190.
- (74) Rapf, R. J.; Dooley, M. R.; Kappes, K.; Perkins, R. J.; Vaida, V. pH Dependence of the Aqueous Photochemistry of α -Keto Acids. *The Journal of Physical Chemistry A* **2017**, *121*, 8368–8379.
- (75) Rapf, R. J.; Perkins, R. J.; Carpenter, B. K.; Vaida, V. Mechanistic Description of Photochemical Oligomer Formation from Aqueous Pyruvic Acid. *The Journal of Physical Chemistry A* **2017**, *121*, 4272–4282.

- (76) Esteve, W.; Nozière, B. Uptake and Reaction Kinetics of Acetone, 2-Butanone, 2,4-Pentanedione, and Acetaldehyde in Sulfuric Acid Solutions. *Journal of Physical Chemistry A* **2005**, *109*, 10920–10928.
- (77) Liggio, J.; Li, S. M. Reactive uptake of pinonaldehyde on acidic aerosols. *Journal of Geophysical Research: Atmospheres* **2006**, *111*, 24303.
- (78) Casale, M. T.; Richman, A. R.; Elrod, M. J.; Garland, R. M.; Beaver, M. R.; Tolbert, M. A. Kinetics of acid-catalyzed aldol condensation reactions of aliphatic aldehydes. *Atmospheric Environment* **2007**, *41*, 6212–6224.
- (79) Nozière, B.; Esteve, W. Light-absorbing aldol condensation products in acidic aerosols: Spectra, kinetics, and contribution to the absorption index. *Atmospheric Environment* **2007**, *41*, 1150–1163.
- (80) Krizner, H. E.; De Haan, D. O.; Kua, J. Thermodynamics and Kinetics of Methylglyoxal Dimer Formation: A Computational Study. *The Journal of Physical Chemistry A* **2009**, *113*, 6994–7001.
- (81) Herrmann, H.; Schaefer, T.; Tilgner, A.; Styler, S. A.; Weller, C.; Teich, M.; Otto, T. Tropospheric Aqueous-Phase Chemistry: Kinetics, Mechanisms, and Its Coupling to a Changing Gas Phase. *Chemical Reviews* **2015**, *115*, 4259–4334.
- (82) Mabey, W.; Mill, T. Critical review of hydrolysis of organic compounds in water under environmental conditions. *Journal of Physical and Chemical Reference Data* **2009**, *7*, 383.
- (83) Altieri, K. E.; Carlton, A. G.; Lim, H.-J.; Turpin, B. J.; Seitzinger, S. P. Evidence for Oligomer Formation in Clouds: Reactions of Isoprene Oxidation Products. *Environmental Science & Technology* **2006**, *40*, 4956–4960.
- (84) Altieri, K. E.; Seitzinger, S. P.; Carlton, A. G.; Turpin, B. J.; Klein, G. C.; Marshall, A. G. Oligomers formed through in-cloud methylglyoxal reactions: Chemical composition, properties, and mechanisms investigated by ultra-high resolution FT-ICR mass spectrometry. *Atmospheric Environment* **2008**, *42*, 1476–1490.
- (85) McNeill, V. F.; Woo, J. L.; Kim, D. D.; Schwier, A. N.; Wannell, N. J.; Sumner, A. J.; Barakat, J. M. Aqueous-phase secondary organic aerosol and organosulfate formation in atmospheric aerosols: A modeling study. *Environmental Science and Technology* **2012**, *46*, 8075–8081.
- (86) Schindelka, J.; Iinuma, Y.; Hoffmann, D.; Herrmann, H. Sulfate radical-initiated formation of isoprene-derived organosulfates in atmospheric aerosols. *Faraday Discussions* **2013**, *165*, 237–259.
- (87) Gaston, C. J.; Riedel, T. P.; Zhang, Z.; Gold, A.; Surratt, J. D.; Thornton, J. A. Reactive uptake of an isoprene-derived epoxydiol to submicron aerosol particles. *Environmental Science and Technology* **2014**, *48*, 11178–11186.
- (88) Cortés, D. A.; Elrod, M. J. Kinetics of the Aqueous Phase Reactions of Atmospherically Relevant Monoterpene Epoxides. *The Journal of Physical Chemistry A* **2017**, *121*, 9297–9305.

- (89) Czoschke, N. M.; Jang, M.; Kamens, R. M. Effect of acidic seed on biogenic secondary organic aerosol growth. *Atmospheric Environment* **2003**, *37*, 4287–4299.
- (90) Tolocka, M. P.; Jang, M.; Ginter, J. M.; Cox, F. J.; Kamens, R. M.; Johnston, M. V. Formation of Oligomers in Secondary Organic Aerosol. *Environmental Science & Technology* **2004**, *38*, 1428–1434.
- (91) Surratt, J. D.; Kroll, J. H.; Kleindienst, T. E.; Edney, E. O.; Claeys, M.; Sorooshian, A.; Ng, N. L.; Offenberg, J. H.; Lewandowski, M.; Jaoui, M.; Flagan, R. C.; Seinfeld, J. H. Evidence for Organosulfates in Secondary Organic Aerosol. *Environmental Science and Technology* **2006**, *41*, 517–527.
- (92) Iinuma, Y.; Müller, C.; Böge, O.; Gnauk, T.; Herrmann, H. The formation of organic sulfate esters in the limonene ozonolysis secondary organic aerosol (SOA) under acidic conditions. *Atmospheric Environment* **2007**, *41*, 5571–5583.
- (93) Song, C.; Gyawali, M.; Zaveri, R. A.; Shilling, J. E.; Arnott, W. P. Light absorption by secondary organic aerosol from α -pinene: Effects of oxidants, seed aerosol acidity, and relative humidity. *Journal of Geophysical Research: Atmospheres* **2013**, *118*, 741–11.
- (94) Han, Y.; Stroud, C. A.; Liggió, J.; Li, S.-M. The effect of particle acidity on secondary organic aerosol formation from α -pinene photooxidation under atmospherically relevant conditions. *Atmospheric Chemistry and Physics* **2016**, *16*, 13929–13944.
- (95) Nestorowicz, K.; Jaoui, M.; Jan Rudzinski, K.; Lewandowski, M.; Kleindienst, T. E.; Spólnik, G.; Danikiewicz, W.; Szmigielski, R. Chemical composition of isoprene SOA under acidic and non-acidic conditions: Effect of relative humidity. *Atmospheric Chemistry and Physics* **2018**, *18*, 18101–18121.
- (96) Liggió, J.; Li, S. M. Organosulfate formation during the uptake of pinonaldehyde on acidic sulfate aerosols. *Geophysical Research Letters* **2006**, *33*, 13808.
- (97) Eddingsaas, N. C.; Vandervelde, D. G.; Wennberg, P. O. Kinetics and products of the acid-catalyzed ring-opening of atmospherically relevant butyl epoxy alcohols. *Journal of Physical Chemistry A* **2010**, *114*, 8106–8113.
- (98) Lin, Y.-H.; Budisulistiorini, S. H.; Chu, K.; Siejack, R. A.; Zhang, H.; Riva, M.; Zhang, Z.; Gold, A.; Kautzman, K. E.; Surratt, J. D. Light-Absorbing Oligomer Formation in Secondary Organic Aerosol from Reactive Uptake of Isoprene Epoxydiols. *Environmental Science & Technology* **2014**, *48*, 12012–12021.
- (99) Chan, K. M.; Huang, D. D.; Li, Y. J.; Chan, M. N.; Seinfeld, J. H.; Chan, C. K. Oligomeric products and formation mechanisms from acid-catalyzed reactions of methyl vinyl ketone on acidic sulfate particles. *Journal of Atmospheric Chemistry* **2013**, *70*, 1–18.
- (100) Molina, M. J.; Ivanov, A. V.; Trakhtenberg, S.; Molina, L. T. Atmospheric evolution of organic aerosol. *Geophysical Research Letters* **2004**, *31*, 22104.
- (101) Jimenez, J. L. et al. Evolution of organic aerosols in the atmosphere. *Science* **2009**, *326*, 1525–1529.

- (102) Cole-Filipiak, N. C.; O'Connor, A. E.; Elrod, M. J. Kinetics of the hydrolysis of atmospherically relevant isoprene-derived hydroxy epoxides. *Environmental Science and Technology* **2010**, *44*, 6718–6723.
- (103) Nozière, B.; Fache, F.; Maxut, A.; Fenet, B.; Baudouin, A.; Fine, L.; Ferronato, C. The hydrolysis of epoxides catalyzed by inorganic ammonium salts in water: Kinetic evidence for hydrogen bond catalysis. *Physical Chemistry Chemical Physics* **2018**, *20*, 1583–1590.
- (104) Barsanti, K. C.; Pankow, J. F. Thermodynamics of the formation of atmospheric organic particulate matter by accretion reactions-Part 3: Carboxylic and dicarboxylic acids. *Atmospheric Environment* **2006**, *40*, 6676–6686.
- (105) Loeffler, K. W.; Koehler, C. A.; Paul, N. M.; De Haan, D. O. Oligomer formation in evaporating aqueous glyoxal and methyl glyoxal solutions. *Environmental Science and Technology* **2006**, *40*, 6318–6323.
- (106) Claffin, M. S.; Krechmer, J. E.; Hu, W.; Jimenez, J. L.; Ziemann, P. J. Functional Group Composition of Secondary Organic Aerosol Formed from Ozonolysis of α -Pinene under High VOC and Autoxidation Conditions. *ACS Earth and Space Chemistry* **2018**, *2*, 1196–1210.
- (107) Zhao, R.; Kenseth, C. M.; Huang, Y.; Dalleska, N. F.; Kuang, X. M.; Chen, J.; Paulson, S. E.; Seinfeld, J. H. Rapid Aqueous-Phase Hydrolysis of Ester Hydroperoxides Arising from Criegee Intermediates and Organic Acids. *Journal of Physical Chemistry A* **2018**, *122*, 5190–5201.
- (108) Kleindienst, T. E.; Jaoui, M.; Lewandowski, M.; Offenberg, J. H.; Docherty, K. S. The formation of SOA and chemical tracer compounds from the photooxidation of naphthalene and its methyl analogs in the presence and absence of nitrogen oxides. *Atmospheric Chemistry and Physics* **2012**, *12*, 8711–8726.
- (109) Jiang, K.; Hill, D. R.; Elrod, M. J. Assessing the Potential for Oligomer Formation from the Reactions of Lactones in Secondary Organic Aerosols. *Journal of Physical Chemistry A* **2018**, *122*, 292–302.
- (110) Nguyen, T. B.; Bates, K. H.; Crounse, J. D.; Schwantes, R. H.; Zhang, X.; Kjaergaard, H. G.; Surratt, J. D.; Lin, P.; Laskin, A.; Seinfeld, J. H.; Wennberg, P. O. Mechanism of the hydroxyl radical oxidation of methacryloyl peroxy nitrates (MPAN) and its pathway toward secondary organic aerosol formation in the atmosphere. *Physical Chemistry Chemical Physics* **2015**, *17*, 17914–17926.
- (111) Bean, J. K.; Hildebrandt Ruiz, L. Gas–particle partitioning and hydrolysis of organic nitrates formed from the oxidation of α -pinene in environmental chamber experiments. *Atmospheric Chemistry and Physics* **2016**, *16*, 2175–2184.
- (112) Liu, S.; Shilling, J. E.; Song, C.; Hiranuma, N.; Zaveri, R. A.; Russell, L. M. Hydrolysis of Organonitrate Functional Groups in Aerosol Particles. *Aerosol Science and Technology* **2012**, *46*, 1359–1369.

- (113) Rindelaub, J. D.; Borca, C. H.; Hostetler, M. A.; Slade, J. H.; Lipton, M. A.; Slipchenko, L. V.; Shepson, P. B. The acid-catalyzed hydrolysis of an α -pinene-derived organic nitrate: kinetics, products, reaction mechanisms, and atmospheric impact. *Atmospheric Chemistry and Physics* **2016**, *16*, 15425–15432.
- (114) Rindelaub, J. D.; McAvey, K. M.; Shepson, P. B. The photochemical production of organic nitrates from α -pinene and loss via acid-dependent particle phase hydrolysis. *Atmospheric Environment* **2015**, *100*, 193–201.
- (115) Takeuchi, M.; Ng, N. L. Chemical composition and hydrolysis of organic nitrate aerosol formed from hydroxyl and nitrate radical oxidation of α -pinene and β -pinene. *Atmospheric Chemistry and Physics* **2019**, *19*, 12749–12766.
- (116) Zare, A.; Fahey, K. M.; Sarwar, G.; Cohen, R. C.; Pye, H. O. Vapor-Pressure Pathways Initiate but Hydrolysis Products Dominate the Aerosol Estimated from Organic Nitrates. *ACS Earth and Space Chemistry* **2019**, *3*, 1426–1437.
- (117) Vasquez, K. T.; Crounse, J. D.; Schulze, B. C.; Bates, K. H.; Teng, A. P.; Xu, L.; Allen, H. M.; Wennberg, P. O. Rapid hydrolysis of tertiary isoprene nitrate efficiently removes NO_x from the atmosphere. *Proceedings of the National Academy of Sciences of the United States of America* **2021**, *117*, 33011–33016.
- (118) Klodt, A. L.; Zhang, K.; Olsen, M. W.; Fernandez, J. L.; Furche, F.; Nizkorodov, S. A. Effect of Ammonium Salts on the Decarboxylation of Oxaloacetic Acid in Atmospheric Particles. *ACS Earth and Space Chemistry* **2021**, acsearthspacechem.1c00025.
- (119) Fraser, M. P.; Lakshmanan, K. Using levoglucosan as a molecular marker for the long-range transport of biomass combustion aerosols. *Environmental Science and Technology* **2000**, *34*, 4560–4564.
- (120) Klodt, A. L.; Romonosky, D. E.; Lin, P.; Laskin, J.; Laskin, A.; Nizkorodov, S. A. Aqueous Photochemistry of Secondary Organic Aerosol of α -Pinene and α -Humulene in the Presence of Hydrogen Peroxide or Inorganic Salts. *ACS Earth and Space Chemistry* **2019**, *3*, 2736–2746.
- (121) Romonosky, D. E.; Li, Y.; Shiraiwa, M.; Laskin, A.; Laskin, J.; Nizkorodov, S. A. Aqueous Photochemistry of Secondary Organic Aerosol of α -Pinene and α -Humulene Oxidized with Ozone, Hydroxyl Radical, and Nitrate Radical. *Journal of Physical Chemistry A* **2017**, *121*, 1298–1309.
- (122) Nguyen, T. B.; Laskin, A.; Laskin, J.; Nizkorodov, S. A. Direct aqueous photochemistry of isoprene high-NO_x secondary organic aerosol. *Physical Chemistry Chemical Physics* **2012**, *14*, 9702–9714.
- (123) Maksymiuk, C. S.; Gayahtri, C.; Gil, R. R.; Donahue, N. M. Secondary organic aerosol formation from multiphase oxidation of limonene by ozone: Mechanistic constraints via two-dimensional heteronuclear NMR spectroscopy. *Physical Chemistry Chemical Physics* **2009**, *11*, 7810–7818.
- (124) Chen, X.; Hopke, P. K. A chamber study of secondary organic aerosol formation by limonene ozonolysis. *Indoor Air* **2010**, *20*, 320–328.

- (125) Chen, X.; Hopke, P. K.; Carter, W. P. Secondary organic aerosol from ozonolysis of biogenic volatile organic compounds: Chamber studies of particle and reactive oxygen species formation. *Environmental Science and Technology* **2011**, *45*, 276–282.
- (126) Greenspan, L. Humidity Fixed Points of Binary Saturated Aqueous Solutions. *Journal of Research of the National Bureau of Standards. Section A, Physics and Chemistry* **1977**, *81*, 89–96.
- (127) Glasius, M.; Duane, M.; Larsen, B. R. Determination of polar terpene oxidation products in aerosols by liquid chromatography-ion trap mass spectrometry. *Journal of Chromatography A* **1999**, *833*, 121–135.
- (128) Kristensen, K.; Cui, T.; Zhang, H.; Gold, A.; Glasius, M.; Surratt, J. D. Dimers in α -pinene secondary organic aerosol: effect of hydroxyl radical, ozone, relative humidity and aerosol acidity. *Atmospheric Chemistry and Physics* **2014**, *14*, 4201–4218.
- (129) Zhang, X.; McVay, R. C.; Huang, D. D.; Dalleska, N. F.; Aumont, B.; Flagan, R. C.; Seinfeld, J. H. Formation and evolution of molecular products in α -pinene secondary organic aerosol. *Proceedings of the National Academy of Sciences of the United States of America* **2015**, *112*, 14168–14173.
- (130) Kristensen, K.; Watne, Å. K.; Hammes, J.; Lutz, A.; Petä, T.; Hallquist, M.; Bilde, M.; Glasius, M. High-Molecular Weight Dimer Esters Are Major Products in Aerosols from α -Pinene Ozonolysis and the Boreal Forest. *Environmental Science & Technology Letters* **2016**, *3*, 280–285.
- (131) Walser, M. L.; Desyaterik, Y.; Laskin, J.; Laskin, A.; Nizkorodov, S. A. High-resolution mass spectrometric analysis of secondary organic aerosol produced by ozonation of limonene. *Physical Chemistry Chemical Physics* **2008**, *10*, 1009–1022.
- (132) Kundu, S.; Fisseha, R.; Putman, A. L.; Rahn, T. A.; Mazzoleni, L. R. High molecular weight SOA formation during limonene ozonolysis: insights from ultrahigh-resolution FT-ICR mass spectrometry characterization. *Atmospheric Chemistry and Physics* **2012**, *12*, 5523–5536.
- (133) Sleighter, R. L.; Chen, H.; Wozniak, A. S.; Willoughby, A. S.; Caricasole, P.; Hatcher, P. G. Establishing a measure of reproducibility of ultrahigh-resolution mass spectra for complex mixtures of natural organic matter. *Analytical Chemistry* **2012**, *84*, 9184–9191.
- (134) Qi, L.; Nakao, S.; Malloy, Q.; Warren, B.; Cocker, D. R. Can secondary organic aerosol formed in an atmospheric simulation chamber continuously age? *Atmospheric Environment* **2010**, *44*, 2990–2996.
- (135) Denjean, C.; Formenti, P.; Picquet-Varrault, B.; Camredon, M.; Pangui, E.; Zapf, P.; Katrib, Y.; Giorio, C.; Tapparo, A.; Temime-Roussel, B.; Monod, A.; Aumont, B.; Doussin, J. F. Aging of secondary organic aerosol generated from the ozonolysis of α -pinene: Effects of ozone, light and temperature. *Atmospheric Chemistry and Physics* **2015**, *15*, 883–897.

- (136) Baumann, M. G. D.; Batterman, S. A.; Zhang, G.-Z. Terpene emissions from particleboard and medium density fiberboard products. *Forest Products Journal* **1999**, *49*, 49–56.
- (137) Nazaroff, W. W.; Weschler, C. J. Cleaning products and air fresheners: exposure to primary and secondary air pollutants. *Atmospheric Environment* **2004**, *38*, 2841–2865.
- (138) Singer, B. C.; Destailats, H.; Hodgson, A. T.; Nazaroff, W. W. Cleaning products and air fresheners: emissions and resulting concentrations of glycol ethers and terpenoids. *Indoor Air* **2006**, *16*, 179–191.
- (139) D’Ambro, E. L.; Schobesberger, S.; Zaveri, R. A.; Shilling, J. E.; Lee, B. H.; Lopez-Hilfiker, F. D.; Mohr, C.; Thornton, J. A. Isothermal Evaporation of α -Pinene Ozonolysis SOA: Volatility, Phase State, and Oligomeric Composition. *ACS Earth and Space Chemistry* **2018**, *2*, 1058–1067.
- (140) Yasmeeen, F.; Vermeylen, R.; Szmigielski, R.; Iinuma, Y.; Böge, O.; Herrmann, H.; Maenhaut, W.; Claeys, M. Terpenylic acid and related compounds: precursors for dimers in secondary organic aerosol from the ozonolysis of α - and β -pinene. *Atmospheric Chemistry and Physics* **2010**, *10*, 9383–9392.
- (141) Fleming, L. T.; Ali, N. N.; Blair, S. L.; Roveretto, M.; George, C.; Nizkorodov, S. A. Formation of Light-Absorbing Organosulfates during Evaporation of Secondary Organic Material Extracts in the Presence of Sulfuric Acid. *ACS Earth and Space Chemistry* **2019**, *3*, 947–957.
- (142) Nguyen, T. B.; Lee, P. B.; Updyke, K. M.; Bones, D. L.; Laskin, J.; Laskin, A.; Nizkorodov, S. A. Formation of nitrogen- and sulfur-containing light-absorbing compounds accelerated by evaporation of water from secondary organic aerosols. *Journal of Geophysical Research: Atmospheres* **2012**, *117*, 1207.
- (143) Carslaw, K. S.; Clegg, S. L.; Brimblecombe, P. A Thermodynamic Model of the System HCl-HNO₃-H₂SO₄-H₂O, Including Solubilities of HBr, from <200 to 328 K. *Journal of Physical Chemistry* **1995**, *99*, 11557–11574.
- (144) Massucci, M.; Clegg, S. L.; Brimblecombe, P. Equilibrium Partial Pressures, Thermodynamic Properties of Aqueous and Solid Phases, and Cl₂ Production from Aqueous HCl and HNO₃ and Their Mixtures. *Journal of Physical Chemistry A* **1999**, *103*, 4209–4226.
- (145) Clegg, S. L.; Brimblecombe, P.; Wexler, A. S. Extended AIM Aerosol Thermodynamics Model.
- (146) Lee, H. J.; Laskin, A.; Laskin, J.; Nizkorodov, S. A. Excitation-emission spectra and fluorescence quantum yields for fresh and aged biogenic secondary organic aerosols. *Environmental Science and Technology* **2013**, *47*, 5763–5770.
- (147) Kristensen, K.; Enggrob, K. L.; King, S. M.; Worton, D. R.; Platt, S. M.; Mortensen, R.; Rosenoern, T.; Surratt, J. D.; Bilde, M.; Goldstein, A. H.; Glasius, M. Formation and occurrence of dimer esters of pinene oxidation products in atmospheric aerosols. *Atmospheric Chemistry and Physics* **2013**, *13*, 3763–3776.

- (148) Wong, C.; Vite, D.; Nizkorodov, S. A. Stability of α -Pinene and d-Limonene Ozonolysis Secondary Organic Aerosol Compounds Toward Hydrolysis and Hydration. *ACS Earth and Space Chemistry* **2021**, *5*, 2555–2564.
- (149) Hallquist, M. et al. The formation, properties and impact of secondary organic aerosol: Current and emerging issues. *Atmospheric Chemistry and Physics* **2009**, *9*, 5155–5236.
- (150) Iinuma, Y.; Böge, O.; Kahnt, A.; Herrmann, H. Laboratory chamber studies on the formation of organosulfates from reactive uptake of monoterpene oxides. *Physical Chemistry Chemical Physics* **2009**, *11*, 7985–7997.
- (151) Duporté, G.; Flaud, P. M.; Kammer, J.; Geneste, E.; Augagneur, S.; Pangui, E.; Lamkaddam, H.; Gratien, A.; Doussin, J. F.; Budzinski, H.; Villenave, E.; Perraudin, E. Experimental Study of the Formation of Organosulfates from α -Pinene Oxidation. 2. Time Evolution and Effect of Particle Acidity. *Journal of Physical Chemistry A* **2020**, *124*, 409–421.
- (152) Priyadarshani, A.; Hettiyadura, S.; Al-Naiema, I. M.; Hughes, D. D.; Fang, T.; Stone, E. A. Organosulfates in Atlanta, Georgia: anthropogenic influences on biogenic secondary organic aerosol formation. *Atmos. Chem. Phys* **2019**, *19*, 3191–3206.
- (153) Wang, Y.; Ren, J.; Huang, X. H.; Tong, R.; Yu, J. Z. Synthesis of Four Monoterpene-Derived Organosulfates and Their Quantification in Atmospheric Aerosol Samples. *Environmental Science and Technology* **2017**, *51*, 6791–6801.
- (154) Yttri, K. E. et al. Source apportionment of the summer time carbonaceous aerosol at Nordic rural background sites. *Atmospheric Chemistry and Physics* **2011**, *11*, 13339–13357.
- (155) Kristensen, K.; Bilde, M.; Aalto, P. P.; Petäjä, T.; Glasius, M. Denuder/filter sampling of organic acids and organosulfates at urban and boreal forest sites: Gas/particle distribution and possible sampling artifacts. *Atmospheric Environment* **2016**, *130*, 36–53.
- (156) Nguyen, Q. T.; Christensen, M. K.; Cozzi, F.; Zare, A.; Hansen, A. M.; Kristensen, K.; Tulinius, T. E.; Madsen, H. H.; Christensen, J. H.; Brandt, J.; Massling, A.; Nøjgaard, J. K.; Glasius, M. Understanding the anthropogenic influence on formation of biogenic secondary organic aerosols in Denmark via analysis of organosulfates and related oxidation products. *Atmospheric Chemistry and Physics* **2014**, *14*, 8961–8981.
- (157) Brüggemann, M.; Van Pinxteren, D.; Wang, Y.; Yu, J. Z.; Herrmann, H. Quantification of known and unknown terpenoid organosulfates in PM10 using untargeted LC–HRMS/MS: contrasting summertime rural Germany and the North China Plain. *Environmental Chemistry* **2019**, *16*, 333–346.
- (158) Ma, Y.; Xu, X.; Song, W.; Geng, F.; Wang, L. Seasonal and diurnal variations of particulate organosulfates in urban Shanghai, China. *Atmospheric Environment* **2014**, *85*, 152–160.

- (159) Kristensen, K.; Glasius, M. Organosulfates and oxidation products from biogenic hydrocarbons in fine aerosols from a forest in North West Europe during spring. *Atmospheric Environment* **2011**, *45*, 4546–4556.
- (160) Hansen, A. M.; Kristensen, K.; Nguyen, Q. T.; Zare, A.; Cozzi, F.; Nøjgaard, J. K.; Skov, H.; Brandt, J.; Christensen, J. H.; Ström, J.; Tunved, P.; Krejci, R.; Glasius, M. Organosulfates and organic acids in Arctic aerosols: Speciation, annual variation and concentration levels. *Atmospheric Chemistry and Physics* **2014**, *14*, 7807–7823.
- (161) Meade, L. E.; Riva, M.; Blomberg, M. Z.; Brock, A. K.; Qualters, E. M.; Siejack, R. A.; Ramakrishnan, K.; Surratt, J. D.; Kautzman, K. E. Seasonal variations of fine particulate organosulfates derived from biogenic and anthropogenic hydrocarbons in the mid-Atlantic United States. *Atmospheric Environment* **2016**, *145*, 405–414.
- (162) Romonosky, D. E.; Ali, N. N.; Saiduddin, M. N.; Wu, M.; Lee, H. J.; Aiona, P. K.; Nizkorodov, S. A. Effective absorption cross sections and photolysis rates of anthropogenic and biogenic secondary organic aerosols. *Atmospheric Environment* **2016**, *130*, 172–179.
- (163) Updyke, K. M.; Nguyen, T. B.; Nizkorodov, S. A. Formation of brown carbon via reactions of ammonia with secondary organic aerosols from biogenic and anthropogenic precursors. *Atmospheric Environment* **2012**, *63*, 22–31.
- (164) Mang, S. A.; Henricksen, D. K.; Bateman, A. E.; Andersen, M. P.; Blake, D. R.; Nizkorodov, S. A. Contribution of carbonyl photochemistry to aging of atmospheric secondary organic aerosol. *Journal of Physical Chemistry A* **2008**, *112*, 8337–8344.
- (165) Docherty, K. S.; Wu, W.; Lim, Y. B.; Ziemann, P. J. Contributions of organic peroxides to secondary aerosol formed from reactions of monoterpenes with O₃. *Environmental Science and Technology* **2005**, *39*, 4049–4059.
- (166) Koch, B. P.; Dittmar, T. From mass to structure: an aromaticity index for high-resolution mass data of natural organic matter. *Rapid Communications in Mass Spectrometry* **2006**, *20*, 926–932.
- (167) Vione, D.; Maurino, V.; Minero, C.; Duncianu, M.; Olariu, R. I.; Arsene, C.; Sarakha, M.; Mailhot, G. Assessing the transformation kinetics of 2- and 4-nitrophenol in the atmospheric aqueous phase. Implications for the distribution of both nitroisomers in the atmosphere. *Atmospheric Environment* **2009**, *43*, 2321–2327.
- (168) Barsotti, F.; Bartels-Rausch, T.; De Laurentiis, E.; Ammann, M.; Brigante, M.; Mailhot, G.; Maurino, V.; Minero, C.; Vione, D. Photochemical Formation of Nitrite and Nitrous Acid (HONO) upon Irradiation of Nitrophenols in Aqueous Solution and in Viscous Secondary Organic Aerosol Proxy. *Environmental Science and Technology* **2017**, *51*, 7486–7495.
- (169) Lee, H. J.; Aiona, P. K.; Laskin, A.; Laskin, J.; Nizkorodov, S. A. Effect of solar radiation on the optical properties and molecular composition of laboratory proxies of atmospheric brown carbon. *Environmental Science and Technology* **2014**, *48*, 10217–10226.

- (170) Ackendorf, J. M.; Ippolito, M. G.; Galloway, M. M. pH Dependence of the Imidazole-2-carboxaldehyde Hydration Equilibrium: Implications for Atmospheric Light Absorbance. *Environmental Science and Technology Letters* **2017**, *4*, 551–555.
- (171) Phillips, S. M.; Bellcross, A. D.; Smith, G. D. Light Absorption by Brown Carbon in the Southeastern United States is pH-dependent. *Environmental Science and Technology* **2017**, *51*, 6782–6790.
- (172) Qin, J.; Zhang, L.; Qin, Y.; Shi, S.; Li, J.; Gao, Y.; Tan, J.; Wang, X. pH-Dependent Chemical Transformations of Humic-Like Substances and Further Cognitions Revealed by Optical Methods. *Environmental Science & Technology* **2022**, *56*, 7578–7587.
- (173) Andreae, M. O. et al. Aerosol characteristics and particle production in the upper troposphere over the Amazon Basin. *Atmospheric Chemistry and Physics* **2018**, *18*, 921–961.
- (174) Twohy, C. H.; Clement, C. F.; Gandrud, B. W.; Weinheimer, A. J.; Campos, T. L.; Baumgardner, D.; Brune, W. H.; Faloon, I.; Sachse, G. W.; Vay, S. A.; Tan, D. Deep convection as a source of new particles in the midlatitude upper troposphere. *Journal of Geophysical Research: Atmospheres* **2002**, *107*, 6–1.
- (175) Weigel, R. et al. In situ observations of new particle formation in the tropical upper troposphere: The role of clouds and the nucleation mechanism. *Atmospheric Chemistry and Physics* **2011**, *11*, 9983–10010.
- (176) Murphy, D. M.; Cziczo, D. J.; Froyd, K. D.; Hudson, P. K.; Matthew, B. M.; Middlebrook, A. M.; Peltier, R. E.; Sullivan, A.; Thomson, D. S.; Weber, R. J. Single-particle mass spectrometry of tropospheric aerosol particles. *Journal of Geophysical Research: Atmospheres* **2006**, *111*, 23–32.
- (177) Laskin, A.; Laskin, J.; Nizkorodov, S. A. Chemistry of Atmospheric Brown Carbon. *Chemical Reviews* **2015**, *115*, 4335–4382.
- (178) Carslaw, K. S.; Peter, T.; Clegg, S. L. Modeling the composition of liquid stratospheric aerosols. *Reviews of Geophysics* **1997**, *35*, 125–154.
- (179) Guenther, A. B.; Jiang, X.; Heald, C. L.; Sakulyanontvittaya, T.; Duhl, T.; Emmons, L. K.; Wang, X. The model of emissions of gases and aerosols from nature version 2.1 (MEGAN2.1): An extended and updated framework for modeling biogenic emissions. *Geoscientific Model Development* **2012**, *5*, 1471–1492.
- (180) Hyvärinen, A. P.; Lihavainen, H.; Gaman, A.; Vairila, L.; Ojala, H.; Kulmala, M.; Viisanen, Y. Surface tensions and densities of oxalic, malonic, succinic, maleic, malic, and cis-pinonic acids. *Journal of Chemical and Engineering Data* **2006**, *51*, 255–260.
- (181) Lignell, H.; Epstein, S. A.; Marvin, M. R.; Shemesh, D.; Gerber, B.; Nizkorodov, S. Experimental and theoretical study of aqueous cis-pinonic acid photolysis. *Journal of Physical Chemistry A* **2013**, *117*, 12930–12945.

- (182) Müller, L.; Reinnig, M. C.; Naumann, K. H.; Saathoff, H.; Mentel, T. F.; Donahue, N. M.; Hoffmann, T. Formation of 3-methyl-1,2,3-butanetricarboxylic acid via gas phase oxidation of pinonic acid - A mass spectrometric study of SOA aging. *Atmospheric Chemistry and Physics* **2012**, *12*, 1483–1496.
- (183) Glasius, M.; Calogirou, A.; Jensen, N. R.; Hjorth, J.; Nielsen, C. J. Kinetic Study of Gas-Phase Reactions of Pinonaldehyde and Structurally Related Compounds. *International Journal of Chemical Kinetics* **1997**, *29*, 527–533.
- (184) Nozière, B.; Barnes, I.; Becker, K. H. Product study and mechanisms of the reactions of α -pinene and of pinonaldehyde with OH radicals. *Journal of Geophysical Research: Atmospheres* **1999**, *104*, 23645–23656.
- (185) Wong, C.; Liu, S.; Nizkorodov, S. A. Highly Acidic Conditions Drastically Alter the Chemical Composition and Absorption Coefficient of α -Pinene Secondary Organic Aerosol. *ACS Earth and Space Chemistry* **2022**, *6*, 2983–2994.
- (186) Nguyen, T. B.; Laskin, A.; Laskin, J.; Nizkorodov, S. A. Brown carbon formation from ketoaldehydes of biogenic monoterpenes. *Faraday Discussions* **2013**, *165*, 473–494.
- (187) Zhang, Y.; Apsokardu, M. J.; Kerecman, D. E.; Achtenhagen, M.; Johnston, M. V. Reaction Kinetics of Organic Aerosol Studied by Droplet Assisted Ionization: Enhanced Reactivity in Droplets Relative to Bulk Solution. *Journal of the American Society for Mass Spectrometry* **2021**, *32*, 46–54.
- (188) Arcus, C. L.; Bennett, G. J. The mechanism of the rearrangement of pinonic acid into homoterpenyl methyl ketone. *Journal of the Chemical Society (Resumed)* **1955**, *28*, 2627–2632.
- (189) Nozière, B.; Esteve, W. Organic reactions increasing the absorption index of atmospheric sulfuric acid aerosols. *Geophysical Research Letters* **2005**, *32*, 1–5.
- (190) Thomas, A. F.; Perret, C. 4-(1-hydroperoxy-1-methylethyl)-1,3-cyclopentadienyl methyl ketone: its formation from α -terpineol and behaviour as a dimethylfulvene epoxide. *Tetrahedron* **1986**, *42*, 3311–3321.
- (191) Bozzato, G.; Bachmann, J. P.; Pesaro, M. Stereoselective addition of methylcuprates to a 2-formyl-cyclohexa-2,5-dienone system. A stereoselective total synthesis of racemic β -vetivone. *Journal of the Chemical Society, Chemical Communications* **1974**, 1005–1006.
- (192) Degrado, S. J.; Mizutani, H.; Hoveyda, A. H. Efficient Cu-catalyzed asymmetric conjugate additions of alkylzincs to trisubstituted cyclic enones. *Journal of the American Chemical Society* **2002**, *124*, 13362–13363.
- (193) Després, V. R.; Alex Huffman, J.; Burrows, S. M.; Hoose, C.; Safatov, A. S.; Buryak, G.; Fröhlich-Nowoisky, J.; Elbert, W.; Andreae, M. O.; Pöschl, U.; Jaenicke, R. Primary biological aerosol particles in the atmosphere: a review. *Tellus, Series B: Chemical and Physical Meteorology* **2012**, *64*, 15598.

- (194) Pan, Y. L. Detection and characterization of biological and other organic-carbon aerosol particles in atmosphere using fluorescence. *Journal of Quantitative Spectroscopy and Radiative Transfer* **2015**, *150*, 12–35.
- (195) Graber, E. R.; Rudich, Y. Atmospheric HULIS: How humic-like are they? A comprehensive and critical review. *Atmospheric Chemistry and Physics* **2006**, *6*, 729–753.
- (196) Pöhlker, C.; Huffman, J. A.; Pöschl, U. Autofluorescence of atmospheric bioaerosols - Fluorescent biomolecules and potential interferences. *Atmospheric Measurement Techniques* **2012**, *5*, 37–71.
- (197) Chen, Q.; Mu, Z.; Song, W.; Wang, Y.; Yang, Z.; Zhang, L.; Zhang, Y. L. Size-Resolved Characterization of the Chromophores in Atmospheric Particulate Matter From a Typical Coal-Burning City in China. *Journal of Geophysical Research: Atmospheres* **2019**, *124*, 10546–10563.
- (198) Barsotti, F.; Ghigo, G.; Vione, D. Computational assessment of the fluorescence emission of phenol oligomers: A possible insight into the fluorescence properties of humic-like substances (HULIS). *Journal of Photochemistry and Photobiology A: Chemistry* **2016**, *315*, 87–93.
- (199) Bones, D. L. et al. Appearance of strong absorbers and fluorophores in limonene-O₃ secondary organic aerosol due to NH₄⁺-mediated chemical aging over long time scales. *Journal of Geophysical Research: Atmospheres* **2010**, *115*, 5203.
- (200) Aiona, P. K.; Luek, J. L.; Timko, S. A.; Powers, L. C.; Gonsior, M.; Nizkorodov, S. A. Effect of Photolysis on Absorption and Fluorescence Spectra of Light-Absorbing Secondary Organic Aerosols. *ACS Earth and Space Chemistry* **2018**, *2*, 235–245.
- (201) Ammor, M. S. Recent advances in the use of intrinsic fluorescence for bacterial identification and characterization. *Journal of fluorescence* **2007**, *17*, 455–459.
- (202) Baboornian, V. J.; Gu, Y.; Nizkorodov, S. A. Photodegradation of Secondary Organic Aerosols by Long-Term Exposure to Solar Actinic Radiation. *ACS Earth and Space Chemistry* **2020**, *4*, 1078–1089.
- (203) Veghte, D. P.; China, S.; Weis, J.; Lin, P.; Hinks, M. L.; Kovarik, L.; Nizkorodov, S. A.; Gilles, M. K.; Laskin, A. Heating-Induced Transformations of Atmospheric Particles: Environmental Transmission Electron Microscopy Study. *Analytical Chemistry* **2018**, *90*, 9761–9768.
- (204) Timko, S. A.; Maydanov, A.; Pittelli, S. L.; Conte, M. H.; Cooper, W. J.; Koch, B. P.; Schmitt-Kopplin, P.; Gonsior, M. Depth-dependent photodegradation of marine dissolved organic matter. *Frontiers in Marine Science* **2015**, *2*, 66.
- (205) Zepp, R. G.; Sheldon, W. M.; Moran, M. A. Dissolved organic fluorophores in southeastern US coastal waters: correction method for eliminating Rayleigh and Raman scattering peaks in excitation–emission matrices. *Marine Chemistry* **2004**, *89*, 15–36.
- (206) Duarte, R. M.; Pio, C. A.; Duarte, A. C. Synchronous scan and excitation-emission matrix fluorescence spectroscopy of water-soluble organic compounds in atmospheric aerosols. *Journal of Atmospheric Chemistry* **2004**, *48*, 157–171.

- (207) Laskin, J.; Laskin, A.; Nizkorodov, S. A.; Roach, P.; Eckert, P.; Gilles, M. K.; Wang, B.; Lee, H. J.; Hu, Q. Molecular selectivity of brown carbon chromophores. *Environmental Science and Technology* **2014**, *48*, 12047–12055.
- (208) Chen, Q.; Miyazaki, Y.; Kawamura, K.; Matsumoto, K.; Coburn, S.; Volkamer, R.; Iwamoto, Y.; Kagami, S.; Deng, Y.; Ogawa, S.; Ramasamy, S.; Kato, S.; Ida, A.; Kajii, Y.; Mochida, M. Characterization of Chromophoric Water-Soluble Organic Matter in Urban, Forest, and Marine Aerosols by HR-ToF-AMS Analysis and Excitation-Emission Matrix Spectroscopy. *Environmental Science and Technology* **2016**, *50*, 10351–10360.
- (209) Lee, B. J.; Kim, B.; Lee, K. Air pollution exposure and cardiovascular disease. *Toxicological Research* **2014**, *30*, 71–75.
- (210) Huffman, J. A. et al. Real-time sensing of bioaerosols: Review and current perspectives. *Aerosol Science and Technology* **2019**, *54*, 465–495.
- (211) Wlodarski, M.; Kaliszewski, M.; Kwasny, M.; Kopczynski, K.; Zawadzki, Z.; Wlodarski, A. M.; Mierczyk, Z.; Mlynczak, J.; Trafny, E.; Szpakowska, M. Fluorescence excitation-emission matrices of selected biological materials. *SPIE Proceedings* **2006**, *6398*, 639806.
- (212) Dalterio, R. A.; Nelson, W. H.; Britt, D.; Sperry, J. F.; Tanguay, J. F.; Suib, S. L. The Steady-State and Decay Characteristics of Primary Fluorescence from Live Bacteria. *Applied Spectroscopy* **1987**, *41*, 234–241.
- (213) Kopczynski, K.; Kwasny, M.; Mierczyk, Z.; Zawadzki Krzysztof Kopczynski, Z.; Zawadzki, Z. Laser induced fluorescence system for detection of biological agents: European project FABIOLA. *Optical Security Systems* **2005**, *5954*, 595405.
- (214) Ramanujam, N. Fluorescence Spectroscopy of Neoplastic and Non-Neoplastic Tissues. *Neoplasia (New York, N.Y.)* **2000**, *2*, 89.
- (215) Billinton, N.; Knight, A. W. Seeing the wood through the trees: A review of techniques for distinguishing green fluorescent protein from endogenous autofluorescence. *Analytical Biochemistry* **2001**, *291*, 175–197.
- (216) Benson, R. C.; Meyer, R. A.; Zaruba, M. E.; McKhann, G. M. Cellular autofluorescence— is it due to flavins? *The journal of histochemistry and cytochemistry : official journal of the Histochemistry Society* **1979**, *27*, 44–48.
- (217) Richards-Kortum, R.; Sevick-Muraca, E. Quantitative optical spectroscopy for tissue diagnosis. *Annual review of physical chemistry* **1996**, *47*, 555–606.
- (218) Avi-Dor, Y.; Olson, J. M.; Doherty, M. D.; Kaplan, N. O. Fluorescence of Pyridine Nucleotides in Mitochondria. *Journal of Biological Chemistry* **1962**, *237*, 2377–2383.
- (219) Bueno, C.; Encinas, M. V. Photophysical and Photochemical Studies of Pyridoxamine. *Helvetica Chimica Acta* **2003**, *86*, 3363–3375.
- (220) Ramanujam, N., *Fluorescence Spectroscopy In Vivo*; John Wiley & Sons, Ltd: 2006.
- (221) Olmstead, J. A.; Gray, D. G. Fluorescence emission from mechanical pulp sheets. *Journal of Photochemistry and Photobiology A: Chemistry* **1993**, *73*, 59–65.

- (222) Castellan, A.; Ruggiero, R.; Frollini, E.; Ramos, L. A.; Chirat, C. Studies on fluorescence of cellulose. *Holzforschung* **2007**, *61*, 504–508.
- (223) Olmstead, J. A.; Gray, D. G. Fluorescence spectroscopy of cellulose, lignin and mechanical pulps : A review. *Journal of pulp and paper science* **1997**, *23*, J571–J581.
- (224) Dreyer, B.; Morte, A.; Pérez-Gilabert, M.; Honrubia, M. Autofluorescence detection of arbuscular mycorrhizal fungal structures in palm roots: an underestimated experimental method. *Mycological Research* **2006**, *110*, 887–897.
- (225) Bonfante-Fasolo, P.; Faccio, A.; Perotto, S.; Schubert, A. Correlation between chitin distribution and cell wall morphology in the mycorrhizal fungus *Glomus versiforme*. *Mycological Research* **1990**, *94*, 157–165.
- (226) Vierheilig, H.; Böckenhoff, A.; Knoblauch, M.; Juge, C.; Van Bel, A. J.; Grundler, F.; Piché, Y.; Wyss, U. In vivo observations of the arbuscular mycorrhizal fungus *Glomus mosseae* in roots by confocal laser scanning microscopy. *Mycological Research* **1999**, *103*, 311–314.